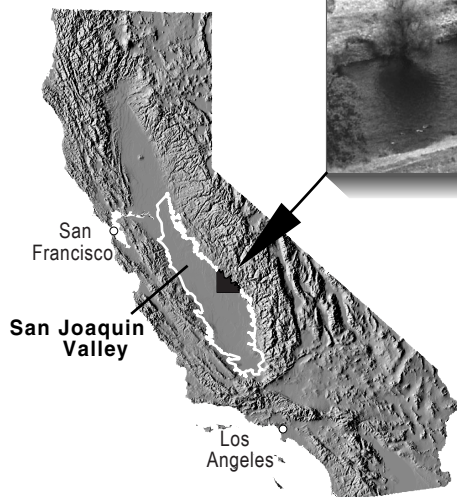# Evaluation of Processes Affecting 1,2-Dibromo-3-Chloropropane (DBCP) Concentrations in Ground Water in the Eastern San Joaquin Valley, California: Analysis of Chemical Data and Ground-Water Flow and Transport Simulations

U.S. GEOLOGICAL SURVEY
Water-Resources Investigations Report 99-4059

San Francisco

San Joaquin Valley

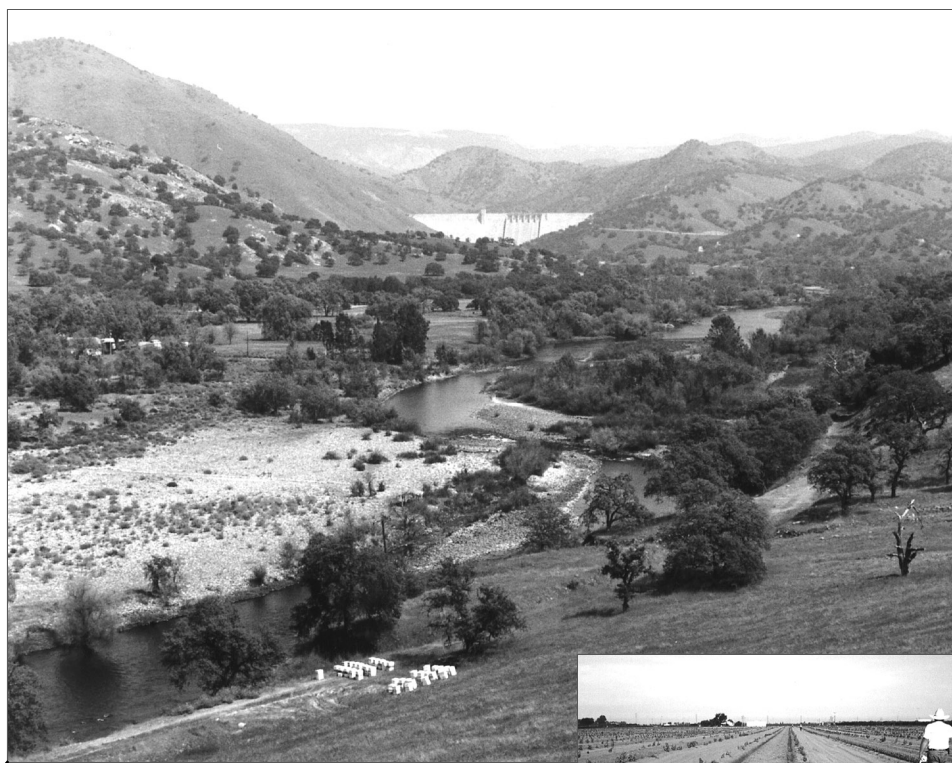Los Angeles

National Water-Quality Assessment Program

Evaluation of Processes Affecting 1,2-Dibromo-3-Chloropropane (DBCP) Concentrations in Ground Water in the Eastern San Joaquin Valley, California: Analysis of Chemical Data and Ground-Water Flow and Transport Simulations

By KAREN R. BUROW[1], SANDRA Y. PANSHIN[1], NEIL M. DUBROVSKY[1], DAVID VANBROCKLIN[2], *and* GRAHAM E. FOGG[2]

[1]U.S. Geological Survey
[2]Hydrologic Sciences, University of California, Davis

6440-53

Sacramento, California
1999

U.S. DEPARTMENT OF THE INTERIOR

BRUCE BABBITT, Secretary

U.S. GEOLOGICAL SURVEY

Charles G. Groat, Director

FOREWORD

The mission of the U.S. Geological Survey (USGS) is to assess the quantity and quality of the earth resources of the Nation and to provide information that will assist resource managers and policymakers at Federal, State, and local levels in making sound decisions. Assessment of water-quality conditions and trends is an important part of this overall mission.

One of the greatest challenges faced by water-resources scientists is acquiring reliable information that will guide the use and protection of the Nation's water resources. That challenge is being addressed by Federal, State, interstate, and local water-resource agencies and by many academic institutions. These organizations are collecting water-quality data for a host of purposes that include: compliance with permits and water-supply standards; development of remediation plans for specific contamination problems; operational decisions on industrial, wastewater, or water-supply facilities; and research on factors that affect water quality. An additional need for water-quality information is to provide a basis on which regional- and national-level policy decisions can be based. Wise decisions must be based on sound information. As a society we need to know whether certain types of water-quality problems are isolated or ubiquitous, whether there are significant differences in conditions among regions, whether the conditions are changing over time, and why these conditions change from place to place and over time. The information can be used to help determine the efficacy of existing water-quality policies and to help analysts determine the need for and likely consequences of new policies.

To address these needs, the U.S. Congress appropriated funds in 1986 for the USGS to begin a pilot program in seven project areas to develop and refine the National Water-Quality Assessment (NAWQA) Program. In 1991, the USGS began full implementation of the program. The NAWQA Program builds upon an existing base of water-quality studies of the USGS, as well as those of other Federal, State, and local agencies. The objectives of the NAWQA Program are to:

- Describe current water-quality conditions for a large part of the Nation's freshwater streams, rivers, and aquifers.
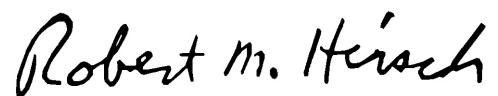- Describe how water quality is changing over time.
- Improve understanding of the primary natural and human factors that affect water-quality conditions.

This information will help support the development and evaluation of management, regulatory, and monitoring decisions by other Federal, State, and local agencies to protect, use, and enhance water resources.

The goals of the NAWQA Program are being achieved through ongoing and proposed investigations of 60 of the Nation's most important river basins and aquifer systems, which are referred to as study units. These study units are distributed throughout the Nation and cover a diversity of hydrogeologic settings. More than two-thirds of the Nation's freshwater use occurs within the 60 study units and more than two-thirds of the people served by public water-supply systems live within their boundaries.

National synthesis of data analysis, based on aggregation of comparable information obtained from the study units, is a major component of the program. This effort focuses on selected water-quality topics using nationally consistent information. Comparative studies will explain differences and similarities in observed water-quality conditions among study areas and will identify changes and trends and their causes. The first topics addressed by the national synthesis are pesticides, nutrients, volatile organic compounds, and aquatic biology. Discussions on these and other water-quality topics will be published in periodic summaries of the quality of the Nation's ground and surface water as the information becomes available.

This report is an element of the comprehensive body of information developed as part of the NAWQA Program. The program depends heavily on the advice, cooperation, and information from many Federal, State, interstate, Tribal, and local agencies and the public. The assistance and suggestions of all are greatly appreciated.

Robert M. Hirsch

Robert M. Hirsch
Chief Hydrologist

CONTENTS

FIGURES

TABLES

CONVERSION FACTORS, VERTICAL DATUM, ABBREVIATIONS, AND WELL-NUMBERING SYSTEM

Conversion Factors

Multiply	By	To obtain
centimeter (cm)	0.3937	inch
meter (m)	3.281	foot
meter per year (m/yr)	3.281	foot per year
kilometer (km)	0.6214	mile
square kilometer (km^2)	0.3861	square mile
liter (L)	33.82	ounce, fluid
liter per second (L/s)	15.85	gallon per minute
millimeters per year (mm/yr)	0.03937	inches per year
Hydraulic conductivity		
meter per second (m/s)	86,400	meter per day
meter per second (m/s)	3.281	foot per second
Transmissivity*		
meter squared per sec (m^2/s)	86,400	meter squared per day
feet squared per second (ft^2/s)	0.0929	meter squared per second

Temperature in degrees Celsius (°C) may be converted to degrees Fahrenheit (°F) as follows:

$$°F = (1.8 \times °C) + 32.$$

Vertical Datum:

Sea level: In this report, "sea level" refers to the National Geodetic Vertical Datum of 1929 (NGVD of 1929)—a geodetic datum derived from a general adjustment of the first-order level nets of both the United States and Canada, formerly called Sea Level Datum of 1929.

Transmissivity: The standard unit for transmissivity is cubic meter per second per square second times meter of aquifer thickness $[(m^3s)/m^2]m$. In this report, the mathematically reduced form, meter squared per second (m^2/s), is used for convenience.

Specific conductance is given in microsiemens per centimeter at 25 degrees Celsius (µS/cm at 25°C). Concentrations of chemical constituents in water are given either in milligrams per liter (mg/L), micrograms per liter (µg/L), or tritium units (TU). The Freundlich isotherm distribution coefficient (K_D) is reported in liters per kilogram (L/kg).

Abbreviations:

mL	milliliter(s)
L/kg	liter(s) per kilogram
μm	micrometer(s)
BAA	2-bromoallyl alcohol
BCP	2-bromo-3-chloropropene
CFC	chlorofluorocarbon
DBCP	1,2-dibromo-3-chloropropane
DBP	2,3-dibromopropene
GC/ECD	gas chromatography/electron-capture detector
MAPP	oxygen-methyl acetylene propadiene stabilized
MCL	maximum contaminant level
NAWQA	National Water Quality Assessment
NWQL	National Water Quality Laboratory
PTFE	polytetrafluoroethylene (Teflon)
PVC	polyvinyl chloride
QC	quality control
TU	tritium unit
USGS	U.S. Geological Survey

Well-Numbering System

Wells are identified and numbered according to their location in the rectangular system for the subdivision of public lands. Identification consists of the township number, north or south; the range number, east or west; and the section number. Each section is divided into sixteen 40-acre tracts lettered consecutively (except I and O), beginning with "A" in the northeast corner of the section and progressing in a sinusoidal manner to "R" in the southeast corner. Within the 40-acre tract, wells are sequentially numbered in the order they are inventoried. The final letter refers to the base line and meridian. In California, there are three base lines and meridians: Humbolt (H), Mount Diablo (M), and San Bernardino (S). All wells in the study area are referenced to the Mount Diablo base line and meridian (M). Well numbers consist of 15 characters and follow the format 014S022E023F001M. In this report, well numbers are abbreviated and written 14S/22E-23F1. The following diagram shows how the number for well 14S/22E-23F1 is derived.
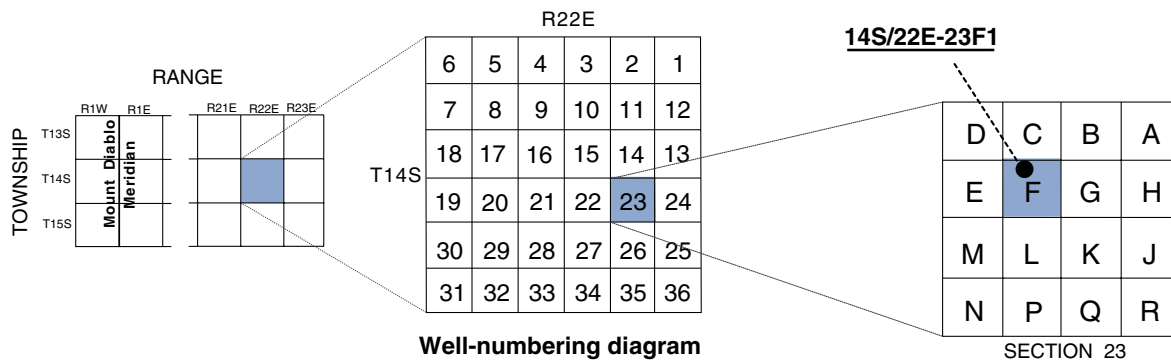
Well-numbering diagram

Evaluation of Processes Affecting 1,2-Dibromo-3-Chloropropane (DBCP) Concentrations in Ground Water in the Eastern San Joaquin Valley, California: Analysis of Chemical Data and Ground-Water Flow and Transport Simulations

By Karen R. Burow, Sandra Y. Panshin, Neil M. Dubrovsky, David VanBrocklin, *and* Graham E. Fogg

ABSTRACT

Future use of the sole-source aquifer near Fresno in the eastern San Joaquin Valley, California, will depend, in part, on how long 1,2-dibromo-3-chloropropane (DBCP), an agricultural fumigant banned from use since the late 1970's, persists at concentrations greater than the maximum contaminant level of 0.2 micrograms per liter (µg/L). Field data indicate that DBCP concentrations in ground water have decreased since the late 1970's. Laboratory experiments by earlier investigators show that DBCP transformed to 2-bromoallyl alcohol (BAA) under conditions similar to in situ conditions, with an estimated half-life ranging from 6.1 (pH 7.8, 21.1 degrees Celsius) to 141 years (pH 7.0, 15 degrees Celsius). For this current study, a detailed hydrogeologic investigation was done to assess the relative importance of chemical transformation, dispersion, and ground-water pumping and reapplication of irrigation water in affecting DBCP concentrations.

Ground-water samples were collected from 20 monitoring wells installed along a 4.6-kilometer transect. DBCP concentrations in these samples ranged from less than the detection limit of 0.03 µg/L to a maximum of 6.4 µg/L. Results of chlorofluorocarbon (CFC) age dating indicate that DBCP occurs in water that ranges in age from about 2 to 41 years. The primary transformation product BAA, which was identified during previous laboratory studies, was not detected at or greater than 0.03 µg/L in any of the 20 ground-water samples. The lack of detection of BAA indicates that transformation to BAA is insignificant relative to other processes controlling DBCP concentrations. Results from this current study indicate that the in situ hydrolysis half-life for DBCP to BAA is much greater than the laboratory-determined values.

Estimated initial concentrations of DBCP, calculated using CFC-estimated travel times and a half-life of 6.1 years, indicate that maximum initial concentrations are consistent with maximum measured concentrations in ground water. In contrast to initial DBCP concentrations, the estimated initial nitrate concentrations indicate that nitrate concentrations in recharge water have increased with time.

A conceptual two-dimensional numerical flow and transport modeling approach was used to test hypotheses addressing dispersion, transformation rate, and in a relative sense, the effects of ground-water pumping and reapplication of irrigation water on DBCP concentrations in the aquifer. The flow and transport simulations, which represent hypothetical steady-state flow conditions in the aquifer, were used to refine the conceptual understanding of the aquifer system rather than to predict future concentrations of DBCP. Results indicate that dispersion reduces peak concentrations, but this process alone does not

account for the apparent decrease in DBCP concentrations in ground water in the eastern San Joaquin Valley. Ground-water pumping and reapplication of irrigation water may affect DBCP concentrations to the extent that this process can be simulated indirectly using first-order decay. Transport simulation results indicate that the in situ "effective" half-life of DBCP caused by processes other than dispersion and transformation to BAA could be on the order of 6 years.

INTRODUCTION

Background

DBCP (1,2-dibromo-3-chloropropane), a soil fumigant used to control nematodes, had been applied to crops nationwide since the 1950's, with the most frequent use between 1960 and 1979. In 1977, agricultural use of DBCP was suspended in California in response to concern about the potential hazardous effects of DBCP on human health. Exposure to DBCP was later linked to temporary sterility and cancer (U.S. Environmental Protection Agency, 1985). Since 1979, DBCP has been detected in more than 2,500 drinking-water wells in California (California Department of Pesticide Regulation, 1992, 1993, 1994), many of which tap the sole-source aquifer near Fresno in the eastern San Joaquin Valley, California (fig. 1). DBCP has persisted in this area at concentrations that exceed the maximum contaminant level (MCL) of 0.2 µg/L (U.S. Environmental Protection Agency, 1996) more than 15 years after it was banned from use. Understanding the processes that control the behavior of DBCP is critical to the management of the ground-water resources in this area.

The application of DBCP is not well documented, although partial reporting of applications to the California Department of Pesticide Regulation indicates that DBCP was used on vineyards, orchards, and various other crops (California Department of Food and Agriculture, 1973; Domagalski, 1997). DBCP was used intermittently to treat nematode problems that occur especially in older, well-established crops. At many locations, it was used only once (California State University, Fresno Foundation, 1994). DBCP commonly was mixed with irrigation water that was applied in excess of the amount needed for a specific crop, which ensured that DBCP was well-distributed within the root zone. Thus, in regions where the unsaturated zone consists of predominantly coarse-grained sediments, DBCP probably was transported rapidly to ground water, with only minor losses owing to microbial transformation or volatilization (Domagalski and Dubrovsky, 1991; California State University, Fresno Foundation, 1994).

This study, a cooperative effort between the University of California at Davis and the U.S. Geological Survey (USGS), was done to evaluate the chemical and physical processes affecting concentrations of DBCP in ground water in the eastern San Joaquin Valley, California. This study is one element of the USGS National Water-Quality Assessment (NAWQA) Program ground-water studies in the San Joaquin-Tulare Basins. The NAWQA Program was designed to assess the status of and trends in the quality of the Nation's ground- and surface-water resources and to use these observations to advance our understanding of the natural and human factors that affect water quality (Gilliom and others, 1995).

Purpose and Scope

This report presents the results of a study of the transport and fate of DBCP in ground water in the eastern San Joaquin Valley, California. Many studies on DBCP have been done in this area, including studies by Peoples and others (1980), Biggar and others (1984), Zalkin and others, (1984), Cohen (1986), Schmidt (1986), and Loague and others (1998a, b). This study differs from the previous studies in that it demonstrates how the process of dispersion caused by macro-scale heterogeneity may affect DBCP concentrations in the aquifer and examines the reliability of laboratory studies in predicting the in situ behavior of chemicals.

Ground-water samples were collected during 1994–95 and analyzed for chlorofluorocarbons (CFCs) and tritium. Data from the ground-water samples, which were collected from 20 monitoring wells installed along a 4.6-km transect, were used to provide a quantitative estimate of the age of ground water in the aquifer; the data also were used to determine the rate and direction of ground-water flow in the aquifer. The estimated age of the ground-water samples was used to evaluate whether advective travel times estimated from
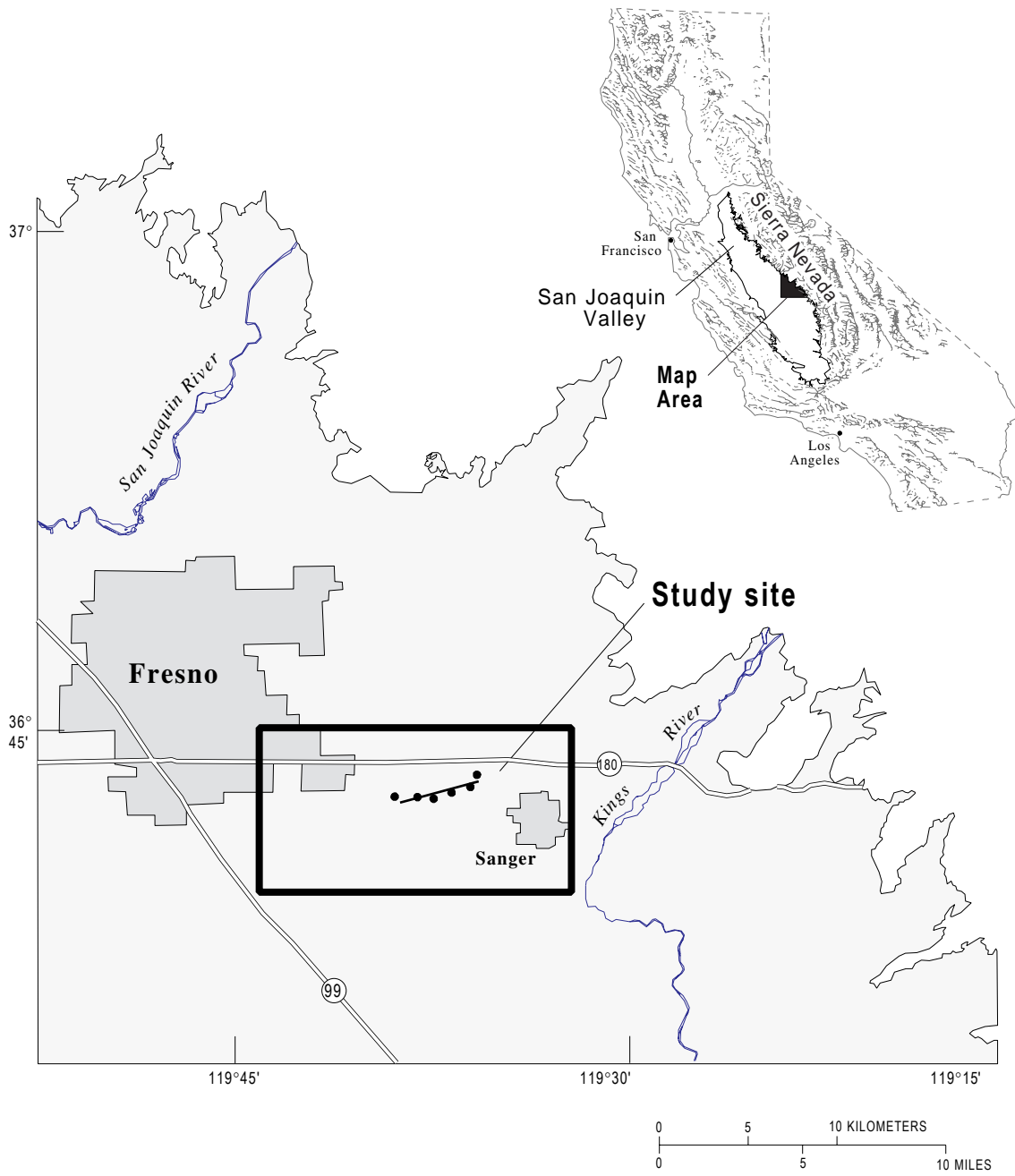
Figure 1. Location of study area, Fresno County, eastern San Joaquin Valley, California.

CFC concentrations were similar to the travel times estimated using a series of two-dimensional, steady-state flow simulations. In addition, ground-water samples were collected and analyzed for DBCP and its primary transformation product 2-bromoallyl alcohol (BAA) to provide an estimate of the in situ rate of transformation of DBCP to BAA.

Two steady-state flow solutions were used in a series of transport simulations incorporating dispersion and first-order decay. The flow and transport simulations, which represent hypothetical steady-state conditions in the aquifer, were used to refine the conceptual understanding of the aquifer system rather than to predict future concentrations of DBCP. The simulated DBCP concentrations were compared with measured DBCP concentrations in ground-water samples from the production wells near Fresno (California Department of Pesticide Regulation, 1992, 1993, 1994) to evaluate the relative extent to which DBCP concentrations in the study area were controlled by chemical transformation, dispersion caused by macro-scale heterogeneity, and in a relative sense, ground-water pumping and the reapplication of irrigation water.

Description of Study Area

The study area is west of the foothills of the Sierra Nevada and east of the San Joaquin Valley trough on the high alluvial fan of the Kings River (fig. 1). The fan encompasses about 2,500 km^2. The alluvial sediments consist of interlayered lenses of gravel, sand, silt, and clay. These sediments were derived from source materials in the Sierra Nevada that consist primarily of granitic rocks, with lesser amounts of metasedimentary and metavolcanic rocks (Page and LeBlanc, 1969; Cehrs and others, 1980). A more complete description of the alluvial sediments in the study area is given in Burow and others (1997).

The principal aquifer in the study area is unconfined. Locally, water-bearing layers of sand and gravel are confined by extensive clay layers, but at the regional scale, the sand layers are interconnected (Page and LeBlanc, 1969). Regional movement of ground water is southwest, toward the axis of the San Joaquin Valley. Locally, ground water is drawn toward Fresno because of extensive pumping by municipal drinking-water suppliers. Ground water is recharged by subsurface inflows from adjacent areas; by natural recharge from precipitation, rivers, and streams; and by artificial recharge from canal seepage and infiltration of excess irrigation water. Pumping is the primary mechanism of ground-water withdrawal in the study area, although some ground water flows downgradient to adjacent areas or discharges into the San Joaquin and Kings Rivers (Muir, 1977).

Ground water in the study area has low to moderate dissolved-solids concentrations, commonly less than 500 mg/L (Bertoldi and others, 1991). The dominant anion is bicarbonate, with lesser amounts of chloride and sulfate. Among the major cations, concentrations typically are higher for calcium and sodium than for magnesium. The major-ion ratios for ground water in the study area resemble the major-ion ratios in surface water that drains the Sierra Nevada and recharges the ground-water system (Davis and others, 1959).

Agriculture is the predominant land use in the eastern San Joaquin Valley. Vineyards cover nearly 900 km^2 in Fresno County (California Department of Water Resources, 1971). Urban areas, such as Fresno, with a population that exceeds 450,000 (U.S. Department of Commerce, 1990), rely almost exclusively on ground water for their water supply. In 1985, ground-water withdrawals in Fresno County, which include the city of Fresno and surrounding agricultural areas, accounted for about 47 percent of the total water use (Fred Stumpf, California Department of Water Resources, written commun., 1988).

Ground-water development in Fresno County began in about 1880. Ground-water withdrawals increased slowly until the 1940's and 1950's when ground-water pumping for irrigation increased sharply (Bertoldi and others, 1991). Beginning in the early 1950's, water from the San Joaquin River was diverted into the Friant-Kern Canal below Millerton Lake, and the Pine Flat Dam was completed on the Kings River (Gronberg and others, 1998). A local network of canals distribute surface water from the Friant-Kern Canal to farms in the study area. The relative proportion of surface water and ground water used for irrigation varies spatially and temporally. Fields adjacent to the irrigation canals likely receive more surface water than fields at greater distances. During wet years, surface-water supplies may be available for the duration of the irrigation season, but during dry years, many farms rely solely on ground water for irrigation.

Chemical and Physical Processes Affecting DBCP Concentrations

Several of the chemical and physical properties of DBCP facilitate its transport to ground water and its continued presence in the aquifer near Fresno. DBCP has a relatively low vapor pressure, 0.8 torr at 21^oC, and a moderate water solubility, 700 to 1,230 mg/L at 20^oC (Burlinson and others, 1982; U.S. Environmental Protection Agency, 1985). Near Fresno, DBCP is weakly sorbed (K_D=0.06 and 0.07 L/kg) owing to the predominantly low organic content of soils in this area (Deeley and others, 1991). Laboratory experiments by Castro and Belser (1968) indicate that DBCP could undergo biological transformation in soils, but DBCP is resistant to biological transformation in well-oxygenated ground water, such as the ground water in the Fresno area (Bloom and Alexander, 1990). One of the potentially significant processes that can affect DBCP concentrations in the aquifer is chemical transformation (fig. 2). During laboratory studies, Burlinson and others (1982) determined that DBCP is transformed primarily by dehydrohalogenation to the intermediate products 2-bromo-3-chloropropene (BCP) and 2,3-dibromopropene (DBP), both of which can then undergo hydrolysis to the stable end product BAA. Because transformation of DBCP is slow under environmental conditions, the experiments of Burlinson and others (1982) were done using temperatures of 40 to 100^oC. Using the Arrhenius plots from these experiments, Burlinson and others (1982) estimated that the half-life for DBCP to BAA is 38 years (pH 7, 25^oC) to 141 years (pH 7, 15^oC). Deeley and others (1991) observed the same primary transformation pathway using DBCP added to a phosphate-buffered aqueous solution, but the temperatures at which their experiments were done (21 to 72^oC) were lower than those used by Burlinson and others (1982). Deeley and others (1991) concluded that, at temperatures ranging from 42 to 72^oC, their
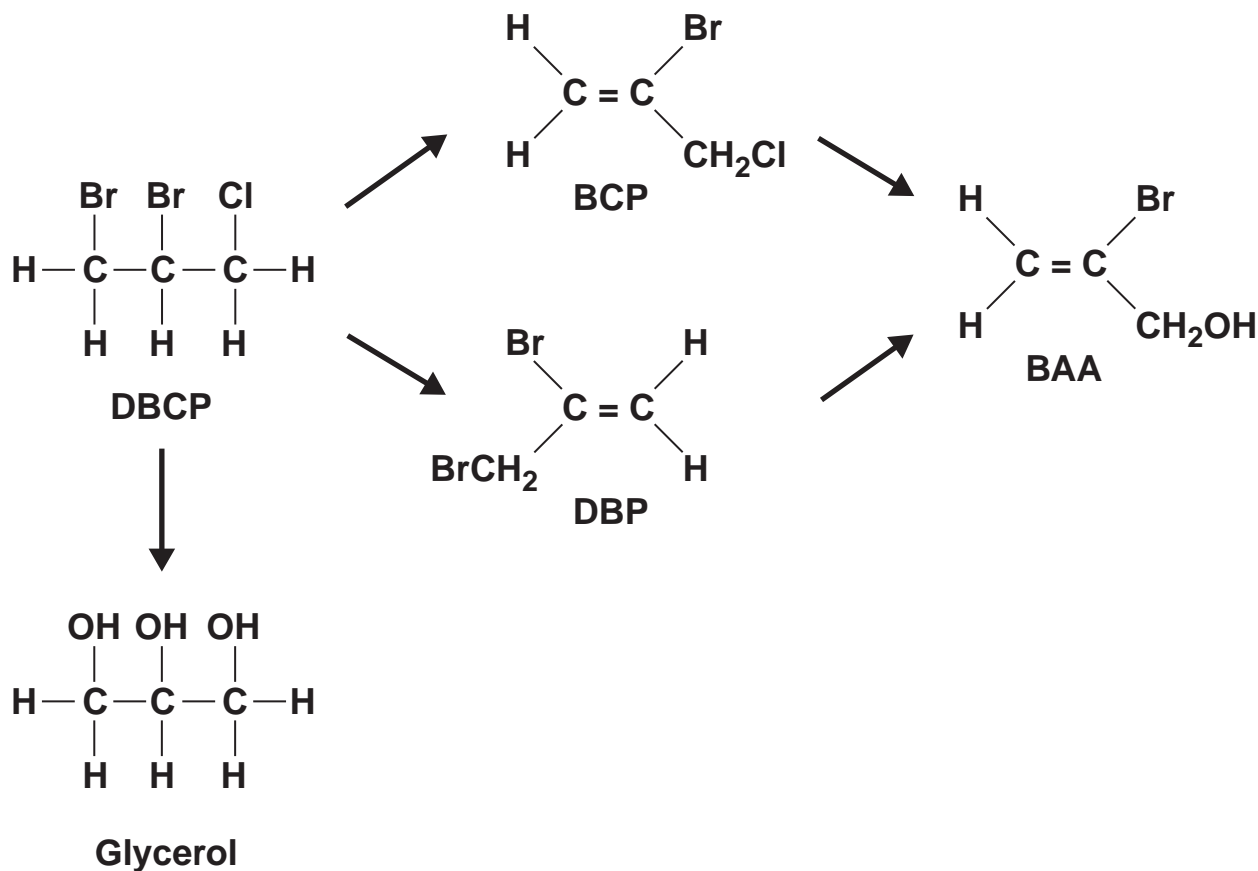
Figure 2. Dominant reaction pathways expected in the aquifer near Fresno in the eastern San Joaquin Valley, California.

results were similar to those of Burlinson and others (1982), but at temperatures less than about 42°C, their results deviate from the linear Arrhenius plot of Burlinson and others (1982). This deviation may indicate a different transformation pathway at temperatures less than about 42°C. During laboratory experiments using Fresno ground water and slurries of ground water and aquifer solids as the reaction matrix, Deeley and others (1991) estimated a half-life for the DBCP to BAA reaction of 6.1 years for conditions similar to those in the aquifer (pH 7.8, 21.1°C). As a result of their experiments using Fresno aquifer materials, Deeley and others (1991) suggest that there is some uncertainty in the significance of the DBCP to BAA reaction pathway. During their experiments, dehydrohalogenation predominated in the phosphate-buffered solution, whereas hydrolysis seemed to predominate in the experiments using the slurries of ground water and aquifer solids. Glycerol concentrations in the slurries of ground water and aquifer solids (calculated on the basis of bromide-ion concentrations) accounted for about 50 percent of the initial mass of added DBCP, indicating that DBCP hydrolysis to glycerol may be a significant reaction pathway in the aquifer. Concentrations of glycerol cannot be measured because it cannot be extracted from solution. Deeley and others (1991) also observed that, in contrast with the phosphate-buffered solutions, BCP accumulated to higher concentrations in the slurries of ground water and aquifer solids than in the phosphate-buffered solutions, and BAA was detected only at trace levels, suggesting that the reaction half-life for DBCP to BAA in conditions similar to conditions in the aquifer may be longer than expected. As discussed by Deeley and others (1991), additional data are needed to fully evaluate the implications of these results.

Physical processes that can affect DBCP concentrations in the aquifer near Fresno include dispersion and processes related to ground-water pumping and reapplication of irrigation water. Mechanical dispersion, caused by spatial variability in hydraulic conductivity, can have a significant effect on the concentrations and the rate of movement of solutes in the aquifer (Sudicky, 1986; U.S. Environmental Protection Agency, 1989; Fogg, 1990). Ground-water velocity may vary more than several orders of magnitude resulting in the complex spreading and mixing of ground water with different DBCP concentrations. Molecular diffusion also can result in the spreading and mixing of DBCP in the aquifer. Solute spreading owing to molecular diffusion, however, is small relative to mechanical dispersion in advection-dominated ground-water systems, such as the aquifer system in the Fresno area.

The process of ground-water pumping and reapplication of irrigation water can reduce DBCP concentrations in the aquifer by mixing recharged surface water (water with no DBCP) with DBCP-contaminated ground water. DBCP concentrations also could be reduced during this process by volatilization, photolysis, or microbial transformation in the root zone (Bloom and Alexander, 1990; Halmann and others, 1992; Litton and Guymon, 1993).

Acknowledgments

WELL NETWORK AND GROUND-WATER SAMPLING METHODS

Monitoring Well Network

To characterize changes in water quality along approximate ground-water flow paths, 20 monitoring wells were installed at six cluster well sites along a 4.6-km transect in 1994–95 (fig. 3). The monitoring well transect generally was aligned in the direction of regional ground-water movement in the study area. Well depths at the sites range from 21.3 to 81.7 m below land surface (table 1). Mud-rotary and hollow-

stem auger drilling methods were used to install 5.1-cm (2 in.) and 10.2-cm (4 in.) diameter wells constructed with polyvinyl chloride (PVC) casing. The length of the screened interval of each well is 1.5 m (5 ft). A more detailed description of well drilling and installation is given in Burow and others (1997).

Water-Quality Data Collection and Analysis

Ground-water samples were collected from the 20 monitoring wells during 1994–95 and analyzed for DBCP, the DBCP transformation products BAA and DBP, and various other constituents, including nitrate and stable isotopes (Willie Kinsey, U.S. Geological Survey, written commun., 1998). In this report, concentrations of nitrate plus nitrite are referred to as nitrate because nitrite was not detected in any of the ground-water samples collected during this study; the detection limit of nitrite is 0.01 mg/L. Ground-water samples also were analyzed for CFC and tritium concentrations to determine the age of the ground water sampled from the monitoring wells.
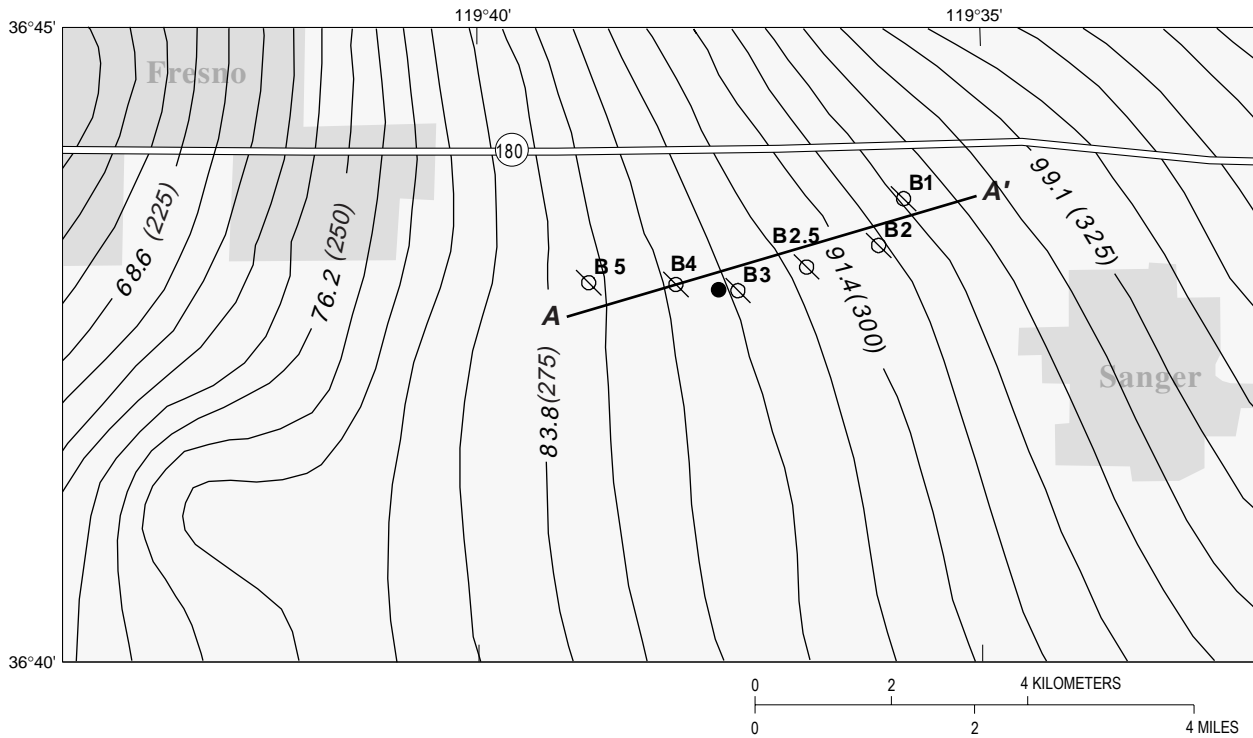
EXPLANATION

——— *68.6 (225)* ——— Line of equal ground-water elevation (1993), in meters (feet in parentheses)

A ——————— *A'* Monitoring well transect (section shown in figure 4)

⌀ **B1** Cluster well site and number

● Irrigation well 14S/22E-18E4

Figure 3. Cluster well sites along the monitoring well transect near Fresno in the eastern San Joaquin Valley, California. Wells are aligned nearly parallel to the regional ground-water gradient (from Fresno Irrigation District, 1993).

Ground-water samples were collected using protocols developed by the NAWQA Program to minimize contamination and to promote the collection of high-quality, consistent ground-water data among NAWQA study units (major hydrologic systems that are the focus of NAWQA studies) throughout the Nation (Koterba and others, 1995). Ground-water samples for all analytes except CFCs were collected using a submersible impeller pump. The sample collection lines were made of polytetrafluoroethylene, or PTFE (Teflon), to minimize cross-contamination between successive sampling locations. Sample collection and preservation chambers were used to reduce contamination from airborne contaminants. Before a sample was collected, each well was purged until readings of pH, dissolved-oxygen concentration, specific conductance, redox potential, turbidity, and temperature became stable (as defined in Koterba and others, 1995). Generally, at least three casing volumes of water were extracted to ensure that the sample was from ground water in the aquifer and not from water stored in the well. The protocols used for sample

collection, processing, storage, and shipment minimized changes in water chemistry until the sample could be analyzed in the laboratory.

Analyses of DBCP and nitrate were completed at the USGS National Water Quality Laboratory (NWQL) in Arvada, Colorado. DBCP samples were collected by filling 40-mL vials with unfiltered water and sealing them with PTFE-lined lids designed to minimize loss owing to volatilization. The DBCP samples were analyzed by liquid/liquid extraction followed by gas chromatography/electron-capture detection (GC/ECD) (Fishman, 1993). Nitrate samples were filtered using a 0.45-µm pleated capsule filter and analyzed using standard methods of analysis (Fishman and Friedman, 1985).

The DBCP transformation products, BAA and DBP, were analyzed at the USGS California District laboratory in Sacramento, California, using liquid/liquid extraction followed by gas chromatography/mass spectrometry (Panshin, 1997). The primary intermediate product, BCP, was not analyzed because a BCP analytical standard was unavailable at the time of

Table 1. Construction characteristics of wells along the monitoring well transect near Fresno in the eastern San Joaquin Valley, California

[State well No.: See well-numbering diagram on p. VIII. Well depth and depth of screened interval are in meters below land surface. Midpoint of screened interval is in meters above sea level]

Well	State well No.	Well depth	Screened interval	Midpoint of screened interval
B1-1	14S/22E-8K3	24.7	21.6–23.2	85.2
B1-2	14S/22E-8K2	51.2	48.2–49.8	58.7
B1-3	14S/22E-8K1	81.7	78.6–80.2	28.2
B2-1	14S/22E-17C1	24.7	21.6–23.2	84.3
B2-2	14S/22E-17C3	27.4	24.4–26.0	81.8
B2-3	14S/22E-17C2	41.2	38.1–39.7	68.1
B2.5-1	14S/22E-18A2	42.7	39.6–41.2	64.2
B2.5-2	14S/22E-18A1	54.0	50.9–52.5	52.9
B3-1	14S/22E-18E3	21.3	18.3–19.9	85.2
B3-2	14S/22E-18E5	34.4	31.4–33.0	72.1
B3-3	14S/22E-18E2	52.4	49.4–51.0	54.1
B3-4	14S/22E-18E6	60.1	57.0–58.6	46.5
B3-5	14S/22E-18E1	80.8	77.7–79.3	25.8
B4-1	14S/21E-13G1	23.8	20.7–22.3	81.2
B4-2	14S/21E-13G4	35.1	32.0–33.6	70.0
B4-3	14S/21E-13G3	56.1	53.0–54.6	48.9
B4-4	14S/21E-13G2	79.6	76.5–78.1	25.4
B5-1	14S/21E-14H3	24.4	21.3–22.9	78.2
B5-2	14S/21E-14H2	48.2	45.1–46.7	54.4
B5-3	14S/21E-14H4	81.7	78.6–80.2	20.9

this study thus precluding documentation of the suitability of the analytical method for measurement of this compound.

Unfiltered, 1-L samples were collected for tritium analysis. The samples were analyzed at the University of Miami Tritium Laboratory using electrolytic enrichment followed by gas counting (Ann Mullin, U.S. Geological Survey, written commun., 1996). Unfiltered, 125-mL samples were collected for the analysis of oxygen and hydrogen isotopes and analyzed at the USGS isotope laboratory in Reston, Virginia, using hydrogen equilibration (Coplen and others, 1991).

As previously mentioned, the ground-water samples for the analytes were collected using the submersible impeller pump. Following collection of these samples a submersible, positive-displacement piston pump with 0.6-cm diameter aluminum tubing was used to collect the samples for analysis of CFC concentrations using methods described by Busenberg and Plummer (1992). The ground-water samples for CFC analysis were collected in 62-mL borosilicate glass ampules that were flushed with ultrapure nitrogen gas and then with native ground water prior to sealing the ampule with a torch fueled with oxygen-methyl acetylene propadiene stabilized gas (MAPP). The samples were analyzed for CFC-12 (dichlorodifluoromethane, CCl_2F_2), CFC-11 (trichlorofluoromethane, CCl_3F), and CFC-113 (trichlorotrifluoroethane, $C_2Cl_3F_3$) by the USGS laboratory in Reston, Virginia, using a purge-and-trap GC/ECD procedure (Busenberg and Plummer, 1992).

Quality-Control Data

Quality-control (QC) samples were collected to evaluate bias and variability while obtaining environmental data. The QC-sample results were aggregated from this study and from two other NAWQA ground-water studies completed in the San Joaquin Valley during the same time period (Burow and others, 1998a, b; Willie Kinsey, U.S. Geological Survey, written commun., 1998). The aggregated QC results provide a more representative measure of bias and variability than do the results from this study alone. The QC samples collected for this study were from monitoring wells, but the QC samples collected for the other two studies were from both domestic and monitoring wells. The QC samples for all three studies

were collected, preserved, and analyzed using the same methods and equipment used to collect the corresponding environmental ground-water samples.

Duplicate ground-water samples were collected to assess the combined effects of field and laboratory procedures on measurement variability. The duplicate samples were collected sequentially. Blank water samples (hereinafter referred to as blanks) were collected to estimate bias. The blanks were obtained by processing, preserving, and analyzing blank solution water (water that is free of the analytes of interest) using the same methods that were used for the environmental samples. Two types of blanks were collected and analyzed for this study: equipment blanks and field blanks. Equipment blanks were collected prior to each sampling season to determine whether the sampling equipment could be a source of contamination to the environmental samples. Field blanks were collected immediately following the collection of the environmental samples. The field blanks were used to determine whether the field-cleaning procedure following each sample collection was adequate for preventing cross-contamination between wells and to determine whether the sample was exposed to atmospheric contamination during sampling.

Twelve pairs of duplicate ground-water samples were analyzed for nitrate (dissolved nitrate plus nitrite, expressed as elemental nitrogen) (Willie Kinsey, U.S. Geological Survey, written commun., 1998). Concentrations were identical in 8 of the 12 duplicate samples, within 0.3 mg/L in 3 of the duplicate samples, and within 1 mg/L in 1 pair of samples. The mean relative percent deviation for all 12 samples was 1.1 percent. The maximum relative percent deviation was 7.4 percent. The small relative percent deviation indicates a high degree of precision in the collection, the processing, and the analysis of the nitrate samples.

Two equipment blanks were analyzed for DBCP—one blank in 1994 and one blank in 1995. DBCP was not detected in either of the blanks. Nineteen field blanks were collected and analyzed for DBCP: 12 blanks were collected at domestic well sites and 7 blanks were collected at monitoring well sites. DBCP was not detected in any of the 19 blanks, indicating that the method of sample collection and the cleaning procedures were successful in prohibiting environmental sample contamination or carry-over for these compounds.

Replicate samples were collected for analysis of CFCs. Five sequential samples were collected from each well because the ampules containing the samples frequently are broken during shipment to the laboratory. Generally, 3 of the 5 samples were analyzed to evaluate the variability in CFC concentrations. One blank collected in 1994 for CFC analysis was from a well that was known to contain old (pre-1945) ground water; the age of the pre-1945 water was determined from tritium and radiocarbon age dates (Bill Gilmour, Altamont Landfill, written commun., 1994). The CFC concentrations in this blank were consistent with the expected concentrations in the pre-1945 water, indicating that the equipment and the sampling method used for this study were reliable and did not cause any significant contamination to the ground-water samples owing to current levels of CFCs in the atmosphere.

HYDROLOGIC AND CHEMICAL CHARACTERIZATION

Hydrologic Data

Regional ground-water flow in the study area is predominantly horizontal (Muir, 1977). On the basis of the hydraulic head measured during November 1995 (fig. 4), the horizontal hydraulic gradient along the monitoring well transect is about 0.002. Local vertical hydraulic gradients in the transect ranged from 0.0003 (between wells B1-2 and B1-3) to 0.1 (between wells B2-1 and B2-2). The spatial variability in the vertical gradients may be caused by local confining clay layers or by hydraulic stresses, such as the pumping of nearby large-volume irrigation wells. For most of the sites, however, there was little change in the magnitude or direction of the vertical gradients between the irrigation season and the nonirrigation season. Site B3 had the largest difference in vertical gradients between the irrigation season (0.08 between wells B3-1 and B3-2) and the nonirrigation season (0.001 between wells B3-1 and B3-2); this difference likely was due to the pumping of a nearby irrigation well.

An aquifer test was done for this study in December 1994. An irrigation well (14S/22E-18E4) located about 200 m west of cluster site B3 (fig. 3) was pumped continuously for about 48 hours at an average pumping rate of 37.8 L/s (600 gpm). Information on the depth and the screened interval of the irrigation well was unavailable, but the well likely draws water from a depth of about 30 to 60 m below land surface, which approximately corresponds to the middle- to lower-parts of the aquifer represented by the monitoring well transect. The estimate of the depth and screened interval of the irrigation well is based on personal communication with the landowner and on the median depth to the top of the screened interval of other wells in the area. Water levels were measured in the irrigation well during pumping and in monitoring wells B3-1, B3-3, B3-5, and B4-1. The water levels in wells B3-1 and B4-1 did not respond during pumping of the irrigation well, indicating that the shallow zone is not hydraulically connected to the zone penetrated by the well at the spatial and the temporal scales of the aquifer pumping test. Water levels in wells B3-3 and B3-5, however, did respond during pumping of the irrigation well. The water level in well B3-3 responded first, about 15 minutes after the start of pumping, whereas the water level in well B3-5 responded about 30 minutes after the start of pumping. Sediment textural data collected during drilling at site B3 (Burow and others, 1997) indicate that it is likely that the pumped irrigation well was drawing a greater proportion of flow from the zone between 30 and 60 m below land surface. In general, the sediments at depths of 30 to 60 m below land surface consist of coarse sands and gravel and the sediments at depths of 60 to 80 m below land surface consist of fine sands, silt, and clay.

Transmissivity values were calculated based on drawdown measured in the pumping well and in monitoring wells B3-3 and B3-5. On the basis of the drawdown in the pumping well, a transmissivity of about 0.011 m^2/s (0.12 ft^2/s) was calculated using methods of Theis (1935), Cooper and Jacob (1946), and Walton (1962). On the basis of drawdown data for wells B3-3 and B3-5 analyzed using the leaky aquifer theory of Walton (1962), estimates of transmissivity were 0.0033 m^2/s (0.036 ft^2/s) and 0.0011 m^2/s (0.012 ft^2/s), respectively. These estimates generally are within one order of magnitude of transmissivity estimates calculated during previous studies done within the Kings River alluvial fan. Transmissivity estimates obtained from aquifer test results from previous studies for wells screened at depths as much as 80 m near the monitoring well transect ranged from 0.0075 m^2/s (0.08 ft^2/s) to 0.023 m^2/s (0.25 ft^2/s) (Nolte, 1957; Page and LeBlanc, 1969; California State University, Fresno Foundation, 1994). A similarity in

hydraulic properties of sediments throughout the study area can be expected because the aquifer sediments in this area were deposited by similar sedimentary processes. Slug-test data were collected for monitoring wells B1-1, B1-2, B1-3, B2-1, B3-1, B3-3, B3-5, B4-1, B5-1, and B5-2. Slug-test data could not be collected in well B5-3 because this well is screened in low-permeability sediments and because the water level in this well did not recover for months after attempts to develop and sample the well. Estimated transmissivities ranged from about 0.0011 m^2/s (0.012 ft^2/s) to 0.0032 m^2/s (0.034 ft^2/s) for wells screened in the most
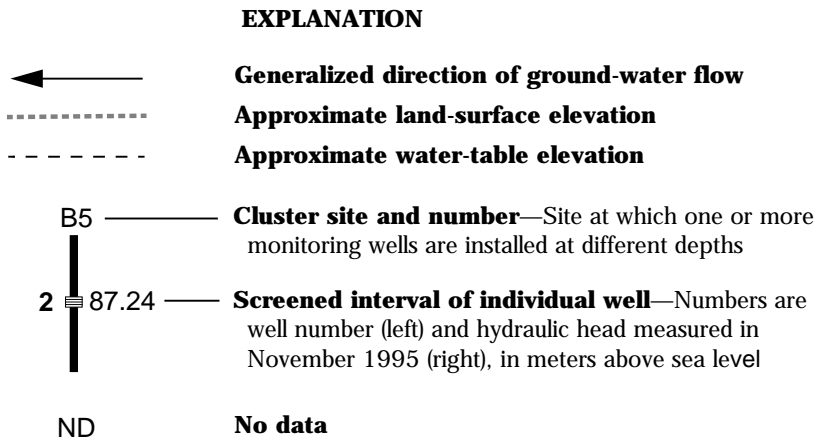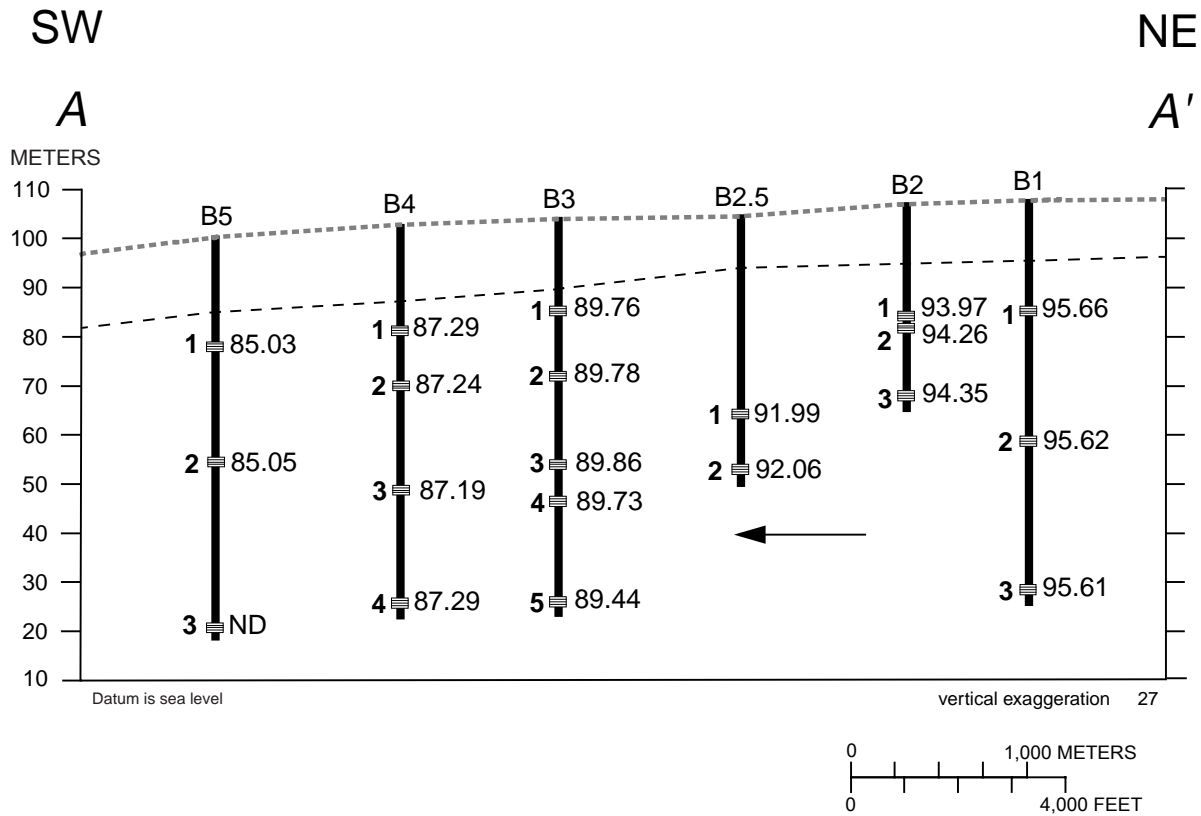
Figure 4. Hydraulic head measured in wells along the monitoring well transect near Fresno in the eastern San Joaquin Valley, California, November 1995.

transmissive zones (B1-3, B2-1, B3-1, and B4-1). Estimated transmissivities ranged from about 7.6×10^{-6} m^2/s (8.2×10^{-5} ft^2/s) to 0.00055 m^2/s (0.006 ft^2/s) for wells screened in the least transmissive zones (B1-1, B1-2, B3-3, B3-5, B5-1, and B5-2). These estimates were calculated using the methods of Cooper and others (1967), Papadopulos and others (1973), and Bouwer and Rice (1976).

Hydraulic conductivity estimates were assigned to each of four hydrogeologic facies categories identified by Burow and others (1997) for numerical modeling during this current study. Hydrogeologic facies are distinct lithologic units that were deposited by similar depositional processes and that have similar hydraulic properties. The four categories identified by the hydrogeologic characterization are, in decreasing order of hydraulic conductivity, gravel, coarse sand or gravel, fine sand, and silt and clay. The hydraulic conductivity of the gravel was estimated from literature values. The hydraulic conductivity of the coarse sand or gravel was determined from transmissivity estimates of the aquifer test analysis (and from previous studies) because this facies is the most abundant water-bearing unit in the monitoring well transect and was assumed to be the principal

contributing unit during the aquifer pumping test. An average hydraulic conductivity calculated from the slug-test data for wells B1-1, B1-2, B3-3, B3-5, and B5-1 was used for the fine sand category (table 2) because these wells are screened in less transmissive sediments than the wells represented in the aquifer pumping test. The hydraulic conductivity for the silt and clay category was estimated from the slug-test data for well B5-2 and from literature values. A more detailed description of the parameters used in the flow model is presented later in this report.

Chemical Data

DBCP, Nitrate, and Specific Conductance

DBCP was detected in at least one ground-water sample from 13 of the 20 wells (65 percent) monitored for this study. Concentrations ranged from less than 0.03 to 6.4 µg/L (table 3), with concentrations greater than the MCL of 0.2 µg/L in samples from 11 of the 13 wells with detections of DBCP; none of these wells, however, are used for drinking-water supply. DBCP concentrations in wells for which more than one ground-water sample was analyzed showed a moderate degree of temporal variability (generally within a factor of two). The variability in concentrations may have been caused by temporal changes in DBCP concentrations in the ground water or by variability in the analytical recovery of DBCP. Because QC data on measurement bias and variability of DBCP were not available and because only 1 to 3 samples were collected from each well for DBCP analysis, the cause of the variability in DBCP concentrations could not be determined.

DBCP was not detected in any ground-water samples from the deep wells (depths greater than 70 m below land surface) (table 1, fig. 5). Concentrations in the shallow wells (depths less than 30 m below land surface), however, were variable ranging from less than 0.03 to 3.0 µg/L. Concentrations in the intermediate depth wells (between 30 and 70 m below land surface) generally were high, with concentrations exceeding the MCL in samples from 7 of 10 wells. The highest concentration of DBCP, 6.4 µg/L, occurred in a ground-water sample from well B2-3, which is screened at an intermediate depth (tables 1 and 3). These patterns of DBCP concentrations generally are consistent with the history of DBCP applications in the study area. The

Table 2. Estimates of hydraulic conductivity derived from the analysis of slug-test data from wells along the monitoring well transect near Fresno in the eastern San Joaquin Valley, California

[Hydrogeologic facies categories are defined in Burow and others, 1997]

Well	Hydraulic conductivity, in meters per second	Hydrogeologic facies category
B1-1	2.6×10^{-5}	Category 3: fine sand
B1-2	5.6×10^{-6}	Category 3: fine sand
B1-3	4.5×10^{-5}	Category 2: coarse sand or gravel
B2-1	9.1×10^{-5}	Category 2: coarse sand or gravel
B3-1	7.6×10^{-5}	Category 2: coarse sand or gravel
B3-3	7.1×10^{-6}	Category 3: fine sand
B3-5	2.5×10^{-6}	Category 3: fine sand
B4-1	1.2×10^{-4}	Category 2: coarse sand or gravel
B5-1	3.2×10^{-5}	Category 3: fine sand
B5-2	1.9×10^{-7}	Category 4: silt and clay

Table 3. Ground-water quality data from wells along the monitoring well transect near Fresno in the eastern San Joaquin Valley, California

[Nitrate concentrations are dissolved nitrate plus nitrite, as nitrogen. DBCP, 1,2-dibromo-3-chloropropane; BAA, 2-bromoallyl alcohol; DBP, 2,3-dibromopropene. $\delta^{18}O$ is stable isotopic ratio of oxygen-18 to oxygen-16; δD is stable isotopic ratio of deuterium to protium. µS/cm, microsiemens per centimeter at 25°C; °C, degree Celsius; mg/L, milligrams per liter; µg/L, micrograms per liter. per mil, parts per thousand. <, actual value is less than value shown; —, no data]

Well	Date sampled	pH	Specific conductance (µS/cm)	Oxygen, dissolved (mg/L)	DBCP (µg/L)	BAA (µg/L)	DBP (µg/L)	Nitrate, dissolved (mg/L, as N)	$\delta^{18}O$ (per mil)	δD (per mil)
B1-1	06/17/94	7.3	710	4.2	2.6	<0.03	—	7.9	-11.5	-86.5
	04/11/95	7.3	735	7.2	3.2	—	—	9.3	—	—
	08/24/95	—	741	—	2.2	—	—	—	—	—
B1-2	08/30/94	7.4	336	6.3	.26	<.03	—	2.2	-9.03	-69.1
	04/11/95	7.6	340	6.5	.32	—	—	2.4	—	—
B1-3	08/30/94	7.4	329	3.7	<.03	<.03	—	1.4	-8.60	-66.6
	04/11/95	7.6	322	3.8	<.03	—	—	1.4	—	—
B2-1	08/04/94	6.8	748	4.7	2.8	<.03	—	12	-12.0	-87.4
	04/12/95	6.4	709	5.6	2.3	—	—	12	—	—
	08/24/95	—	694	—	2.8	—	—	—	—	—
B2-2	08/23/95	7.0	791	8.1	3.0	<.03	<0.01	14	—	—
B2-3	08/23/95	7.4	719	6.6	6.4	<.03	<.01	11	—	—
B2.5-1	08/22/95	7.4	665	3.8	<.03	<.03	<.01	1.9	—	—
B2.5-2	08/22/95	7.6	437	7.5	.86	<.03	<.01	3.3	—	—
B3-1	06/16/94	6.6	749	3.6	<.03	<.03	—	5.9	-10.7	-80.7
	03/07/95	6.5	744	5.4	<.03	—	—	6.7	—	—
	08/24/95	—	809	—	.06	—	—	—	—	—
B3-2	08/09/95	7.0	1,030	3.6	.30	<.03	<.01	11	—	—
B3-3	08/03/94	7.3	744	3.7	<.03	<.03	—	5.1	-10.6	-80.3
	03/07/95	7.1	728	6.8	.05	—	—	5.1	—	—
B3-4	08/09/95	7.6	462	6.2	.46	<.03	<.01	2.9	—	—
B3-5	08/03/94	7.6	374	4.7	<.03	<.03	—	2.3	-7.89	-62.7
	03/07/95	7.5	370	6.8	<.03	—	—	2.3	—	—
B4-1	08/04/94	6.6	767	3.6	<.03	<.03	—	6.2	-10.2	-77.3
	04/12/95	6.7	712	4.2	<.03	—	—	5.7	—	—
B4-2	08/08/95	6.9	795	5.8	<.03	<.03	<.01	6.1	—	—
B4-3	08/08/95	7.5	559	6.0	.86	<.03	<.01	4.1	—	—
B4-4	08/08/95	7.6	352	5.5	<.03	<.03	<.01	2.6	—	—
B5-1	09/01/94	6.8	1,920	5.0	1.7	<.03	—	31	-7.76	-63.1
	03/08/95	6.8	1,910	5.7	.86	—	—	31	—	—
B5-2	08/31/94	7.2	1,170	1.9	2.0	<.03	—	8.8	-8.19	-64.3
	04/10/95	7.4	1,000	3.6	1.9	—	—	7.4	—	—
B5-3	08/31/94	7.2	972	.4	<.03	<.03	—	6.2	-9.80	-74.1
	03/08/95	7.3	488	2.6	<.03	—	—	3.8	—	—

lack of DBCP in ground water from the deepest wells along the transect likely reflects water that entered the aquifer system before the use of DBCP, and the generally high DBCP concentrations in wells screened at intermediate depths likely reflect water that entered the aquifer system at the time that DBCP was widely applied. The variable concentrations in ground-water samples from the shallow wells may reflect differences in land-use management, such as the amount of DBCP applied or the time of the last application near the well, or the differences in the source of irrigation water. The variability in concentrations also may be caused by differences in sediment texture. Low-permeability soils may restrict leaching of DBCP below the root zone, allowing more time for DBCP to volatilize or undergo microbial transformation; however, DBCP movement
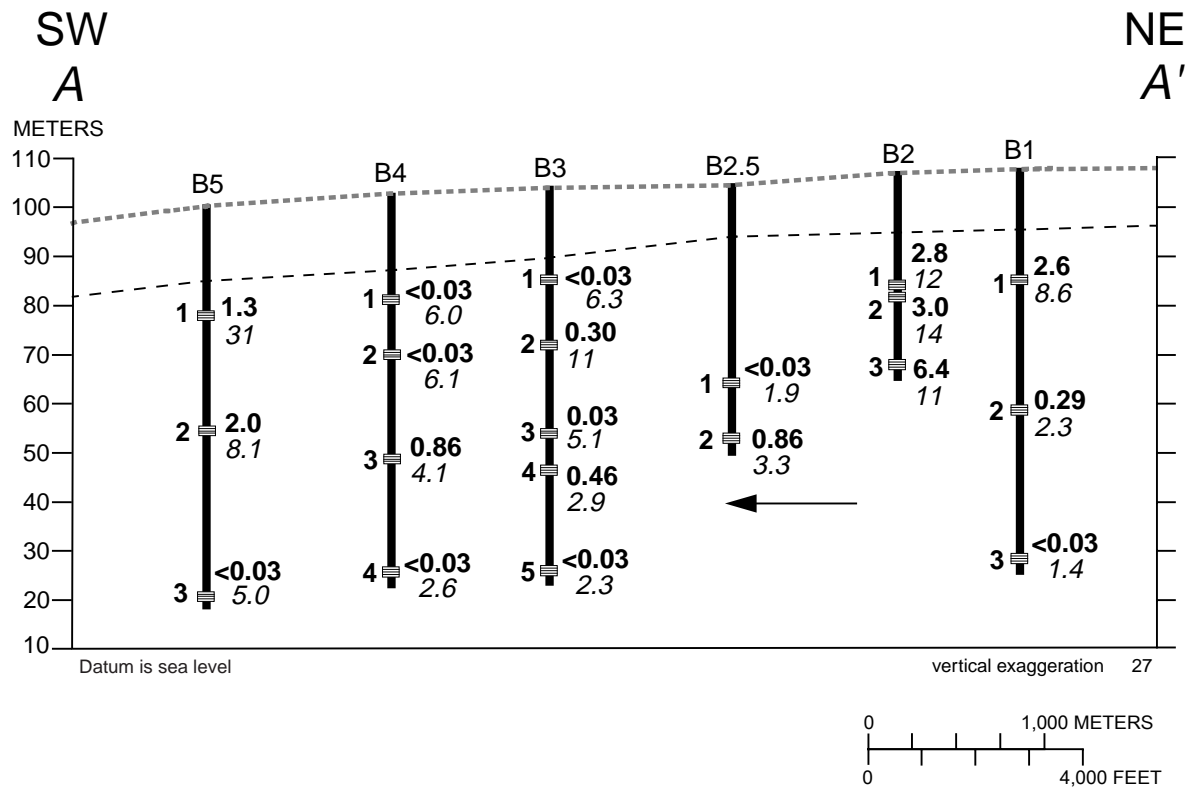
Figure 5. Concentrations of 1,2-dibromo-3-chloropropane (DBCP) and nitrate in ground-water samples from monitoring wells in the eastern San Joaquin Valley, California. Median concentrations of DBCP and nitrate are shown where more than one ground-water sample was collected (table 3).

also may be restricted in the low-permeability layers beneath the soil zone. Conversely, coarse-grained sediments may promote rapid recharge, replacing water containing DBCP with water recharged after DBCP use was discontinued.

Nitrate concentrations and specific conductance data from the monitoring wells along the transect were evaluated to provide additional information on processes that may affect DBCP concentrations in the aquifer. Because nitrate is transported conservatively in well-oxygenated ground water, the relation between nitrate and DBCP concentrations can provide insight on the transport of DBCP. In agricultural areas, nitrate concentrations are influenced by the use of nitrogen fertilizers (Nightingale, 1972; Owens and others, 1992), confined animal feeding operations, and rural septic systems. Nitrogen fertilizer use generally has increased since the 1950's (Alexander and Smith, 1990), and DBCP use increased from 1950 until it was banned in the late 1970's. Nitrogen fertilizers were applied more consistently than DBCP, and application has continued after DBCP use was banned. Specific conductance, which is related to the total ion composition of ground water, is an indicator of salinity. In the study area, increased salinity is caused, in part, by the effects of agriculture (Nightingale, 1972; Burow and others, 1998a, b).

Nitrate concentrations and specific conductance generally decreased with depth (fig. 5, table 3). Similar to the DBCP concentrations, nitrate concentrations and specific conductance were less than background levels in ground-water samples from 3 of the 4 deep wells (wells B1-3, B3-5, and B4-4), which possibly reflects the presence of relatively old ground water that had not been significantly affected by agriculture. Nitrate concentrations that were less than 1.0 to 3.0 mg/L likely represent ground water that had not been affected by human activities (Madison and Brunett, 1985; Mueller and Helsel, 1996). In this report, the background levels for nitrate concentrations in the study area are assumed to be less than 3.0 mg/L. The background levels for dissolved-solids concentrations in this ground-water system typically are less than 500 mg/L (Bertoldi and others, 1991), which is assumed to be approximately equal to a specific conductance value of 650 to 900 µS/cm (Hem, 1989). Ground-water samples from the wells at cluster sites B2 and B5 generally had the highest concentrations of DBCP, nitrate, and specific conductance (fig. 5).

Nitrate and DBCP concentrations were positively correlated (rho=0.42, p=0.002; Spearman's rank correlation; Lehmann, 1975) using data collected from the monitoring wells sampled during this study and data from another NAWQA study in the eastern San Joaquin Valley (Burow and others, 1998a), during which 20 domestic and 10 monitoring wells were sampled in a vineyard land-use setting (fig. 6). The significance level used for hypothesis testing for this report was 5 percent (α=0.05). For compounds with reported concentrations that were less than the detection limit, a concentration of one-half the minimum detection limit was used in the statistical analysis. The positive correlation between nitrate and DBCP concentrations indicates that most of the sampled ground water in the eastern San Joaquin Valley that has been affected by DBCP has also been affected by the use of nitrogen fertilizer or other sources of nitrate even though the spatial and temporal application patterns of DBCP were different from the application patterns of nitrogen fertilizer. Nitrogen fertilizer has been applied annually over broad areas for a variety of crops; DBCP, however, was applied only on selected fields of a limited variety of crops. Nitrogen fertilizers were still being applied at the time of this study (1995),

Figure 6. Concentrations of 1,2-dibromo-3-chloropropane (DBCP) and nitrate in ground-water samples from domestic and monitoring wells in the eastern San Joaquin Valley, California.

but DBCP has not been used since the late 1970's. The widespread application of DBCP, combined with the natural tendency of solute plumes to spread over wider areas in the unsaturated zone may have resulted in a widespread, diffuse source of DBCP at the water table. Areas with elevated concentrations of nitrate and no detectable DBCP may have been areas where DBCP was not applied. The co-occurrence of nitrate and DBCP may reflect the susceptibility of individual wells to contamination; susceptibility may be controlled by factors, such as sediment texture and distance from the contaminant source, that affect travel time through the subsurface (Schmidt, 1972, 1986; Teso and others, 1988; Burow and others, 1998a).

Chlorofluorocarbon and Tritium Concentrations

Chlorofluorocarbons (CFCs) are stable volatile compounds that are used as refrigerants, aerosol propellants, cleaning agents, solvents, and blowing agents in the production of foam rubber and plastics. The CFC refrigerant CFC-12 was first produced in the 1930's, followed by the production of CFC-11 in the 1940's. Atmospheric concentrations of CFCs have steadily increased since these compounds were first produced, although their use has recently been restricted because CFCs contribute to the depletion of stratospheric ozone and because of their potential to contribute to greenhouse warming. Equilibrium calculations, which combine atmospheric CFC growth curves that are based on CFC measurements and production estimates, and Henry's Law solubilities allow estimation of the expected concentrations of CFC-12 and CFC-11 in water recharged between 1940 and the 1990's (Plummer and others, 1993).

Ground-water samples from the monitoring wells were analyzed for CFC-12 and CFC-11 concentrations to estimate when the ground water in these wells was recharged. The ground-water samples also were analyzed for concentrations of CFC-113; however, recharge dates could not be interpreted from the CFC-113 concentrations because the measured concentrations were consistently higher than the concentrations expected in the ground water. Local concentrations of CFCs commonly exceed the maximum historical North American continental atmospheric concentrations, although generally by less than 10 percent except in heavily industrialized or urban areas. Measured concentrations of CFC-113 that

were more than 10 percent higher than the average global concentrations indicate that the samples likely were contaminated. Bu and Warner (1995) noted problems with CFC-113 contamination during their study; they attributed the contamination to the widespread use of CFC-113 as a manufacturing solvent. Anomalously high concentrations of CFC-12 and CFC-11 are less common and may be caused by local releases of CFCs into the air in urban areas by plastic containers, air conditioners, aerosol can propellants, and sewage effluent (Plummer and others, 1993). The calculated recharge dates for CFC-12 and CFC-11 (table 4) were determined from the lowest CFC concentrations for each of the replicate samples analyzed. Samples with the lowest concentrations were from the oldest water. The oldest recharge date for each sample was used as the calculated recharge date because of the measurement bias toward trace contamination of CFCs, which would have resulted in a calculated age of water younger than its actual age. The recharge dates were estimated assuming a recharge temperature of 17°C, which is the mean annual air temperature in the study area. The assigned recharge date (the date used to interpret the data for this report) for each well was selected from the calculated recharge dates for CFC-12 and CFC-11 (table 4). The oldest calculated CFC-12 date generally was used as the assigned recharge date because CFC-12 is more resistant to microbial transformation than CFC-11. Microbial transformation, however, probably is not a dominant process affecting CFC-11 concentrations because the aquifer sediments in the study area are low in organic content and the ground water generally is well-oxygenated. Because the measured CFC concentrations were substantially higher than the concentrations estimated using the North American atmospheric CFC growth curves, some of the samples probably were contaminated with CFC-12 or CFC-11. For the samples contaminated by CFC-12, the oldest CFC-11 recharge date was used. Using this approach to interpret the CFC data, the assigned recharge date is the date of the oldest interpretable recharge and represents the maximum travel time since the ground water was recharged.

The CFC data for wells along the monitoring well transect indicate that ground water near the water table was recharged within the past 10 years, whereas ground water at greater depths was recharged as much as 55 years before the 1994–95 sampling (table 4;

Table 4. Tritium concentrations, recharge dates, and ground-water travel times determined from chlorofluorocarbon (CFC) concentrations in ground-water samples from wells along the monitoring well transect near Fresno in the eastern San Joaquin Valley, California

[Recharge dates were assigned from the oldest estimated CFC-12 date. If CFC-12 date was not available, the oldest CFC-11 date was used. TU, tritium units; CFC, chlorofluorocarbon. <, actual value is less than value shown; —, no data]

Well	Date sampled	Tritium, dissolved (TU)	Calculated recharge date		Assigned recharge date (year)	Travel time (year)
			CFC-11 (year)	CFC-12 (year)		
B1-1	06/17/94	—	1974.5	1986	1986	8
	04/11/95	8.8	1977	1992		
	08/24/95	—	1980	([1])		
B1-2	08/30/94	<.09	([1])	1959.5	1954	41
	04/11/95	—	1956.5	1954.5		
B1-3	08/30/94	—	1978.5	1969.5	1947	48
	04/11/95	<.09	1958.5	1947.5		
B2-1	08/04/94	15.0	1981	1992	1992	2
	04/12/95	15.3	1980.5	([1])		
	08/24/95	—	1979.5	([1])		
B2-2	08/23/95	17.5	1986	1991	1991	4
B2-3	08/23/95	15.3	1973	1977	1977	18
B2.5-1	08/22/95	4.4	1964.5	1956	1956	39
B2.5-2	08/22/95	2.7	1966.5	1963	1963	32
B3-1	06/16/94	5.9	1989.5	1992	1992	3
	03/07/95	—	([1])	1993.5		
	08/24/95	—	([1])	1992		
B3-2	08/09/95	11.3	([1])	1979	1979	16
B3-3	08/03/94	2.4	1963	1961.5	1961	33
	03/07/95	—	1969	1966.5		
B3-4	08/09/95	1.0	1966	1954	1954	41
B3-5	08/03/94	<.09	1961.5	1947.5	1940	55
	03/07/95	—	1960	1940		
B4-1	08/04/94	—	1988.5	1992	1992	2
	04/12/95	6.3	([1])	([1])		
B4-2	08/08/95	6.9	([1])	([1])	—	—
B4-3	08/08/95	3.8	([1])	([1])	—	—
B4-4	08/08/95	<.09	([1])	1965.5	1965	30
B5-1	09/01/94	3.8	1982	1989.5	1989	6
	03/08/95	—	1981.5	1989		
B5-2	08/31/94	2.2	([1])	1974	1970	25
	04/10/95	—	1969	1970		
B5-3	08/31/94	4.1	—	—	—	—

[1]CFC concentrations owing to atmospheric deposition were higher than expected.

fig. 7). Ground-water age generally increases with depth because a longer time is required for ground water to move deeper in the flow system. Ground-water recharge dates are variable across the monitoring well transect, which perhaps reflects the three-dimensional heterogeneity of the flow system. Although the monitoring well transect is aligned with the approximate direction of regional ground-water flow, it is likely that locally a substantial component of the flow is perpendicular to the plane of the transect as it flows through the highest permeability sediments (water table maps are gross representations of much more complex flow systems).

Ground-water samples also were analyzed for tritium, a radioactive isotope of hydrogen, to further evaluate ground-water travel times in the study area.
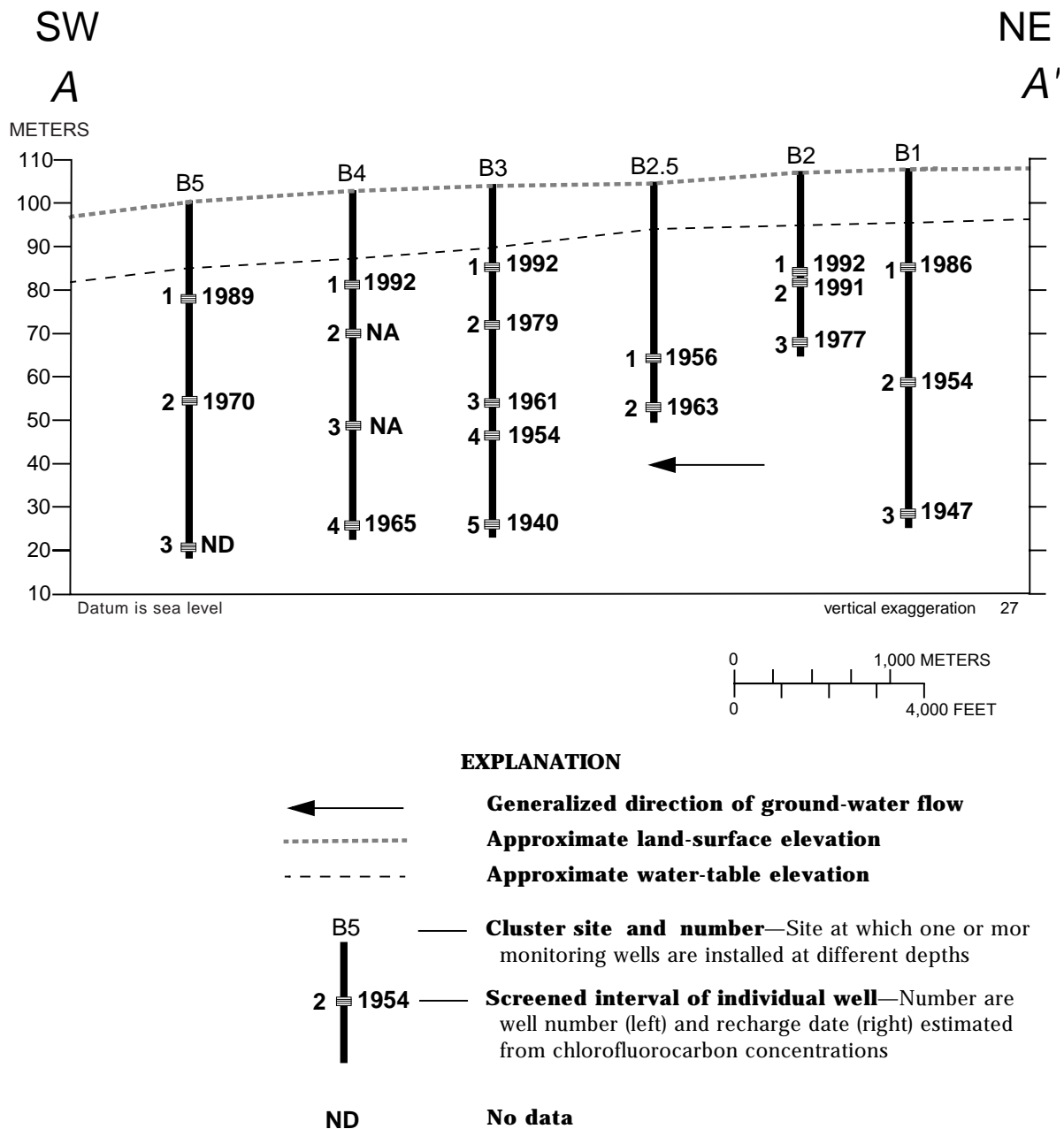
Figure 7. Estimated ground-water recharge dates determined from chlorofluorocarbon (CFC) concentrations in ground-water samples from wells along the monitoring well transect near Fresno in the eastern San Joaquin Valley, California.

Elevated concentrations of tritium were introduced to the atmosphere by large-scale atmospheric testing of thermonuclear bombs between about 1952 and 1962. Since this time, tritium has been removed from the atmosphere in precipitation and recharged to the ground-water system. Because the tritium atom (^{3}H) substitutes for the hydrogen atom (^{1}H) in the water molecule, tritium travels through the aquifer at the same rate as water. Tritium concentrations, measured in tritium units, or TU (where 1 TU represents one atom of ^{3}H for every 10^{18} atoms of ^{1}H), can be used to distinguish ground water that was recharged prior to 1952 from ground water that was recharged after 1952. Tritium undergoes radioactive decay with an estimated half-life of 12.4 years. Ground water recharged prior to 1952 is currently expected to have maximum tritium concentrations of 0.2 to 0.8 TU (Michel, 1989; Plummer and others, 1993).

Tritium concentrations in ground-water samples from the monitoring wells ranged from less than 0.09 to 17.5 TU (table 4). Tritium concentrations were less than 0.09 TU in ground-water samples from four monitoring wells (wells B1-2, B1-3, B3-5, and B4-4), indicating that the ground water sampled from these wells was recharged prior to 1952. Except for well B4-4, a pre-1952 recharge date is consistent with the recharge dates determined from the CFC concentrations for these wells. These observations are supported by a negative correlation between tritium concentrations and travel times estimated from CFC concentrations (rho=-0.78, p less than 0.001; Spearman's rank correlation). Furthermore, both nitrate concentrations and specific conductance were negatively correlated with travel time (rho=-0.80, p less than 0.001 and rho=-0.68, p=0.002, respectively; Spearman's rank correlation) and were positively correlated with tritium concentrations (rho=0.75, p less than 0.001 and rho=0.58, p=0.007, respectively; Spearman's rank correlation), indicating that the highest nitrate concentrations and specific conductance generally occurred in ground water that had recently been recharged. DBCP concentrations, however, were not significantly correlated with travel time (rho=-0.38, p=0.13; Spearman's rank correlation) and were only weakly correlated with tritium concentrations (rho= 0.45, p=0.048; Spearman's rank correlation). The lack of correlation between DBCP and ground-water age may be caused by the spatial and temporal patterns of DBCP applications or by some other process that may affect only DBCP concentrations, such as transformation or volatilization during initial application or during reapplication of DBCP-containing irrigation water.

In summary, different depth zones along the monitoring well transect can be distinguished on the basis of the ground-water chemistry data. Ground water at shallow and intermediate depths near cluster sites B1 and B2 (wells B1-1, B2-1, B2-2, and B2-3) is characterized by high DBCP, nitrate, and tritium concentrations; moderate salinity (as indicated by specific conductance); and generally short (less than 10 years) ground-water travel times. Shallow ground water near cluster sites B3 and B4 is characterized by elevated nitrate and salinity (as indicated by specific conductance) but low DBCP concentrations (wells B3-1, B3-2, B4-1, B4-2). Ground water at cluster site B5 (wells B5-1 and B5-2) is characterized by high salinity, DBCP, and nitrate concentrations. Ground water at depth along the monitoring well transect is relatively old (equal to or greater than 30 years), with low salinity and low concentrations of DBCP, nitrate, and tritium (wells B1-2, B1-3, B3-4, B3-5, and B4-4). Concentrations of DBCP, nitrate, and tritium in the shallow ground water along the transect are more variable than concentrations in the deep ground water probably because of differences in land-use practices, local ground-water pumping, heterogeneity in sediment texture, and increased mixing as solutes travel to the deeper parts of the aquifer.

EVALUATION OF DBCP INPUT AND PROCESSES AFFECTING DBCP CONCENTRATIONS

DBCP concentrations in the ground-water samples collected from the monitoring wells in 1994–95 reflect the net effect of all the processes that control the transport and fate of DBCP. Initial concentrations of DBCP were estimated using CFC recharge dates and the measured DBCP concentrations in the ground-water samples. The estimated initial concentrations of DBCP were compared to DBCP concentrations measured in ground water sampled from production wells in the study area. The processes of chemical transformation, dispersion, and ground-water pumping and reapplication of irrigation water were evaluated using the ground-water sampling data to investigate the relative importance of these three processes on concentrations of DBCP in the aquifer.

Estimation of Initial Concentrations of DBCP

Initial DBCP concentrations were estimated for each well using DBCP concentrations and corresponding CFC recharge dates. Assuming that the transformation of DBCP was a first-order process, first-order rate reaction equations were used for these calculations (Domenico and Schwartz, 1990):

$$C_o = C(t)e^{kt} \tag{1}$$

and

$$k = \frac{0.693}{t_{1/2}}, \tag{2}$$

where

C_o	is the initial DBCP concentration,
$C(t)$	is the DBCP concentration at time, t,
t	is the time since beginning of reaction,
k	is the rate constant for a first-order chemical reaction, and
$t_{1/2}$	is the half-life for the reaction.

Initial concentrations of DBCP were calculated using half-life estimates of 6.1 and 40 years for DBCP transformation (fig. 8). The 6.1-year half-life is a maximum rate of transformation; this rate was determined during laboratory studies by Deeley and others (1991). Average temperature and pH measurements from the monitoring wells along the transect were used to estimate the 40-year half-life for DBCP; this value was estimated using the Arrhenius parameters provided by Burlinson and others (1982). The resulting initial DBCP concentrations estimated using the 6.1-year half-life value show three apparent peaks of DBCP concentrations between 30 and 50 µg/L (fig. 8). The first peak occurred in the early 1950's, which is consistent with the reported date that DBCP applications began. The maximum initial concentrations estimated using a 6.1-year half-life are about 50 µg/L, which is similar to maximum concentrations in ground water sampled from production wells in the study area during the early 1980's (California Department of Pesticide

Regulation, 1992, 1993, 1994). The actual DBCP concentrations in the aquifer during the 1980's may have been higher than the concentrations measured at that time because the ground-water samples were collected from long-screened irrigation, municipal, and domestic wells in which high concentrations in the discrete zones of the aquifer may have been diluted by zones containing low concentrations. By using a longer half-life to calculate initial DBCP concentrations, the calculated maximum concentrations were lower than the concentrations estimated using a 6.1-year half-life. For example, the maximum initial concentration estimated using a half-life of 40 years is 8.7 µg/L for the peak DBCP concentration for the 1970's. The earlier peak DBCP concentration is much lower than the peak for the 1970's; the peak concentrations for the 1950's for a 40-year half-life is 0.94 µg/L. If 50 µg/L is the maximum measured concentration of DBCP in the aquifer, these data suggest that the 6.1-year half-life would be a minimum half-life for DBCP transformation because the calculated initial concentration would be higher than the 50 µg/L using a

EXPLANATION

- —△— DBCP, 6.1-year half-life
- —+— DBCP, 40-year half-life
- ⋯○⋯ Nitrate, conservative
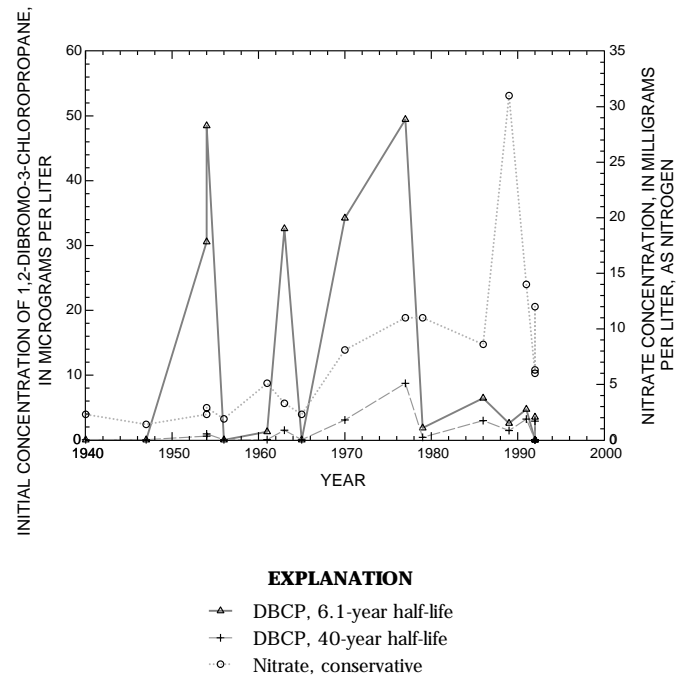
Figure 8. Initial concentrations of 1,2-dibromo-3-chloropropane (DBCP) and nitrate and recharge dates estimated from chlorofluorocarbon (CFC) concentrations in ground-water samples collected from wells along the monitoring well transect near Fresno in the eastern San Joaquin Valley, California. Initial DBCP concentrations were calculated assuming first-order transformation of DBCP.

longer half-life. It is important to note that these calculated initial concentrations may not represent temporal variations in DBCP application if the effects of spatial variations in application and heterogeneity of the flow system are significant.

In contrast to the DBCP input concentrations, estimated initial nitrate concentrations (fig. 8) indicate that the initial nitrate concentrations increased with time, assuming that nitrate is transported conservatively. The apparent temporal variability in the initial DBCP concentrations is consistent with the lack of correlation between DBCP concentrations and travel time noted previously.

Although the actual spatial and temporal variations in applications of DBCP along the transect are not known, DBCP concentrations and recharge dates estimated from CFC concentrations generally are consistent with the overall period of DBCP applications, except in the shallowest monitoring wells which had high DBCP concentrations and recharge dates after 1980. The DBCP in the ground-water samples from these wells may have derived from the leaching of DBCP from fine-grained layers, from recharge of irrigation water that was pumped from a zone containing high DBCP concentrations, or from a recent application of DBCP. Additional data are required to evaluate these mechanisms and to determine the cause of the high concentrations of DBCP in recently recharged ground water.

Chemical Transformation

Data on concentrations of DBCP transformation products can be used to test the hypotheses on the importance of chemical transformation, relative to other processes, in controlling DBCP concentrations in the aquifer. BAA, a stable end-product of DBCP transformation by dehydrohalogenation and then hydrolysis (fig. 2), was not detected in any ground-water samples from the 20 monitoring wells (table 3). DBP, a minor intermediate product of DBCP, also was not detected in any of the ground-water samples selected for analysis of this compound.

Concentrations of BAA that can be expected over time for different values of the transformation half-life are shown in figure 9; these concentrations are based on the assumptions that (1) the transformation of DBCP to BAA is a first-order process that can be described by equations 1 and 2; (2) BAA is a stable end

product; and (3) BAA is the sole product of DBCP transformation. Using a conservative estimate of 5.0 µg/L for the initial DBCP concentration, the BAA concentration after 10 years should be at least 10 times the detection limit if the half-life was less than 100 years (fig. 9). Most of the ground water with high DBCP concentrations, however, is older than 10 years, and therefore, BAA concentrations can be expected to be higher than 10 times the detection limit. The lack of detection of BAA indicates that the laboratory results from previous studies (Burlinson and others, 1982; Deeley and others, 1991) do not accurately reflect the rate of transformation of DBCP to BAA in the aquifer and that the half-life for DBCP to BAA is likely on the order of hundreds of years. The fact that BAA concentrations were less than the detection limit of 0.03 µg/L indicates that DBCP transformation to BAA is not a significant process affecting DBCP concentrations in the aquifer.
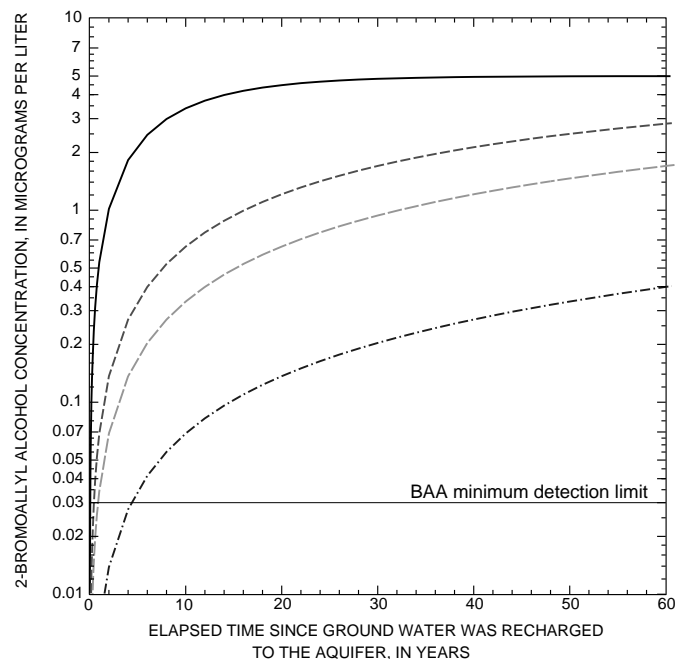
Figure 9. Hypothetical concentrations of 2-bromoallyl alcohol (BAA) for different reaction rates, assuming an initial concentration of 1,2-dibromo-3-chloropropane (DBCP) of 5.0 micrograms per liter. BAA curves were calculated assuming first-order transformation of DBCP.

Deeley and others (1991) used bromide ion concentrations to estimate concentrations of glycerol, a transformation product of DBCP resulting from hydrolysis; they suggest that hydrolysis may be more dominant than the reactions of dehydrohalogenation followed by hydrolysis for conditions similar to conditions in the aquifer. Although bromide concentrations were analyzed in ground-water samples from some of the wells along the monitoring well transect, two factors precluded using the bromide data to estimate concentrations of glycerol: (1) the date and the initial concentrations of DBCP were unknown, and (2) the bromide concentrations in the ground-water samples were at least an order of magnitude higher than the maximum measured concentrations of DBCP, indicating that bromide in the aquifer may have been from other sources. During drilling for this study, sodium-bromide was added to the drilling mud as a tracer in three of the wells sampled for bromide to ensure that the wells were developed adequately before sampling. Although the source of bromide from the sodium-bromide tracer is unique to this study, the lack of information on the initial concentrations of DBCP and other potential sources of bromide can be a problem in many areas.

In summary, the lack of detection of BAA indicates that transformation of DBCP to BAA is not a significant process affecting DBCP concentrations in the aquifer. Although BAA may readily be consumed in situ by unknown chemical or biochemical processes, laboratory studies to date indicate that BAA is a stable end-product. Estimates of initial DBCP concentrations determined using the CFC recharge dates indicate that maximum initial concentrations estimated for a half-life of 6.1 years are similar to the maximum measured concentrations of DBCP in the ground-water samples. This suggests that other processes, such as dispersion and mixing of ground water owing to ground-water pumping and reapplication of irrigation water are the dominant processes affecting DBCP concentrations in ground water.

Dispersion and Ground-Water Pumping and Reapplication of Irrigation Water

The heterogeneous distribution of sediments in the aquifer near Fresno results in large contrasts in ground-water velocity, causing dispersion of DBCP concentrations. The effects of dispersion can be reflected by the variability of DBCP concentrations as the DBCP in ground water travels along preferred pathways or by a gradual decrease in concentration long after applications have ceased. The monthly median DBCP concentrations in ground-water samples from production wells in the Fresno area (fig. 10A) (California Department of Pesticide Regulation, 1992, 1993, 1994) indicate that DBCP concentrations are variable but tend to decrease over time. The monthly DBCP concentrations in ground-water samples from well 14S/21E-3R in the Fresno area (fig. 10B) seem to decrease very gradually. The decrease in concentrations in production wells may have been caused by dispersion, although these apparent decreases in concentration over time may have been caused by spatial and temporal changes in DBCP applications.
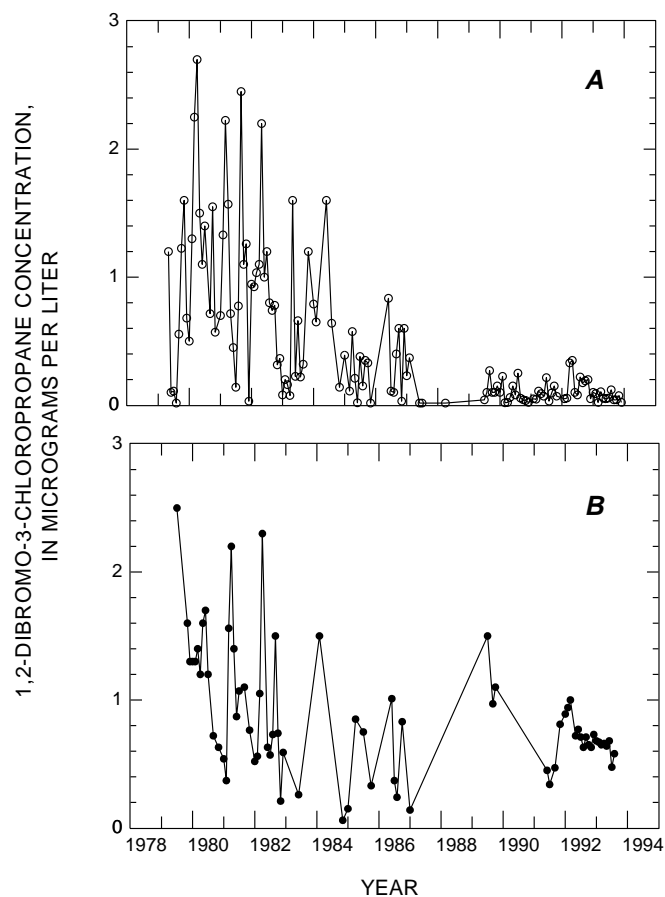
Figure 10. Concentrations of 1,2-dibromo-3-chloropropane (DBCP) in ground-water samples from production wells in the Fresno area in the eastern San Joaquin Valley, California. (California Department of Pesticide Regulation, 1992, 1993). **A,** Median DBCP concentrations in ground-water samples collected monthly. **B,** DBCP concentrations in ground-water samples from well 14S/21E-3R.

The results of the analysis of tritium concentrations and CFC recharge dates indicate that the ground water in the study area may have been pumped and reapplied as irrigation water. Although the concentrations of tritium were low in relatively old ground water and the negative correlation between tritium and ground-water travel times was statistically significant (rho=-0.78, p less than 0.001; Spearman's rank correlation), tritium concentrations in many of the ground-water samples did not correspond to the expected concentrations for tritium in precipitation recharged to ground water for the year indicated by the CFC recharge dates (fig. 11). The estimated concentration of tritium in precipitation (Michel, 1989) was corrected for tritium decay from the date that the ground water was recharged. Tritium concentrations in ground water recharged between 1961 and 1970 were lower than expected, and concentrations in ground water recharged in 1986, 1991, and 1992 were higher than expected compared with the tritium concentrations in precipitation, assuming that tritium concentrations in precipitation either have remained stable or decreased since 1983.

One possible explanation for the apparently anomalous tritium results is the process of ground-water pumping and reapplication. As ground water is pumped and reapplied at land surface for irrigation, the CFC concentrations quickly reequilibrate with the concentrations of CFCs in the atmosphere. Because the equilibration rate for tritium is relatively slow, the tritium concentrations are relatively unaffected by this process. The CFC concentrations, therefore, are representative of the most recent recharge date of the sampled ground water, whereas the tritium concentrations may represent the original recharge date prior to reapplication.

The negative correlation observed between tritium concentrations and ground-water travel time may be because three of the four wells in which no tritium was detected (B1-2, B1-3, and B3-5) are screened below the depth from where most of the irrigation water is pumped (about 25 to 50 m below land surface). The fourth well (B4-4) has a ground-water recharge date of 1965, which is inconsistent with the lack of detectable tritium and the depth of this well. Furthermore, DBCP and nitrate concentrations and specific conductance in ground water sampled from this well indicate that the water in this well is relatively old. For these reasons, the ground-water sample

collected from well B4-4 is believed to have been contaminated with CFCs.

Ground-water samples from selected wells in the monitoring well transect were analyzed for stable isotopes (table 3) to provide additional information on the source of the ground water in the aquifer near Fresno. Stable-isotopic ratios of oxygen-18 (^{18}O) relative to oxygen-16 (^{16}O) and deuterium (D or ^{2}H) relative to protium (^{1}H) are reported relative to the Vienna Standard Mean Ocean Water in delta (δ) notation as parts per thousand (per mil). Because ^{18}O and D are part of the water molecule, they are transported conservatively in ground water. Values of δ^{18}O and δD in recharge water that has infiltrated deep enough or recently enough so as not to be affected by evaporative processes can be used to help distinguish different sources of water and to infer the amount of mixing of ground-water sources. As moist marine air moves inland from the Pacific Ocean over California, the heavier stable isotopes of oxygen, ^{18}O, and hydrogen, and D, are progressively depleted in the air mass as isotopic fractionation removes disproportionate amounts of ^{18}O and D in rain and snow during condensation. Isotopic fractionation also is dependent on temperature and altitude and thus shows patterns in precipitation that are related to topography and proximity to the ocean (Coplen and
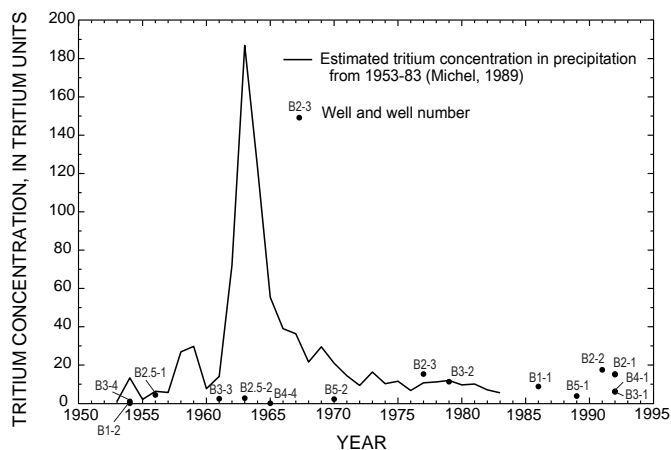
Figure 11. Tritium concentrations and recharge dates estimated from chlorofluorocarbon (CFC) concentrations in ground-water samples from wells along the monitoring well transect near Fresno in the eastern San Joaquin Valley, California. The tritium concentrations in precipitation were averaged for latitudes between 35 and 39 degrees north and longitudes 120 and 125 degrees west. Tritium concentrations and ground-water recharge dates estimated from CFC concentrations were from ground-water samples collected in 1994–95.

others, 1985; Davis and Coplen, 1989; Plummer and others, 1993). The distribution of ^{18}O and D and the processes affecting the stable-isotopic composition of precipitation, stream water, and major ground-water facies in the San Joaquin Valley have been described in detail by Davis and Coplen (1989); the study area of their investigation, however, is west of the study area in this report. Few samples were collected for this current study, and the sample data represent only a local area, but some of the isotopic trends identified by Davis and Coplen (1989) are relevant to the characterization of ground water for the local area of this study.

The δ^{18}O and δD data for the samples from the monitoring well transect (fig. 12) fall along a line that is similar to the local ground water line of Davis and Coplen (1989) (the data deviate slightly from the local line), which suggests that the stable-isotope ratios have not noticeably been affected by evaporation. The δ^{18}O data from the ground-water samples from wells B1-1, B2-1, B3-1, B3-3, B4-1, and B5-3, which for the most part are shallow wells, range from about -9.7 to -12.0 per mil, which is similar to the range of δ^{18}O values for the Kings River facies described by Davis and Coplen (1989). Water from these six wells reflect the mixing of

Figure 12. Isotopic composition of ground-water samples collected from wells along the monitoring well transect near Fresno in the eastern San Joaquin Valley, California, and of selected surface-water samples (from Davis and Coplen, 1989) and ground-water samples (from Willie Kinsey, U.S. Geological Survey, written commun., 1998) near the monitoring well transect.

surface water from runoff in the Sierra Nevada with native ground water. Wells B1-1, B2-1, B3-1, and B3-3 are the most depleted in ^{18}O, indicating that the water in these wells is derived predominantly from recharge of surface water. CFC and tritium data (fig. 11) indicate, however, that the ground water sampled from these wells likely is water that has been pumped and reapplied.

CFC data for samples from wells B1-2, B1-3, and B3-5 indicate that the ground water in these wells most recently was recharged during the 1940's and 1950's, just prior to the completion of the first canals that provided surface water for irrigation in the early 1950's. The isotopic composition of ground water from wells B1-2, B1-3, and B3-5 is enriched in ^{18}O, with δ^{18}O ranging from about -7.9 to -9.0 per mil (fig. 12). The water in these wells likely reflect the isotopic composition of relatively old native ground water recharged from local precipitation and streams draining the Sierra Nevada in the more distant past. Because the CFC and tritium data indicate no evidence that this water was pumped and reapplied for irrigation, the DBCP concentration in well B1-2 likely resulted from the application of DBCP in the early 1950's. Ground-water samples from wells B5-1 and B5-2 also are enriched in ^{18}O, which indicates that the water in these wells may have derived from similar sources; however, CFC and tritium data indicate that the water in these wells likely is water that was pumped and reapplied for irrigation more recently. DBCP detected in the samples from these wells, therefore, may have derived either from DBCP applications in the 1950's or from more recent applications.

GROUND-WATER FLOW AND DBCP TRANSPORT MODELING

A conceptual two-dimensional numerical flow and transport modeling approach was used during this study to test hypotheses addressing dispersion, transformation rate, and in a relative sense, the effects of ground-water pumping and reapplication of irrigation water on DBCP concentrations in the aquifer. The flow and transport simulations, which represent hypothetical steady-state flow conditions in the aquifer, were used to refine the conceptual understanding of the aquifer system rather than to predict future concentrations of DBCP. The hydraulic head and water chemistry data collected from the monitoring wells along the transect were not expected to precisely match

simulated travel times and simulated DBCP concentrations because (1) the model is two-dimensional, (2) the distribution of hydrogeologic facies between cluster well sites likely varies from the actual distribution, (3) the history of DBCP applications along the transect is not known, and (4) long-term data on DBCP concentrations along the monitoring well transect were not available. Using a similar conceptual modeling approach, Loague and others (1998b) evaluated the effects of sorption, chemical transformation, and dispersion of DBCP in ground water in a series of three-dimensional simulations of DBCP transport in the Fresno area. They used quantitative estimates of regional scale DBCP loading at the water table for transport simulations of the saturated zone by simulating multiple nonpoint-source applications at the regional scale and by accounting for different soil types and changes in land use and water-table depth (Loague and others, 1998a). Loague and others (1998b) determined that the highest simulated concentrations of DBCP in ground water were nearly two orders of magnitude lower than the highest measured concentrations of DBCP in the aquifer.

Particle travel times were calculated for a series of steady-state flow simulations to compare the resulting advective travel times with travel times estimated from CFC recharge dates. As demonstrated by Reilly and others (1994), the combined use of numerical modeling and ground-water tracers, such as CFCs and tritium, provides independent estimates of travel time. These estimates can be used to improve the conceptual understanding of the ground-water flow system under investigation and to indicate where further data and analysis are needed. A series of transport simulations were done for this study after the particle tracking analysis was completed. The simulations incorporated stochastically generated hydrogeologic facies distributions to explicitly evaluate the effects of dispersion owing to macro-scale heterogeneity on DBCP concentrations in the aquifer. Additional transport simulations were done to test the effects of a varying rate-reaction constant (expressed as half-life) on the concentrations of DBCP in the aquifer.

Simulation of Ground-Water Flow

A two-dimensional, steady-state modeling approach was used for this study to approximate average ground-water flow conditions in the aquifer.

Ground-water pumpage and irrigation recharge may vary seasonally and from year to year, but because primarily grapes have been grown in the area since the early 1900's, land-use management practices in the study area likely have not changed significantly during the past 50 years. Although pumping for irrigation may significantly affect ground-water flow in the study area, pumping was not explicitly modeled because it could not be accurately represented in two dimensions. To improve the quantification of the flow system, the results of the flow simulations were compared to the horizontal and the vertical gradients in the study area and simulated particle travel times were compared with the travel times estimated from CFC concentrations.

A numerical, finite-difference ground-water flow model (McDonald and Harbaugh, 1988), commonly referred to as MODFLOW, was used to simulate the distribution of hydraulic heads and ground-water flow rates along the monitoring well transect. Steady-state three-dimensional movement of ground water of constant density through a heterogeneous anisotropic medium of porous earth material is described by the following general partial differential equation,

$$\partial X\left(K_{xx}\frac{\partial h}{\partial X}\right) + \partial Y\left(K_{yy}\frac{\partial h}{\partial Y}\right) + \partial Z\left(K_{zz}\frac{\partial h}{\partial Z}\right) - W = 0, \quad (3)$$

where K_{xx}, K_{yy}, and K_{zz} are values of the hydraulic conductivity along the x, y, and z coordinate axes, which are assumed to be parallel to the major axes of hydraulic conductivity, in meters per second; h is the hydraulic head, in meters; and W is a volumetric flux per unit volume (in per second) and represents sources and (or) sinks. An approximate solution of equation 3 was obtained using the finite-difference method where a continuous system is replaced by a finite set of discrete points in space (McDonald and Harbaugh, 1988).

The model of the transect was discretized into a uniform grid of finite-difference cells and simulated as a vertical plane of unit width in the y direction with no flow orthogonal to the x-z plane. The grid consisted of 151 layers [each 0.6 m (2 ft) thick] and 401 columns [each 15 m (50 ft) wide]. The model discretization and the relation between the grid and the monitoring well transect is shown in figure 13. Hydraulic conductivity was specified in the horizontal (x) and vertical (z) directions for each grid cell for stochastically generated distributions of hydrogeologic facies. These
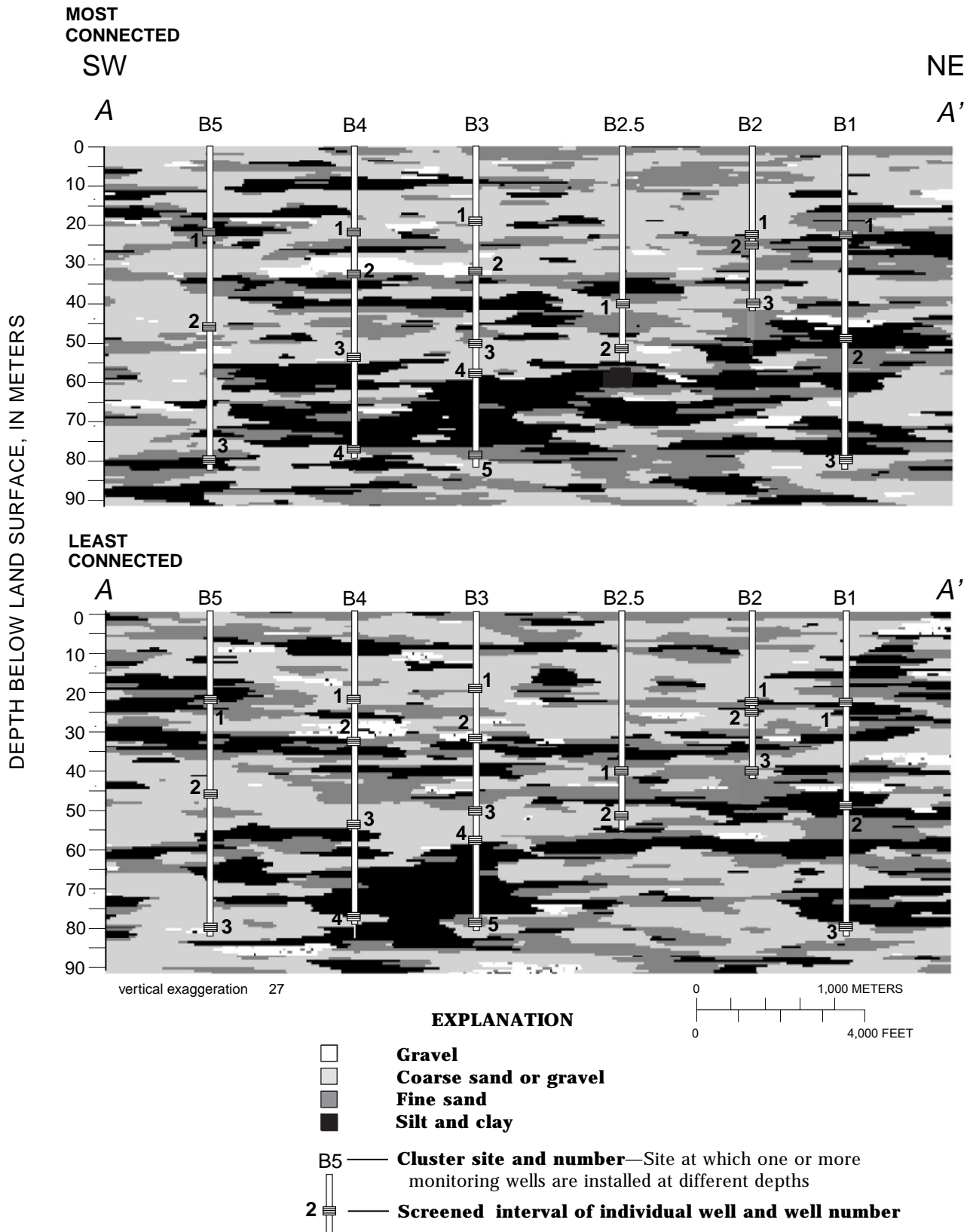
Figure 13. Distributions of hydrogeologic facies (Burow and others, 1997) used in the flow simulations. "Most" and "least" connected refer to the amount of horizontal interconnection of high permeability facies (gravel and coarse sand or gravel). The top of the cross section coincides with land surface.

distributions were generated using a conditional indicator approach which incorporates a transition-probability Markov method (Carle and Fogg, 1996, 1997; Carle, 1997; Carle and others, 1998). This method uses a transition-probability model to define the statistical correlation structure of discrete hydrogeologic facies. Hydrogeologic characterization data, which were collected earlier in this study (Burow and others, 1997), were accurately retained in the conditional simulations; the simulations provided multiple "realizations" of the hydrogeologic facies. Two distributions were selected from a series of 50 equiprobable realizations of the hydrogeologic facies—the "most" and the "least" connected distributions in terms of the degree of horizontal interconnection of high permeability categories (gravel and coarse sand or gravel categories). These distributions are not an exact representation of the distribution of the hydrogeologic facies along the transect; the method used to generate these distributions, however, accurately retains the borehole data and preserves the estimated structure of the hydrogeologic facies distribution by using stochastic interpolation between boreholes (Journel and Huijbregts, 1978). The distributions of hydrogeologic facies in figure 13 were generated using statistical correlation functions which represent the probability of a transition in space from one hydrogeologic facies to another. The most and the least connected distributions differ only in the distribution of hydrogeologic facies between boreholes. The top of the distributions coincide with land surface because the simulations of hydrogeologic facies extended above the water table; in the flow model, the uppermost 26 layers were inactive.

A series of flow simulations was done using a range of parameters for each of the two hydrogeologic facies distributions (table 5). A hydraulic conductivity was assigned to the finite-difference cells for each of the four hydrogeologic facies categories. For the first flow simulation (simulation r1), which represents a best estimate or "average" condition, a hydraulic conductivity of 0.001 m/s (0.0034 ft/s) was used for the coarse sand or gravel facies (category 2). This value for hydraulic conductivity was based on values of transmissivity reported from previous studies (Nolte, 1957; Page and LeBlanc, 1969; California State University, Fresno Foundation, 1994) and from values estimated during this study for wells screened in coarse-grained sediments. Hydraulic conductivity was estimated from an average transmissivity value of $0.016 \ m^2/s$ ($0.17 \ ft^2/s$). The irrigation well used during the pumping test was assumed to have a screened interval length of 30.5 m (100 ft), but because the coarse-grained sediments account for about 50 percent of the sediments in the transect (Burow and others, 1997), the transmissive zone was assumed to have a thickness of only 15.2 m (50 ft). A more detailed description of the aquifer testing done during this study is presented in the "Hydrologic Data" section of this report. Hydraulic conductivity values for the other categories were based on the results of slug tests and literature values (Bouwer, 1978; Freeze and Cherry, 1979; Domenico and Schwartz, 1990). On the basis of the literature values, the assigned hydraulic conductivities are within reasonable ranges for these types of sediments. Hydraulic conductivity was assumed to be isotropic within each cell because the anisotropy of the flow system was represented by a

Table 5. Recharge rates and hydraulic conductivity for hydrogeologic facies categories used in the flow simulations

[Hydrogeologic facies categories are defined in Burow and others, 1997]

Simulation	Recharge rate, in millimeters per year	Hydraulic conductivity, in meters per second			
		Category 1: gravel	Category 2: coarse sand or gravel	Category 3: fine sand	Category 4: silt and clay
r1 ("average" recharge rate and hydraulic conductivity)	150	0.01	0.001	1.0×10^{-5}	1.0×10^{-7}
r2 (maximum hydraulic conductivity)	150	0.034	0.0024	3.0×10^{-5}	2.1×10^{-7}
r3 (minimum hydraulic conductivity)	150	0.007	0.00028	4.6×10^{-6}	1.5×10^{-8}
r4 (minimum recharge rate)	75	0.01	0.001	1.0×10^{-5}	1.0×10^{-7}
r5 (maximum recharge rate)	300	0.01	0.001	1.0×10^{-5}	1.0×10^{-7}

detailed distribution of the hydrogeologic facies and because the anisotropy was not expected to be significant over the 0.6 m (2 ft) thickness of each grid cell. In subsequent flow simulations, hydraulic conductivity was varied for each of the hydrogeologic facies categories to represent maximum hydraulic conductivity (simulation r2) and minimum hydraulic conductivity (simulation r3) along the transect (table 5). The maximum and minimum hydraulic conductivities for each facies were based on literature values (Bouwer, 1978; Freeze and Cherry, 1979; Domenico and Schwartz, 1990); these values were within reasonable ranges for these types of sediment.

The boundary condition for the top boundary of the model of the transect (beginning at layer 27) represents the water table with a constant rate of recharge. Ground-water flow into and out of the model through the upgradient, downgradient, and lower boundaries were simulated with head-dependent (general head) flow boundaries (McDonald and Harbaugh, 1988). Ground-water flow across head-dependent flow boundaries is proportional to the difference in hydraulic head at the boundary and a prescribed hydraulic head at a point exterior to the boundary and is constrained by a proportionality constant. Hydraulic head was specified at a distance from the model boundary to effectively simulate ground-water flow without expanding the grid to encompass the boundaries of the regional flow system (Kipp, 1986; Anderson and Woessner, 1992). The actual hydraulic head in each layer, however, could not be determined because of the complexity of the distribution of the hydrogeologic facies and because the vertical gradients calculated from the measured head in the monitoring wells are averaged across coarse- and fine-grained layers. The proportionality constant was specified at the upgradient and downgradient boundaries as the horizontal conductance of the geologic material adjacent to the modeled area. Because actual conductance was not measured, conductance was determined by assuming a horizontal hydraulic conductivity of 0.001 m/s and adjusting the distance and prescribed head to match a horizontal hydraulic-head gradient of about 0.002 within the boundaries of the model. Vertical conductance was determined for the lower boundary of the model by assuming a vertical hydraulic conductivity of 1.0×10^{-5} m/s (which accounted for anisotropy of two orders of magnitude below the bottom boundary of the model) and adjusting the

distance and prescribed hydraulic head to allow leakage through the bottom boundary while maintaining vertical gradients within the range of measured values. The adjusted horizontal and vertical conductance values were used for all the flow simulations (table 5) and the resulting horizontal and vertical gradients were maintained within the range of measured values.

The average annual recharge rate was estimated using a water balance calculation.

$$R = P + I - ET, \qquad (4)$$

where R is average annual recharge, P is average annual precipitation, I is the amount of irrigation water applied, and ET is evapotranspiration for vineyards. Assuming that evapotranspiration for vineyards near the study area is about 800 mm/yr and that average annual precipitation is about 250 mm/yr, seasonal irrigation requirements for vineyards are about 550 mm/yr (Williams and Matthews, 1990). The average amount of irrigation water applied between 1973 and 1983 was about 850 mm/yr (California Department of Water Resources, 1986), which represents an average annual recharge rate of about 300 mm/yr. Beginning in the 1970's, however, irrigation efficiency was relatively high because of a drought (Larry Williams, University of California, oral commun., 1995). An average annual recharge rate of 150 mm/yr, which represents an irrigation efficiency of about 84 percent, was used in simulations r1, r2, and r3 (table 5) because of the increase in irrigation efficiencies and because these recharge rates were assumed to correspond with the peak DBCP concentrations measured in the early 1980's. The estimated annual recharge rate of 300 mm/yr was used to represent the maximum recharge rate (simulation r5), and one-half of the average annual recharge rate (75 mm/yr) was used to represent the minimum recharge rate (simulation r4).

The results of the series of steady-state ground-water flow simulations were evaluated to determine whether selected model parameters resulted in a reasonable approximation of the flow system along the monitoring well transect. The results of these simulations were similar among the different combinations of parameters shown in table 5. The simulations were calibrated by adjusting conductance and prescribed hydraulic head to match the approximate horizontal and vertical gradients; all
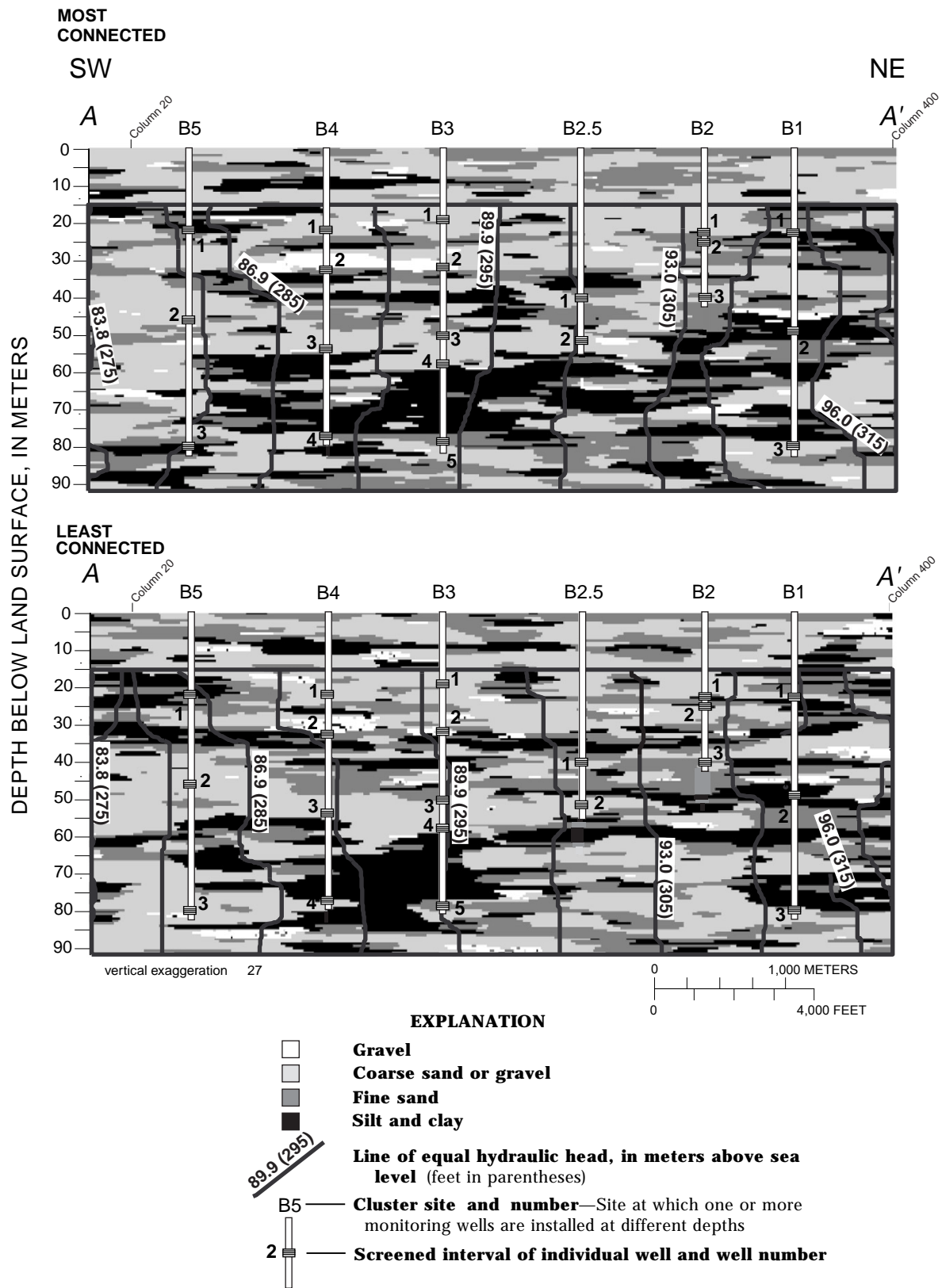
Figure 14. Steady-state hydraulic-head distribution for flow simulations r1-most and r1-least. See table 5 for parameters used in these simulations.

simulations had a horizontal hydraulic gradient of 0.002 and variable vertical hydraulic gradients of less than 0.05, which is consistent with the measured gradients. The relative proportion of water entering through the top recharge boundary and the upgradient boundary varied among the different simulations in response to the recharge rate and the hydraulic conductivities assigned. The overall steady-state hydraulic-head distributions for the simulations with average parameters (simulation r1) were similar between the most and the least connected hydrogeologic facies distributions (fig. 14); the horizontal and vertical gradients varied locally, however, depending on the distribution of hydrogeologic facies. As expected, the horizontal and vertical gradients in these simulations were large in the areas where low-permeability sediments predominate relative to areas where high-permeability sediments predominate. Simulated flow in the two-dimensional model, however, is constrained by the two-dimensionality of the model. The low-permeability hydrogeologic facies may be discontinuous in the third dimension, allowing ground water to flow around these layers.

Simulation of Advective Transport by Particle Tracking

Ground-water path lines and advective travel times for each flow simulation were calculated using the program MODPATH (Pollock, 1989). MODPATH uses cellular volumetric fluxes from the MODFLOW simulations and effective porosity to calculate linear velocity. The x and z components of the linear velocities were used to generate a velocity vector field using simple linear interpolation of the components between adjacent faces of the finite-difference cells. For steady-state simulations, an analytical expression for the flow path in each cell was calculated by direct integration of the velocity components. The travel time calculated using this method represents an average travel time for the advection of a "particle" of water or conservative solute.

An effective porosity of 0.25 was assigned to the entire grid for each MODPATH computation. The effective porosity for each hydrogeologic facies category could not be specified because effective porosity can be specified only by layer. A total porosity of 40 percent was estimated for the transect using

average values (Domenico and Schwartz, 1990) weighted according to the proportion of each hydrogeologic facies category in the transect; however, effective porosity can be as much as one order of magnitude lower than the total porosity, depending on the degree of interconnection of the pore spaces. Because the pore spaces in the geologic materials along the transect probably are well connected (compared with crystalline rocks, for example), an effective porosity of 0.25 was assumed. The effective porosity was not varied for different MODPATH simulations. Because the calculated particle travel times are a linear function of the effective porosity, travel times for these calculations would be about 17 percent longer if an effective porosity of 30 percent was used.

Calculated particle travel times were compared with the travel times estimated from the CFC concentrations to determine whether the flow model results reasonably represent the hydrologic system along the monitoring well transect (see also Reilly and others, 1994). Because the model is two dimensional and because the modeled distribution of hydrogeologic facies may not reflect actual distribution, the calculated particle travel times to the locations in the grid corresponding to the monitoring well screens were not expected to precisely match the travel times determined from the CFC concentrations. The transect, therefore, was divided into four zones (fig. 15) on the basis of the distribution of the hydrogeologic facies, the chemical data from the monitoring wells along the transect, and the screened intervals of production wells in the study area to compare the calculated particle travel times with the CFC-estimated travel times. The shallow zone (from the water table to 24 m below the top of the model grid) is most influenced by the top recharge boundary and represents the shallowest monitoring wells along the transect. Intermediate zone 1 (INT1) is 43 to 55 m below the top of the model grid and intermediate zone 2 (INT2) is 55 to 76 m below the top of the model grid. The intermediate zone was divided into two zones on the basis of the distribution of hydrogeologic facies and the chemical data from the monitoring wells. These zones correspond to the depth and length of the screened intervals typical of production wells (domestic and irrigation) in the study area. The intermediate zone was divided into two zones to enable comparison between simulated concentrations of DBCP and concentrations in ground-water samples from production wells in the area. The

deep zone (55 to 76 m below the top of the model grid) is characterized by a substantially greater percentage of low-permeability hydrogeologic facies than the upper three zones of the model.

Particle travel times were calculated for each flow simulation (table 5) to compare the model results with the travel times estimated from CFC recharge dates. Particle travel times were calculated using backward tracking, that is, particles were tracked backward along their path lines to the boundary where they enter the model. The particles were tracked backward from column 20, which is 289.6 m upgradient from the downgradient boundary (fig. 14) to the top recharge boundary or to column 400, which is
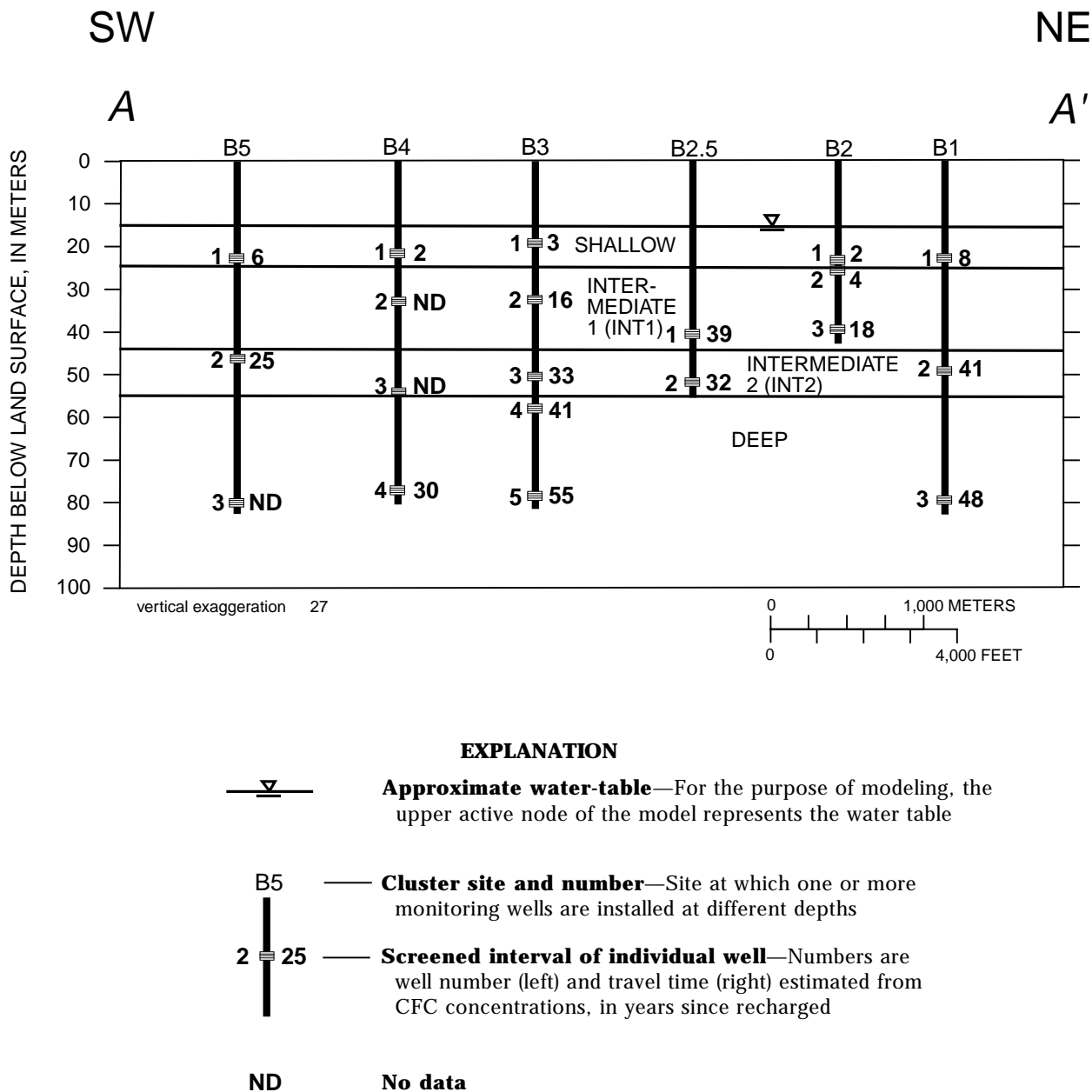
Figure 15. Zones used for comparison between water-quality data and simulation results, travel time since ground water was recharged, and screened intervals for wells along the monitoring well transect near Fresno in the eastern San Joaquin Valley, California. Travel times are based on chlorofluorocarbon (CFC) concentrations. Delineation of the zones was based on the distribution of hydrogeologic facies, chemical data from monitoring wells along the transect, and the typical screened depth interval of production wells in the study area.

15.2 m downgradient from the upgradient boundary. The backward particle path lines were stopped at column 400 to avoid the effects of the upgradient boundary—additional vertical flow in the boundary cells is influenced by the difference between the averaged gradient specified at the boundary and the local gradient caused by the heterogeneity in hydrogeologic facies between cells.

The backward particle travel times were averaged for each of the different depth zones (table 6; fig. 15). Because the model is two-dimensional and because the distribution of hydrogeologic facies probably do not reflect the actual distribution, the calculated particle travel times to the different zones were not expected to exactly match the travel times determined from the CFC concentrations in the monitoring wells. Because the travel times estimated from CFC concentrations represent the time since a particle of water was recharged at the water table, the travel times for particles that stopped at column 400 were corrected to account for the additional amount of time required to travel from the water table to the depth where the particle was stopped. For each particle that stopped at column 400, the additional amount of time added to the computed travel time was determined using a regression equation relating particle travel time to depth for those particles whose paths were tracked backwards to the top recharge boundary (r^2 ranged from 0.69 to 0.96; p less than 0.001).

Particle travel times for the intermediate zones generally were similar to the CFC-estimated travel times for simulations r1, r3, and r5 (table 6). Calculated particle travel times were considered to be reasonable if they did not differ from the range of CFC-estimated travel times by more than about 20 percent. Particle travel times for the shallow zone also were generally similar to the CFC-estimated travel times. Most of the particle travel times for the deep zone were unreasonably long compared with the CFC-estimated travel times. During the two-dimensional simulations, many of the particles in the deep zone were forced to exit the bottom boundary of the model or to move into low-permeability hydrogeologic facies because of the large proportion of silt and clay at depths greater than 55 m below land surface (fig. 14). In the ground-water flow system, however, most ground water likely flows around the low-permeability materials rather than through them. The unreasonably long particle travel times also may have resulted from inaccuracies in the

distribution of the hydrogeologic facies in the deep zone or from low hydraulic conductivity values assigned to the fine-grained facies. The calculated particle travel times for the deep zone, therefore, were considered unreasonable, and thus, the processes for this part of the model (depths greater than 55 m below land surface) were not interpreted.

In most cases, the calculated particle travel times were longer than the average CFC-estimated travel times (except for simulation r5-least; see table 6) indicating that the flow rates for the model simulations may represent minimum flow rates compared with flow rates estimated from CFC travel times. The fairly long calculated travel times (compared with the CFC-estimated travel times) may be due to the lack of representation of irrigation pumpage in the flow simulations, the representation of the flow system in two dimensions, or the method of comparison between travel times determined from CFC data collected at the monitoring well screens and particle travel times averaged over the designated depth zones in the model. Because of the variability in CFC-estimated travel times within each depth zone, the method used to compare the simulated travel times and average CFC-estimated travel times may be misleading.

The differences in calculated particle travel times among simulations with different parameters may be affected by the relative contribution of water from the top recharge and upgradient boundaries. The particle travel times for the r4 simulations are unreasonably long compared with the CFC-estimated travel times for all depth zones (table 6). Because a minimum recharge rate (75 mm/yr) was used for the r4 simulations, flow in the transect was dominated by the inflow from the upgradient boundary; however, when a relatively high recharge rate (150 or 300 mm/yr) was used, the flow in the transect was dominated by the inflow from the top recharge boundary. To evaluate the relative proportions of flow through different parts of the model transect, equal-volume flow tubes were computed for the r1 simulations (fig. 16) by placing a particle at or adjacent to the inflow boundaries at equal volume increments. An approximately equal volume of water flowed between each of the path lines, which indicates that the largest proportion of flow is channeled through the interconnecting cells of the high-permeability sand or gravel facies in the shallow part (less than about 40 m below land surface) of the transect. A relatively small proportion of flow occurred

Table 6. Summary of simulated particle travel times and comparison with travel times estimated from chlorofluorocarbon (CFC) concentrations

[Simulated particle travel times were calculated for each depth zone by averaging travel times for particles tracked backwards from column 20 to the recharge boundary or to column 400. The travel times for particles that stopped at column 400 were corrected to account for the additional amount of time required to travel from the water table to the depth where the particle was stopped. The average ground-water velocity was calculated by averaging the travel times for all particles that tracked backwards from column 20 to column 400. "Most" and "least" refer to the hydrogeologic facies distribution used for the simulation. CFC, chlorofluorocarbon; m, meter; >, actual value is greater than value shown; —, no data]

|	CFC-estimated travel times, range and average (in parentheses), in years	Simulation r1, average hydraulic conductivity and recharge rate		Simulation r2, maximum hydraulic conductivity		Simulation r3, minimum hydraulic conductivity		Simulation r4, minimum recharge rate		Simulation r5, maximum recharge rate	
		Particle travel time, in years									
		Most	Least	Most	Least	Most	Least	Most	Least	Most	Least
Shallow zone (15-24 m below land surface)	2–8 (4)	10	6.5	8.9	6.6	16	6.5	17	13	5.7	3.2
Intermediate zone 1 (INT1) (24-43 m below land surface)	4–39 (19)	27	19	27	25	24	29	110	50	11	10
Intermediate zone 2 (INT2) (43-55 m below land surface)	25–41 (33)	62	42	93	34	36	43	220	81	26	17
Deep zone (55-76 m below land surface)	30–55 (44)	>2,500	110	260	81	110	150	3,000	200	2,600	62
Average ground-water velocity, in meters per year	—	180	120	360	320	38	27	150	95	190	110
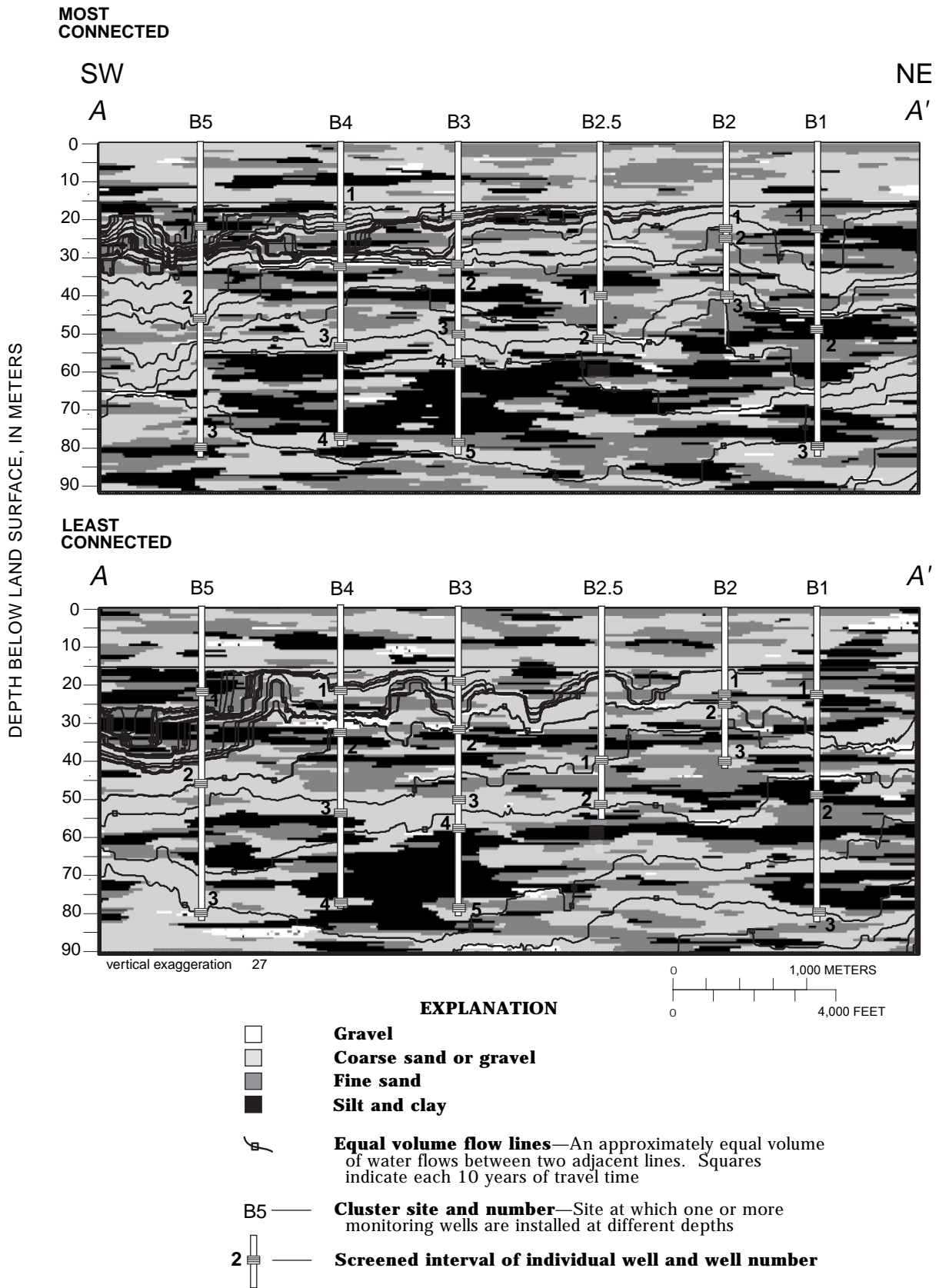
Figure 16. Equal-volume flow tubes for simulations r1-most and r1-least. See table 5 for parameters used in these simulations.

in the deepest part (greater than about 55 m below land surface) of the transect. The source of the water contributed to each layer near the downgradient boundary was determined by the arrangement of the hydrogeologic facies upgradient from that layer and its proximity to the top recharge boundary. Because of the preferential flow through the high-permeability facies, the locations of the observation points in the simulations of DBCP transport are relevant to the interpretation of the simulation results.

Another calculation using particle travel times was done to further evaluate whether the model results were consistent with the independent estimates of ground-water velocities through the system. The average ground-water velocities in table 6 represent the average rate of horizontal flow across the transect; they were calculated by averaging the travel times for all particles (in all zones) that tracked backwards from column 20 to column 400. The travel times for particles that did not track backwards all the way across the transect were not included in the calculation of average ground-water velocity because this velocity was intended to represent horizontal flow across the entire transect. The calculated average ground-water velocities for simulations r1-, r4-, and r5-least were the most reasonable compared with the independent estimates of ground-water velocities in the study area. Previous investigators estimated ground-water velocities of about 90 to 120 m/yr in the study area (California State University, Fresno Foundation, 1994); for this current study, we used regional hydraulic gradients and estimated hydraulic conductivity to calculate an average linear velocity. Our calculations indicate an estimated velocity of about 120 to 260 m/yr. The average ground-water velocities for simulation r3 were smaller (27 and 38 m/yr) than the ground-water velocities for the independent estimates, whereas average velocities for simulation r2 were larger (320 and 360 m/yr) than the velocities from the independent estimates. Although the average ground-water velocities for the r4 simulations were within the range of velocities for the independent estimates, the particle travel times for these simulations do not match the CFC-estimated travel times. The average ground-water velocities for the r5 simulations also were within the range of velocities for the independent estimates; however, the particle travel time for zone INT2 was faster than the CFC-estimated travel time in simulation r5-least.

In conclusion, in spite of the inherent limitations of the two-dimensional, steady-state flow model in representing the ground-water flow system in the study area, the comparisons between calculated particle travel times and ground-water travel times estimated from CFC concentrations obtained from this study and from previous studies indicate that the model boundary conditions and "average" parameters used in the r1 simulations provide a reasonable approximation of the flow system for depths of less than 55 m below land surface. The results of the r1 flow simulations were used in the transport simulations. The flow simulations, however, did not accurately represent conditions at depths greater than 55 m below land surface possibly because the model was two-dimensional and therefore water was forced to flow through the large proportion of low-permeability hydrogeologic facies at greater depth resulting in extremely long particle travel times. Inaccuracies in the distribution of the hydrogeologic facies in this zone or low hydraulic conductivity values assigned to the fine-grained facies also probably have contributed to the inaccurate representation of conditions at depths greater than 55 m below land surface. Because most of the wells in the study area that were sampled for DBCP are screened at depths less than 55 m below land surface and because DBCP was detected in samples from only 1 of the 5 monitoring wells screened at depths greater than 55 m below land surface, the lack of a realistic model to interpret DBCP transport at depths greater than 55 m below land surface is not expected to significantly affect the understanding of the processes affecting DBCP transport and fate.

Simulation of DBCP Transport and Decay

A series of transport simulations was done to evaluate the combined effects of dispersion owing to macro-scale heterogeneity and first-order decay on DBCP concentrations in the model transect. Simulated DBCP concentrations were compared with measured concentrations in the ground-water samples from production wells in the Fresno area to determine whether the changes in measured concentrations with time are reflected by those processes simulated in the model.

Transport Modeling Approach and the MT3D Model

The three-dimensional solute-transport model MT3D (Zheng, 1992, 1993) was used to simulate the concentrations of DBCP in the transect. MT3D uses simulated hydraulic heads, intercell flows, and source and (or) sink terms from the MODFLOW output in the solution of the advection-dispersion equation,

$$\frac{\partial C}{\partial t} = \frac{\partial}{\partial x_i}\left(D_{ij}\frac{\partial C}{\partial x_j}\right) - \frac{\partial}{\partial x_i}(v_i C) + \frac{q_s}{n_e}C_s + \sum_{k=1}^{N} R_k, \quad (5)$$

where

C is the concentration of the dissolved solute,

t is time,

x is the distance along the respective Cartesian coordinate axis,

D_{ij} is the dispersion coefficient,

v_i is the average linear velocity of ground water,

q_s is the volumetric flux of water per unit volume of aquifer representing sources (positive) and sinks (negative),

n_e is the effective porosity of the porous medium,

C_s is the concentration of solute in the sources and (or) sinks, and

$\sum_{k=1}^{N} R_k$ is the chemical reaction term.

The advection-dispersion equation 5 accounts for the process of advection in which the solute travels at the average linear velocity of ground water and for the processes of dispersion and chemical reactions. Dispersion refers to the spreading of the solute; it accounts for the movement of the solute that does not travel at the average linear velocity of ground water. The chemical reaction used in the analysis of DBCP transport assumes first-order decay. The chemical reaction term in equation 5 is expressed as

$$\sum_{k=1}^{N} R_k = -\frac{\rho_b}{n_e}\frac{\partial \overline{C}}{\partial t} - \lambda\left(C + \frac{\rho_b}{n_e}\overline{C}\right) = -\frac{\rho_b}{n_e}\frac{\partial C}{\partial t}\frac{\partial \overline{C}}{\partial C} - \lambda\left(C + \frac{\rho_b}{n_e}\overline{C}\right), \quad (6)$$

where

ρ_b is the bulk density of the porous medium,

$\overline{C}$ is the concentration of solute sorbed on the porous medium, and

λ is the first-order rate reaction constant.

Substituting equation 6 for the last term in equation 5, equation 5 can be rewritten as

$$R\frac{\partial C}{\partial t} = \frac{\partial}{\partial x_i}\left(D_{ij}\frac{\partial C}{\partial x_j}\right) - \frac{\partial}{\partial x_i}(v_i C) + \frac{q_s}{n_e}C_s - \lambda\left(C + \frac{\rho_b}{n_e}\overline{C}\right), \quad (7)$$

where

R is the retardation factor, defined as

$$R = 1 + \frac{\rho_b}{n_e}\frac{\partial \overline{C}}{\partial C} . \quad (8)$$

The MT3D solute-transport model solves equation 7 by using different approaches for the advection (second) and dispersion (first) terms. The transport model uses the forward particle-tracking method of characteristics (MOC) approach (Konikow and Bredehoeft, 1978) to solve the advection term of the equation. The MOC approach involves placing several particles in each cell of the finite-difference grid. Each particle has a concentration and position associated with it. Particles are tracked forward in time in proportion to flow velocity using small time increments. At the end of each increment, the concentration within a given cell owing to advection is calculated by averaging the concentration of all the moving particles in the cell. The change in concentration caused by dispersion, mixing of sources and (or) sinks, and chemical reactions is then calculated using an explicit finite-difference solution of the dispersion term. The MOC method is computationally intensive because it keeps track of the concentration and the position of a large number of particles moving forward in time. A modified version of MOC, referred to as MMOC, designed to reduce the total number of moving particles needed in a given simulation, also is included in the MT3D model. The MMOC approach is similar to the MOC approach

except in the treatment of the advection term in which only one particle is placed at the nodal point of the fixed grid and tracked backward in time to find its position at the previous time level. Linear interpolation is used to determine the concentration at this new position, which then is used to approximate the concentration at the nodal point at the new time level. The MMOC approach generally requires less computational time than MOC, but one of the benefits of using the MOC approach is that it minimizes numerical dispersion (artificial dispersion resulting from the numerical calculations). The MMOC approach introduces more numerical dispersion than MOC, especially for problems with sharp concentration fronts. A hybrid (HMOC) of the two methods was used for the transport of DBCP during this analysis. For sharp concentration fronts, the advection term was solved by the MOC approach; whereas in other parts of the grid where sharp concentration fronts are absent, the advection term was solved using the MMOC approach.

MT3D uses cellular volumetric fluxes from the flow model and effective porosity to solve for the advective term in equation 7. An effective porosity was specified for each active cell according to the hydrogeologic facies category defined for that cell. Effective porosities were estimated at the low end of a range of total porosity values (Domenico and Schwartz, 1990). An effective porosity of 0.25 was used for the gravel facies (category 1); 0.30 was used for the coarse sand or gravel facies (category 2); 0.35 was used for the fine sand facies (category 3); and 0.40 was used for the silt and clay facies (category 4). The proportion of the transect represented by each of these categories is 46 percent sand or gravel, 26 percent fine sand, 25 percent silt and clay, and only 3 percent gravel; therefore, the weighted average effective porosity of the entire transect is about 34 percent. The effective porosity values used in the MT3D simulations were considered to be more realistic than the single effective porosity of 0.25 used for the entire grid in the MODPATH simulations. The difference in travel times resulting from the use of different values of effective porosity between the MODPATH and MT3D simulations could not be determined by direct comparison because the results were dependent on the volume of flow in each cell, although most of the flow occurred in the coarse-grained hydrogeologic facies categories which have effective porosities of 0.25 and 0.30. The difference in travel times was not expected to

affect the interpretation of the DBCP transport simulations. The specified effective porosities were not varied among the different transport simulations because of the significant computational time required to complete each simulation.

MT3D incorporates an isotropic dispersion coefficient in which mechanical dispersion is defined by two independent dispersivities (longitudinal and transverse). A longitudinal dispersivity of 0.03 m (0.1 ft) was specified for each layer in the grid, and a ratio of 0.1 of the longitudinal dispersivity was specified for both the horizontal and vertical transverse dispersivities. An effective molecular diffusion coefficient also can be specified, but because the effect of molecular diffusion was expected to be minor in comparison to mechanical dispersion in this advection-dominated system, the effective molecular diffusion coefficient was specified as zero. The representation of the dispersion process with the dispersion term used in this and other transport models has been the subject of continuing debate and research (Anderson and Woessner, 1992). Although the process of mechanical dispersion caused by variations in ground-water velocity is reasonably understood, quantifying these variations is difficult, if not impossible. Another complicating factor is the apparent scale-dependence of dispersivity (Domenico and Schwartz, 1990). In the analysis described in this report, variations in velocity caused by macro-scale heterogeneities have been accounted for by directly incorporating the macro-scale structure of the porous media into the flow model. In the model, dispersivity was specified as a small value to distinguish the effects of macro-scale heterogeneity from local-scale dispersion (on the scale of the grid cell) and because the local-scale dispersion was expected to be minor. On the basis of estimates of apparent longitudinal dispersivity presented later in this report, the local-scale dispersion is less than 1 percent of the dispersion caused by macro-scale heterogeneity.

The chemical reaction term in equation 6 is used in MT3D to incorporate equilibrium-controlled linear and non-linear sorption and first-order decay reactions. Because DBCP is weakly sorbed in the low organic content soils (K_D=0.06 and 0.07 L/kg) near Fresno (Deeley and others, 1991), the process of sorption was not simulated. The first-order decay term in MT3D uses a rate constant, λ, that is analogous to k in the first-order rate reaction equation 2 when the rate of loss in both the dissolved and sorbed phase is equal. A series

of transport simulations were completed using a range of values for λ (expressed as half-life, or $t_{1/2}$) varying from no decay (conservative transport) to 6.1 years. The 6.1-year half-life was the maximum rate determined during laboratory studies by Deeley and others (1991). Transport simulations using intermediate values of 141 years (Burlinson and others, 1982), 33 years, and 40 years also were done. Half-life values of 33 and 40 years were estimated using the experimental Arrhenius parameters provided by Burlinson and others (1982) but substituting average measurements of temperature (20 to 23°C) and pH (7.2 to 7.3) collected from the monitoring wells along the transect. The 33-year half-life was a preliminary estimate used in two of the simulations, whereas the 40-year half-life was a revised estimate calculated with more complete temperature and pH data. Because the difference in model results between the 33- and 40-year half-life was negligible, only one simulation with a 40-year half-life was completed. Although the results of the analyses of BAA, the primary transformation product of DBCP, indicate that the transformation of DBCP to BAA does not significantly affect DBCP concentrations in ground water, the simulation of DBCP transport and first-order decay allows for an evaluation of whether DBCP is transported conservatively in ground water or whether other physical or chemical processes may be causing a change in concentrations that resembles a first-order reaction.

For the transport simulations, the top recharge boundary in the flow model was specified as an areally distributed source of concentration, whereas the cells along the head-dependent boundaries in the flow model were specified as point sources. Because the maximum concentration of DBCP in ground water sampled during the 1980's was about 50 µg/L (California Department of Pesticide Regulation, 1992, 1993, 1994), recharge at the water table was assigned a constant concentration of 50 µg/L for the first 15 years simulated. Maximum DBCP concentrations in the aquifer during that time, however, may have been higher than 50 µg/L because the ground-water samples were collected from long-screened irrigation, municipal, and domestic wells in which high concentrations in the discrete zones of the aquifer may have been diluted by zones containing low concentrations. A concentration of 50 µg/L, therefore, probably represents a reasonable minimum concentration for DBCP in ground-water recharge.

Although DBCP may have been applied at the region scale for a 20-year period, an application period of 15 years was simulated because applications at the local scale were intermittent and likely spanned a shorter time period. Initial concentrations of DBCP were set to 0 µg/L for each active cell in the transport model except for the source cells along the upgradient boundary. Source concentrations of DBCP were introduced at cells along the upgradient boundary to simulate the concentrations of DBCP contributed from areas upgradient from the model boundary. The DBCP concentrations assigned to these cells changed with time and decreased with depth (table 7) and were approximately equal to the simulated concentrations exiting the model at the downgradient boundary. The model simulated DBCP transport for 100 years.

As in the particle-tracking analysis, the monitoring well transect was divided into zones (fig. 15) in the transport model to compare simulated concentrations of DBCP, averaged for each zone, with measured concentrations from production wells in the area. Because the model is two dimensional and the distribution of geologic materials is heterogeneous and probably does not reflect the true hydrogeologic facies distribution, simulated concentrations at the locations in the model corresponding to the monitoring well screens were not expected to exactly match measured concentrations.

Table 7. 1,2-dibromo-3-chloropropane (DBCP) concentrations assigned at upgradient model boundary for transport simulations

[Simulation time is years since simulation began. Depth of cells is in meters below land surface. DBCP, 1,2-dibromo-3-chloropropane; m, meter; µg/L, microgram per liter. —, no sources specified]

Simulation time (years)	Range of depths of upgradient boundary of source cells (m)	Range of DBCP concentrations assigned to upgradient boundary of source cells (µg/L)
0 to 5	15.8 to 36.0	50 to 0.5
5 to 10	15.8 to 42.1	50 to 2.7
10 to 15	15.8 to 45.1	50 to 2.0
15 to 20	15.8 to 48.2	45 to 2.6
20 to 25	15.8 to 51.2	35 to 0.2
25 to 30	15.8 to 51.2	20 to 2.6
30 to 100	—	—

Simulated DBCP Concentrations and Comparison with Existing Water-Quality Data

A series of transport simulations were done using a range of half-life values for DBCP (table 8). Preferential flow through the high-permeability hydrogeologic facies caused the simulated concentrations of DBCP to spread unevenly throughout the model transect (fig. 17). After a 50-year simulation with the 33-year half-life, computed concentrations remained high near the water table in the low-permeability hydrogeologic facies but generally decreased by an order of magnitude from the time DBCP input at the top recharge boundary ceased (15 years). Although only a small proportion of flow reached the deep zone, DBCP concentrations greater than the detection limit (0.03 µg/L) reached the deep zone for all simulations except those with a half-life of 6.1 years. The concentrations in the deep zone probably were derived from the source cells along the upgradient boundary of the model (table 7). Results of the analysis of particle travel times computed using MODPATH indicate that the model does not adequately represent advective transport in the deep zone; the simulated

concentrations for the deep zone therefore should be interpreted with caution.

The computed arrival times of DBCP at concentrations greater than or equal to the MCL (0.2 µg/L) are similar among simulation results (table 8). Simulated concentrations were averaged from concentrations in the individual cells for zones INT1 and at the grid columns corresponding to monitoring wells at cluster sites B3, B4, and B5 (fig. 15) to demonstrate the spatial variability in breakthrough curves and to represent the effects of varying proximity to a recharge source of DBCP. As was expected, the time of first arrival was shortest for simulations with the longest half-life. Concentrations remained greater than or equal to the MCL for 47 to 59 years (median of 55 years) for simulations using a 6.1-year half-life, whereas concentrations remained greater than or equal to the MCL for at least 80 years for all the other simulations with a half-life longer than 6.1 years (table 8).

The first arrival and duration times for simulated DBCP concentrations greater than or equal to the MCL were nearly identical for a 141-year half-life and conservative transport simulations because the

Table 8. Arrival and duration times and maximum concentrations of 1,2-dibromo-3-chloropropane (DBCP) in transport simulations

[Arrival times are for the first 1,2-dibromo-3-chloropropane (DBCP) concentrations greater than or equal to the maximum contaminant level of 0.2 microgram per liter. Numbers in brackets are duration times in years for DBCP concentrations equal to or greater than 0.2 µg/L. A duration time greater than 100 years indicates that the average concentrations in the observation cells had not yet dropped below 0.2 µg/L after 100 years, which is the end of the simulation time. Depth of intermediate zone 1 (INT1) is 24 to 43 meters below land surface. Depth of intermediate zone 2 (INT2) is 43 to 55 meters below land surface. µg/L, micrograms per liter; >, actual value is greater than value shown; —, no data]

Transport simulation name	Rate reaction constant, expressed as half-life (years)	Arrival and duration times, in years						Maximum concentration in model at elapsed simulation time of 50 years (µg/L)
		Intermediate zone 1 (INT1)			Intermediate zone 2 (INT2)			
		Site B5	Site B4	Site B3	Site B5	Site B4	Site B3	
Most connected (r1-most)								
rx6.1	6.1	6 [56]	5 [55]	11 [58]	14 [57]	34 [53]	16 [52]	2.3
rx33	33	6 [86]	5 [90]	9 [86]	12 [92]	22 [94]	13 [82]	18
rx141	141	6 [>100]	5 [>100]	9 [>100]	12 [>100]	22 [>100]	12 [>100]	34
Conservative	none	6 [>100]	5 [>100]	9 [>100]	12 [>100]	21 [>100]	12 [>100]	41
Least connected (r1-least)								
rx6.1	6.1	6 [47]	8 [57]	5 [57]	18 [55]	37 [54]	24 [59]	1.5
rx33	33	3 [90]	7 [>100]	5 [100]	14 [>100]	22 [>100]	18 [97]	18
rx40	40	3 [94]	7 [>100]	5 [>100]	14 [>100]	21 [>100]	18 [>100]	20
rx141	141	2 [>100]	7 [>100]	5 [>100]	13 [>100]	21 [>100]	17 [>100]	33
Conservative	none	2 [>100]	7 [>100]	5 [>100]	13 [>100]	20 [>100]	17 [>100]	41

SIMULATION TIME = 15 YEARS
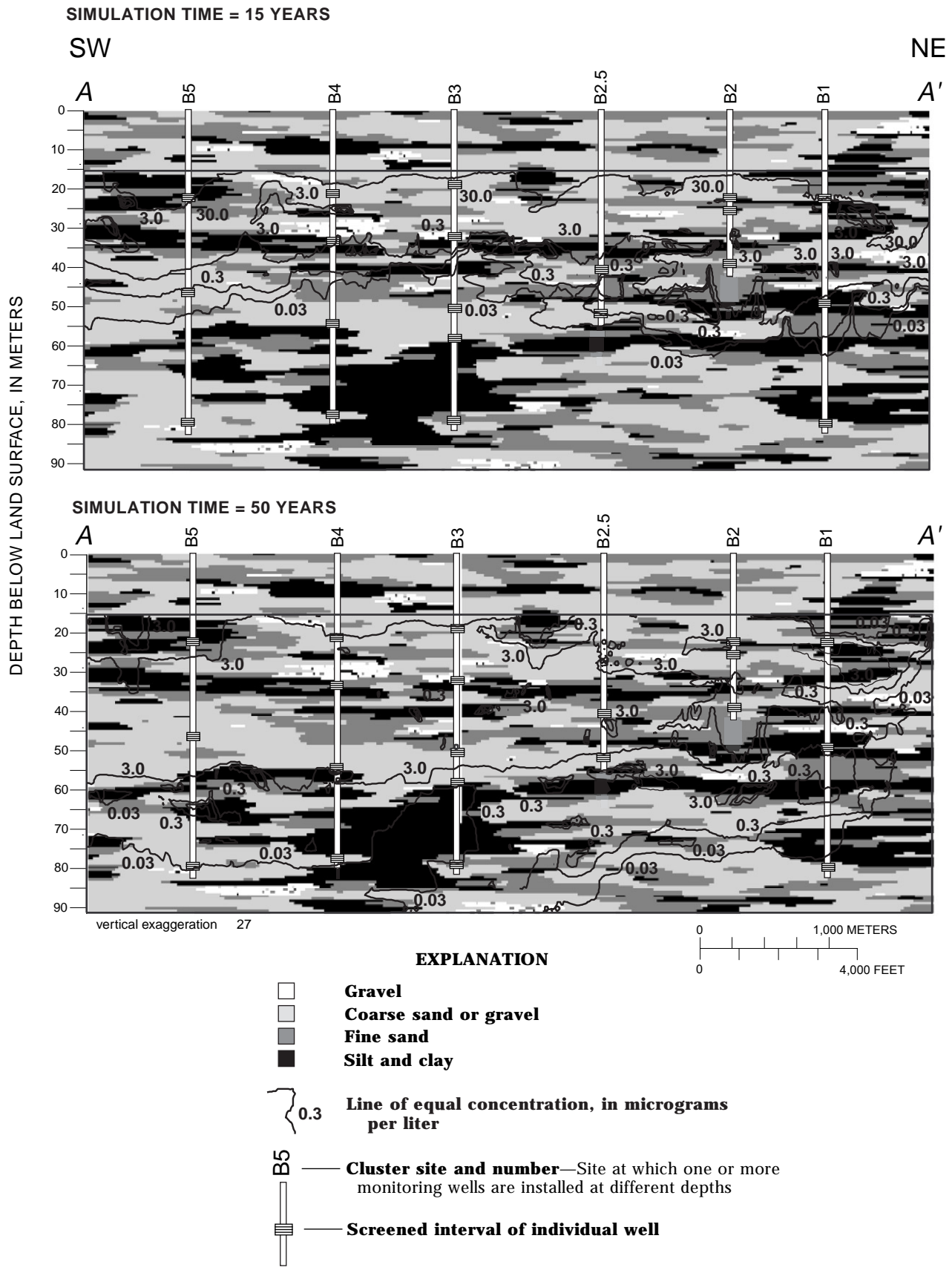
Figure 17 . Concentrations of 1,2-dibromo-3-chloropropane (DBCP) for transport simulation r1-least, assuming a 33-year half-life for decay.

maximum simulation time (100 years) was not long enough to reflect the long-term effects of a 141-year half-life. The maximum computed DBCP concentrations for an elapsed simulation time of 50 years were about 18 percent lower for simulations with a 141-year half-life than the concentrations for the conservative transport simulations (table 8). For an elapsed simulation time of 50 years, maximum DBCP concentrations were different among the simulations with different half-lives. The simulations with a 6.1-year half-life had the lowest maximum concentrations, about 2 µg/L (table 8). Although it may be useful to compare simulated DBCP concentrations among the various transport simulations, these concentrations must be interpreted with caution because the actual concentrations of DBCP in ground-water recharge were not measured and because complete data on the duration and frequency of DBCP applications were not available. Furthermore, because the simulations assumed steady-state flow conditions and the DBCP input concentration for recharge water was specified at a constant rate, the concentrations in the simulated breakthrough curves could be increased to match measured concentrations by a linear increase in input concentrations.

The breakthrough curves for simulation r1-least, which used a half-life of 6.1 and 40 years and conservative transport, indicate that the time of first arrival of the DBCP concentration front is similar among the simulations; for conservative transport, however, maximum DBCP concentrations arrived later and the concentrations remained high for longer times (fig. 18*A*, *B*, and *C*). The simulated concentrations were averaged for zones INT1 and INT2 for those cells designated as high-permeability hydrogeologic facies (gravel and coarse sand or gravel) to compare the simulated concentrations with DBCP concentrations measured in production wells in the area, and thus, represent concentrations that might be measured in a long-screened production well. The concentrations were normalized by dividing the concentration for each zone at each monitoring well cluster site by the maximum averaged concentration at each site to compare the shape of the simulated breakthrough curves with measured DBCP concentration curves.

The computed concentrations in the breakthrough curves among the different cluster well sites and zones were more variable for the 6.1-year half-life simulations than for the 40-year half-life and

the conservative transport simulations (fig. 18*A*, *B*, and *C*). The variability among the breakthrough curves for the 6.1-year and 40-year half-life simulations reflects the combined effects of dispersion and decay on DBCP concentrations. In the conservative transport simulation, the differences in maximum concentrations and in the spreading of the breakthrough curves reflect only the effects of macro-scale dispersion. For the 6.1-year half-life simulation, concentrations at cluster sites B4 and B3 in zone INT1 are 70 to 80 percent lower than the concentrations at cluster site B5 in zone INT1. The breakthrough curve for the 6.1-year half-life simulation at cluster site B5 in zone INT1 reflects the contribution of DBCP from the top recharge boundary because most of the DBCP mass from the upgradient source cells degrades before it reaches cluster site B5. At cluster sites B4 and B3, the subtle indication of a second peak for the breakthrough curves reflects the contribution of the DBCP mass from the upgradient source cells because these sites are closer to the upgradient boundary than cluster site B5. The two peaks in the breakthrough curves for the 40-year half-life and the conservative transport simulations at cluster site B5 in zone INT1 also reflect the separate contributions from the top recharge boundary and from the upgradient sources. These simulated breakthrough curves indicate that the DBCP concentrations contributed from farther upgradient have decreased only slightly in comparison with concentrations near the top recharge boundary. The relative contribution from the top recharge boundary and the upgradient source cells are indistinguishable in the breakthrough curves for the deeper intermediate zone (INT2) for all three simulations. Because zone INT2 is deeper, simulated DBCP concentrations are more dispersed and have had more time to degrade than concentrations in the shallower zones. Also, the contribution from the top recharge boundary is small relative to the contribution from the upgradient source cells in this zone.

Concentrations of DBCP in ground-water samples (fig. 18*D* and *E*) from the production wells in the Fresno area (California Department of Pesticide Regulation, 1992, 1993, 1994) and in the simulated breakthrough curves (for example, fig. 18*A*) are variable. The variability in concentrations may reflect the distance between the screened interval of the sampled wells and the source of DBCP. The maximum measured DBCP concentrations (fig. 18*D*) are the highest DBCP concentrations measured in all ground-
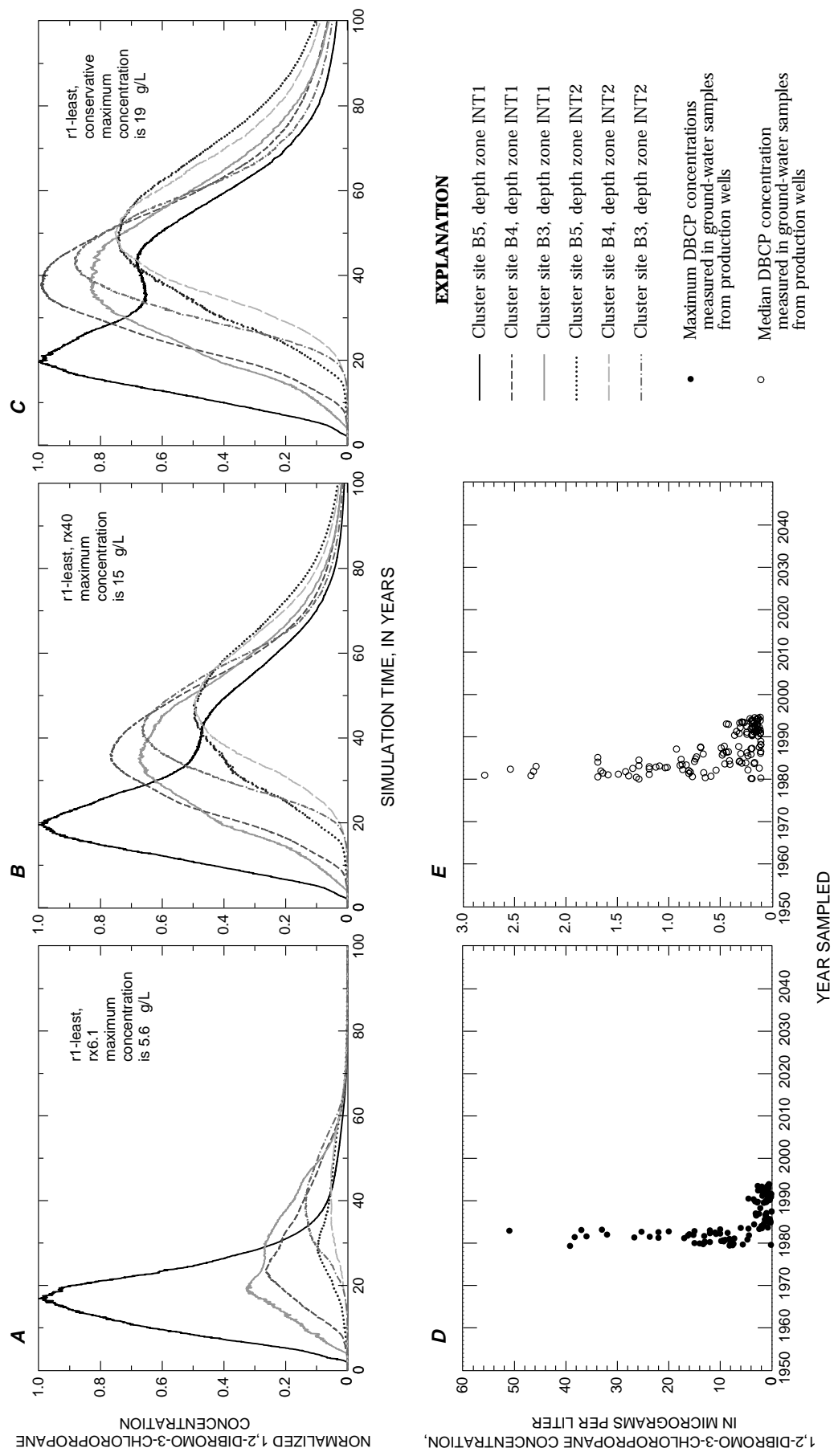
Figure 18. Simulated concentrations of 1,2-dibromo-3-chloropropane (DBCP) and maximum and median DBCP concentrations for ground-water samples collected monthly from production wells in the eastern San Joaquin Valley, California (California Department of Pesticide Regulation, 1992, 1993). Simulated DBCP concentrations are the averaged concentrations for intermediate zone 1 (INT1) 24 to 43 meters below land surface and intermediate zone 2 (INT2) 43 to 55 meters below land surface for high permeability hydrogeologic facies categories and are normalized by the maximum averaged concentration in INT1 and INT2. See table 8 for transport simulation names.

water samples collected from the production wells monthly between 1979–93; similarly, the median measured DBCP concentrations (fig. 18E) are the median DBCP concentrations measured in all samples collected monthly during the same period. Measured DBCP concentrations decreased in the early 1980's; the concentrations in figure 18E resemble the concentrations in the tail-end of the simulated breakthrough curve (fig. 18A), but the measured concentrations decrease more rapidly than any of the simulated breakthrough curves. The sharp decrease in measured concentrations may have been influenced by the significant decrease in the number of wells sampled after about mid-1983. The largest number of samples were collected during 1981–83, which corresponds to the highest measured DBCP concentrations. The number of wells sampled increased again in 1986 and 1989, but DBCP concentrations remained less than 10 μg/L. The decrease in the measured DBCP concentrations is consistent with the decrease in the calculated initial concentration of DBCP (fig. 8) in the 1980's.

The concentrations of DBCP in the breakthrough curve for the 6.1-year half-life simulation for cluster site B5 in zone INT1 (fig. 18A) more closely resembles the measured DBCP concentrations (fig. 18D, E) than the concentrations in any of the other simulated curves because of the relatively sharp decrease in concentration and the slightly concave appearance of the tail-end of the curve. For the transport simulation, most of the flow contributed to this zone is derived from the top recharge boundary (fig. 16). Discrepancies among measured and simulated concentrations in areas dominated by flow from the upgradient boundary indicate that specified concentrations at that boundary are too high or too dispersed even though the assigned concentrations of DBCP in the source cells at the upgradient boundary were selected to resemble concentrations exiting at the downgradient boundary. The effect of the source cells at the upgradient boundary is reflected by the breakthrough curves for the deeper intermediate zone, INT2 (fig. 18A), in which the DBCP concentration at cluster site B3 was higher than the concentration at cluster site B5.

Although DBCP concentrations in ground-water samples from the production wells (fig. 18D, E) seem to represent only the DBCP concentrations for the tail end of the curve, a comparison between the tail end of the measured concentrations with the tail end of the

simulated concentrations allows an evaluation of whether the simulated arrival times for initial and maximum simulated DBCP concentrations are consistent with expected dates for the first DBCP applications and the maximum DBCP concentrations. The arrival times for maximum DBCP concentrations are similar among all the simulations, although the maximum concentration for the 6.1-year half-life simulation arrived about 2.5 years earlier than the maximum concentration for the 40-year half-life and the conservative transport simulations for the shortest travel times (site B5, zone INT1, fig. 18A, B, and C). On the basis of historical DBCP applications and CFC-estimated recharge dates, the first DBCP concentrations may have arrived at the well screens as early as the 1950's (fig. 8), although maximum DBCP concentrations likely occurred between 1960 and 1983 when DBCP was commonly applied (fig. 18D). On the basis of the period of the maximum concentrations for the simulation curves for a 6.1- and a 40-year half-life and for conservative transport at cluster site B5 in zone INT1, if maximum DBCP concentrations in the aquifer occurred as late as 1983, the maximum DBCP concentrations in recharge at the water table would have occurred during the 1960's. The calculated initial concentrations of DBCP in samples from the monitoring wells (fig. 8), however, suggest that the maximum DBCP concentrations in recharge occurred in the 1970's. The arrival times for the maximum concentrations at cluster site B4 and B3 in zone INT1 for the 6.1-year half-life simulation (figure 18A) indicate that the maximum DBCP input would have occurred after about 1960, and the arrival times of the maximum concentrations at these sites for the 40-year half-life and conservative transport simulations would have occurred during the 1940's or earlier, which is inconsistent with available information. The simulated arrival times in the transport model may be longer than the actual arrival times, however, because the calculated particle travel times in the MODPATH simulations (representing advective flow) were about 10 years longer than the average CFC-estimated travel times in the intermediate zones in the model (table 6).

The simulated DBCP concentrations for cluster sites B3, B4, and B5 in zone INT2 (fig. 19A, B, and C) were compared with measured concentrations in samples from well 14S/22E-23F1 near Sanger (fig. 19D) because the concentrations shown in figures 18D and E were collected from wells throughout the region
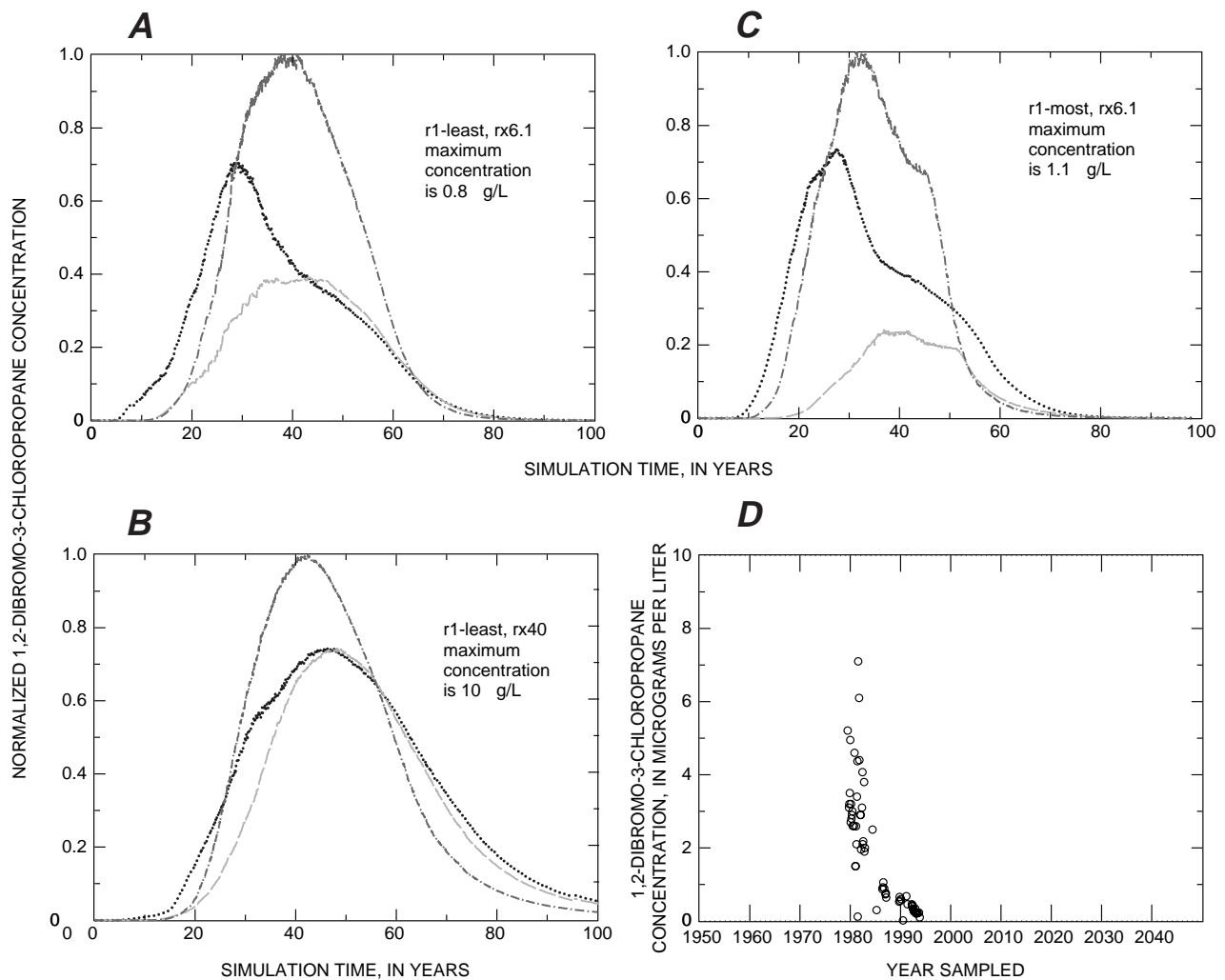
Figure 19. Simulated concentrations of 1,2-dibromo-3-chloropropane (DBCP) and measured DBCP concentrations in ground-water samples from production well 14S/22E-23F1 near Sanger in the eastern San Joaquin Valley, California (California Department of Pesticide Regulation, 1992, 1993). Simulated DBCP concentrations are the averaged concentrations for intermediate zone 2 (INT2) 43 to 55 meters below land surface for high permeability hydrogeologic facies categories and are normalized by the maximum average concentration in INT2. See table 8 for transport simulation names.

and thus do not represent concentrations from any single well in the study area. The depth of well 14S/22E-23F1 is about 58 m below land surface. Simulated breakthrough curves for the intermediate zone 2 (INT2), which is 43 to 55 m below land surface, were used in the comparison. Similar to the maximum and median measured concentrations collected from wells throughout the region (fig. 18D and E), the DBCP concentrations in ground-water samples from well 14S/22E-23F1 decreased sharply after the early 1980's. The data for well 14S/22E-23F1 resemble the concentration data in the tail end of the breakthrough curve (fig. 19), although not all wells in the Fresno area show such a sharp decrease in the concentrations. The measured concentration data for well 14S/22E-23F1 most closely resemble the concentration data in the breakthrough curves for the 6.1-year half-life simulation for r1-most at cluster site B3 and B4 (fig. 19C); if the data for well 14S/22E-23F1 are aligned with the data in the tail end of the breakthrough curve for cluster site B3, the initial concentration front would have arrived in the 1940's, which probably is earlier than the first applications of DBCP. If the simulated arrival times are about 10 years too long, then the first arrival would have been in the 1950's and the maximum concentrations would have been in the 1970's, which is within expected ranges.

The decreasing concentrations of DBCP simulated in the breakthrough curves for simulations for a 40-year half-life and for conservative transport (fig. 18B and C and fig. 19B) are too gradual to resemble the measured DBCP concentrations (fig. 18D and E and fig. 19D). Although the concentrations specified at the upgradient source cells may be unrealistically high, some contribution from upgradient is expected and the concentrations still would be dispersed during transport across the model transect.

Effects of Averaging and a Constant Source of DBCP on Simulation Results

The breakthrough curves for simulated DBCP concentrations for individual layers within each depth zone were evaluated to determine the effects of averaging concentrations across the high-permeability layers. Peak concentrations differed by as much as 30 percent from the averaged peak concentration for the 40-year half-life simulation at cluster site B5 in zone INT1 (fig. 20A). Arrival times of the concentration front also varied by a few years; but for simulation times greater than 50 years, the concentrations were similar among the different layers. The overall effects of averaging do not significantly affect the shape of the concentration breakthrough curves, and therefore, the breakthrough curves for the averaged concentrations may better represent concentrations measured in long-screened production wells.

The simulated DBCP concentrations also may be different from the measured concentrations because of the constant source of DBCP specified at the top recharge boundary for the first 15 years simulated. The constant concentration may not represent the actual DBCP input, although widespread DBCP applications, combined with the dispersive effects of solute movement in the unsaturated zone, could have resulted in a widespread, diffuse source of DBCP at the water table. A simulation was done using two separate pulses of DBCP input to test the effect of a pulsed source of DBCP on concentrations. Recharge at the water table was assigned a constant concentration of 100 µg/L for simulation times from 0 to 5 years and 10 to 15 years. The assigned DBCP concentration for recharge was 0 µg/L for simulation times of 5 to 10 years and 15 to 100 years. The assigned source concentrations at the upgradient boundary were reduced to about half of those used in the earlier simulations (table 7) for simulation periods greater than about 20 years. The breakthrough curves for the resulting DBCP concentrations (fig. 20B) are similar to the breakthrough curves using the constant source concentrations (fig. 18B), except that the curves for the constant-source simulation are more smooth than those for the pulsed source. The arrival time of the peak concentration in the constant-source simulation is similar to the arrival time in the pulsed-source simulation; however, the maximum concentration for zone INT1 at cluster site B5 (24 µg/L; fig. 20B) in the pulsed-source simulation was 55 percent higher than the maximum concentration in the same zone in the constant-source simulation (15 µg/L; fig. 18B) even though the total DBCP mass entering the top recharge
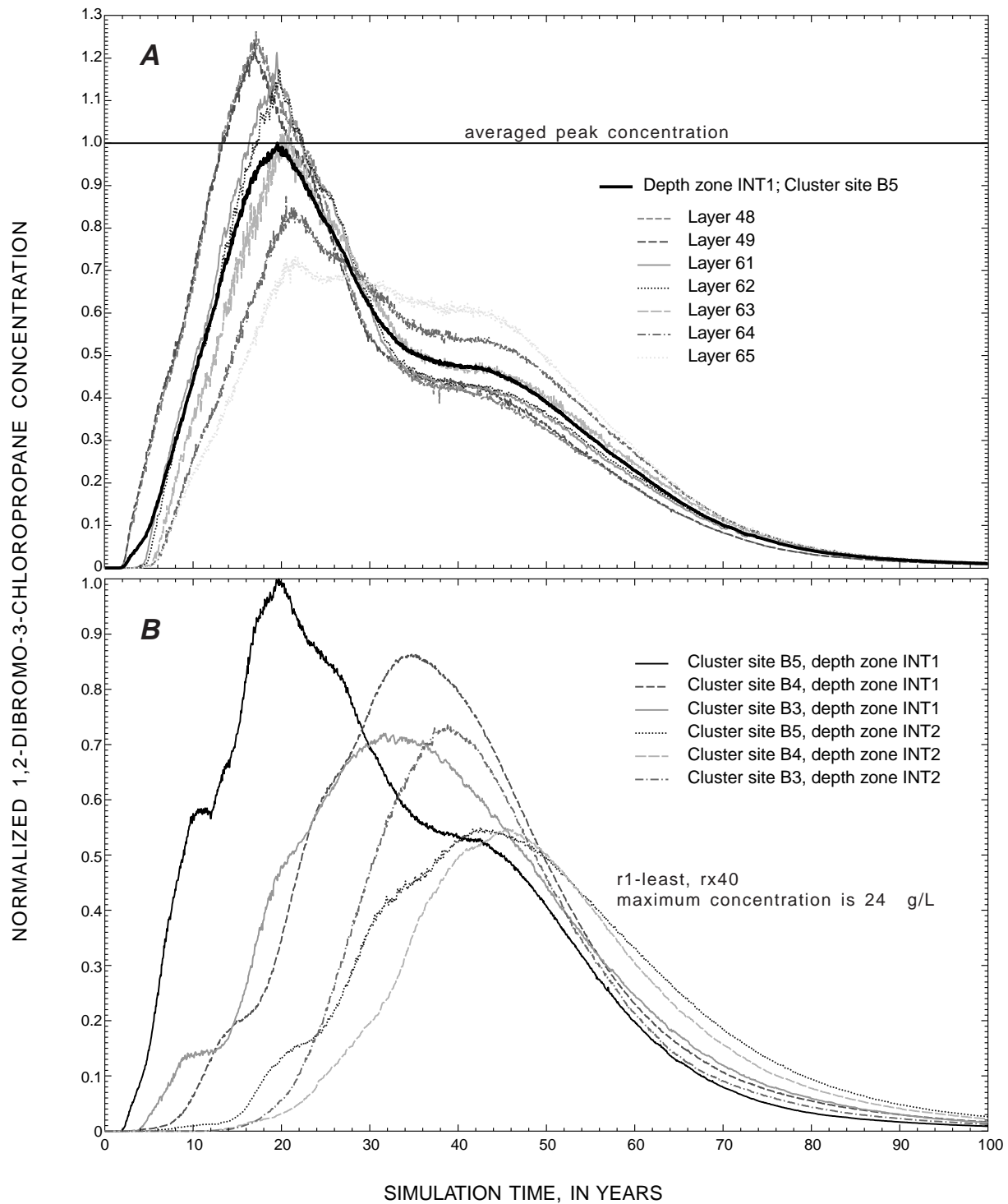
Figure 20. Simulated concentrations of 1,2-dibromo-3-chloropropane (DBCP) for transport simulation r1-least with a 40-year half-life. **A,** Concentrations of DBCP in individual model layers (concentrations are normalized by the maximum averaged concentration for intermediate zone 1(INT1) 24 to 43 m). **B,** Concentrations of DBCP using a pulsed input (concentrations are averaged for zone INT1 and intermediate zone 2 (INT2) 43 to 55 m below land surface and normalized by the maximum averaged concentration of zone INT1 or zone INT2). See table 8 for transport simulation names.

boundary and the upgradient boundary sources increased by only 26 percent overall. This difference in concentrations may reflect the mixing of the two 100 µg/L pulses of DBCP or the arrival of DBCP concentrations from the upgradient boundary, which was specified at a higher concentration than concentrations in the constant-source simulations for the first 20 years simulated. Although the two pulses of DBCP input were separated by 5 years of simulation with no DBCP input, the pulses blend together into one irregularly shaped peak in the breakthrough curve because of the dispersion of DBCP. Perhaps a series of discrete pulses of DBCP in ground-water recharge for the 20- to 25-year period when DBCP was applied could have resulted in a single, irregular pulse at the depths of the production wells in the aquifer. Increasingly widespread and intermittent applications of DBCP would result in increasing dispersion of concentrations in the aquifer.

Simulation of the Effects of Dispersion Using Heterogeneous and Homogeneous Hydraulic Conductivity Distributions

The effects of dispersion on the simulated DBCP concentrations were evaluated by comparing the breakthrough curves simulated using heterogeneous hydrogeologic facies distributions (fig. 18) with those simulated using a homogeneous distribution of hydraulic conductivity (fig. 21). The homogeneous simulation had the same boundary conditions and transport parameters as the heterogeneous simulations. The flow parameters in the homogeneous simulation were adjusted to simulate a volume of flow through each of the boundaries that was approximately equal to the volume of flow in the heterogeneous simulations. In contrast with the heterogeneous simulations, however, the sources of DBCP were not introduced at cells along the upgradient boundary because the breakthrough curves for the heterogeneous simulations most similar to the measured DBCP concentrations were the least influenced by the upgradient boundary. DBCP concentrations were averaged for the same depth zones (fig. 15) as the heterogeneous simulations to facilitate these comparisons.

The resulting breakthrough curves from the homogeneous simulation for conservative transport (fig. 21) had relatively sharp increases and decreases in

concentration. The apparent double peak corresponds to the passing of the peak DBCP concentrations contributed from the upgradient part of the top recharge boundary as water with no DBCP concentrations displaced water with high DBCP concentrations. The peak concentration of 19 µg/L (fig. 18C) in the breakthrough curves, which were simulated using the heterogeneous hydrogeologic facies distribution for conservative transport, was higher than the peak concentration of 5.2 µg/L (fig. 21) in the homogeneous simulation. The breakthrough curves generally were more broad in the heterogeneous simulations than in the homogeneous simulation.

The DBCP breakthrough curve from the homogeneous simulation is most similar to the breakthrough curve from the heterogeneous simulation which used a 6.1-year half-life (fig. 18A) for cluster site B5 in zone INT1, except that the concentrations in the
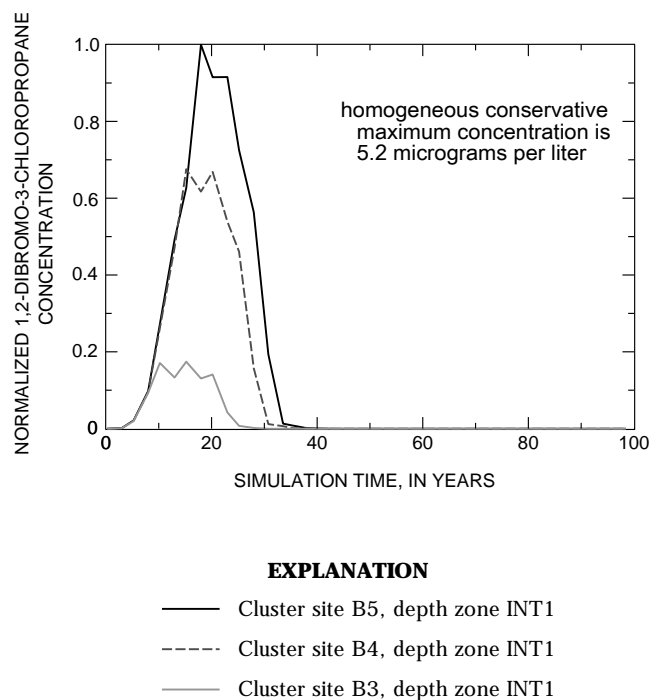
Figure 21. Simulated concentrations of 1,2-dibromo-3-chloropropane (DBCP) using a homogeneous hydraulic conductivity distribution. Simulations used flow and transport parameters similar to heterogeneous simulations. DBCP concentrations are the averaged concentrations for intermediate zone 1 (INT1) 24 to 43 meters below land surface and intermediate zone 2 (INT2) 43 to 55 meters below land surface and normalized by the maximum averaged concentration in zone INT1 or zone INT2.

heterogeneous simulation for the 6.1-year half-life decreased more gradually after the peak than the concentrations in the homogeneous simulation. The steep, slightly concave shape and gradual tail in the concentration breakthrough curve for the heterogeneous simulation may be caused by both the dispersion of concentrations contributed from farther upgradient and the loss of mass attributed to a 6.1-year half-life. Simulated concentrations in the zone INT2 for the homogeneous simulation are nearly zero (less than 0.02 µg/L) because the top recharge boundary is the only source of DBCP and because the DBCP did not move deeper in the transect. The steepness of the breakthrough curves from the homogeneous simulation (fig. 21) resembles the steep decrease in measured concentrations (fig. 18*D* and *E*), except that the measured concentrations decrease more gradually at the tail end of the data.

Simulations of Dispersion

A second series of flow and transport simulations was done to further evaluate the dispersion of DBCP caused by macro-scale heterogeneity in aquifer sediments. Because flow along the transect is predominantly horizontal and because the relative contribution of DBCP from the recharge and upgradient boundaries in the model complicates the evaluation of dispersion alone, the dispersion of DBCP was evaluated in the horizontal direction using a different flow field. The hydrogeologic facies distributions (most and least connected) and the hydraulic conductivity values from the previous r1 simulations (table 5) were used in the analysis. The results of the heterogeneous simulations were then compared with the results of a simulation using a homogeneous distribution of hydraulic conductivity.

The boundary conditions for the top and bottom of the model were no-flow boundaries. Ground-water flow into and out of the model through the upgradient and downgradient boundaries were again assumed to be dependent on hydraulic head and were simulated with head-dependent flow boundaries. The head-dependent boundaries were adjusted to obtain an approximately equal volume of flow through the transect for the heterogeneous and homogeneous hydraulic conductivity distributions and to maintain a horizontal gradient of 0.002. A constant DBCP concentration of 1,000 µg/L was specified at each cell at the upgradient boundary for 150 years of simulation time. As in the previous simulations, a longitudinal dispersivity of 0.03 m (0.1 ft) was specified for each layer in the grid, and a ratio of 0.1 of the longitudinal dispersivity was specified for both the horizontal and the vertical transverse dispersivities. The effective molecular diffusion coefficient was specified as zero. As described previously, the variations in velocity caused by macro-scale heterogeneities were accounted for by directly incorporating the macro-scale structure of the porous media into the flow model. DBCP concentrations were simulated assuming conservative transport. The homogeneous simulation used the same boundary conditions as the heterogeneous simulations; conductance and hydraulic conductivity then were adjusted to obtain an equal amount of flow through the transect. An effective porosity of 34 percent was used in the homogeneous simulation, which is the weighted average effective porosity for the heterogeneous hydrogeologic facies distributions.

The breakthrough curves for the heterogeneous simulations reflect the dispersion of DBCP caused by macro-scale velocity variations across the transect (fig. 22). DBCP concentrations were averaged for each layer in the column corresponding to cluster site B5 and divided by the input concentration assigned at the upgradient boundary. The breakthrough curves are asymmetric, with a long tail for concentrations at simulation times greater than 100 years (fig. 22). Concentrations arrive earliest in the most connected heterogeneous simulation (table 9), consistent with the determination that the most connected distribution had the highest degree of horizontal interconnection of high-permeability categories. The average velocity for the least connected heterogeneous simulations (116 m/yr) was slightly higher than the velocity for the most connected heterogeneous simulation (110 m/yr) on the basis of mean breakthrough arrival times. The breakthrough curve for the homogenous simulation represents an average travel time across the transect without preferential flow paths. On the basis of an arrival time of 52 years, the average velocity in the homogeneous simulation is about 110 m/yr, which is the same as the most connected heterogeneous simulation. These generally insignificant differences in average velocity and the breakthrough curves indicate that the difference in the amount of interconnected high-permeability categories is minor between the most and least connected heterogeneous simulations. The model that generated these hydrogeologic facies

distributions generally was well-constrained over the extent of this two-dimensional transect.

An apparent longitudinal dispersivity was calculated from the relative concentration breakthrough curves for the heterogeneous simulations using a graphical method that relates the variance of the curve, travel time, and velocity to dispersivity (Domenico and Schwartz, 1990):

$$\alpha_L = \frac{v(\sigma_t)^2}{2t} \tag{9}$$

where α_L is the apparent longitudinal dispersivity, in m; v is velocity, in m/s; σ_t is the standard deviation in time, in years; and t is travel time, in years. The apparent longitudinal dispersivities calculated for the most and least connected hydrogeologic facies distributions (fig. 22) were 1,600 and 1,400 m, respectively, for a distance of 5,300 m across the transect. The velocity used to calculate the dispersivity in equation 6 was determined from an independent estimate of the effective hydraulic conductivity of 0.0015 m/s derived from an analysis of a three-dimensional hydrogeologic facies distribution of the
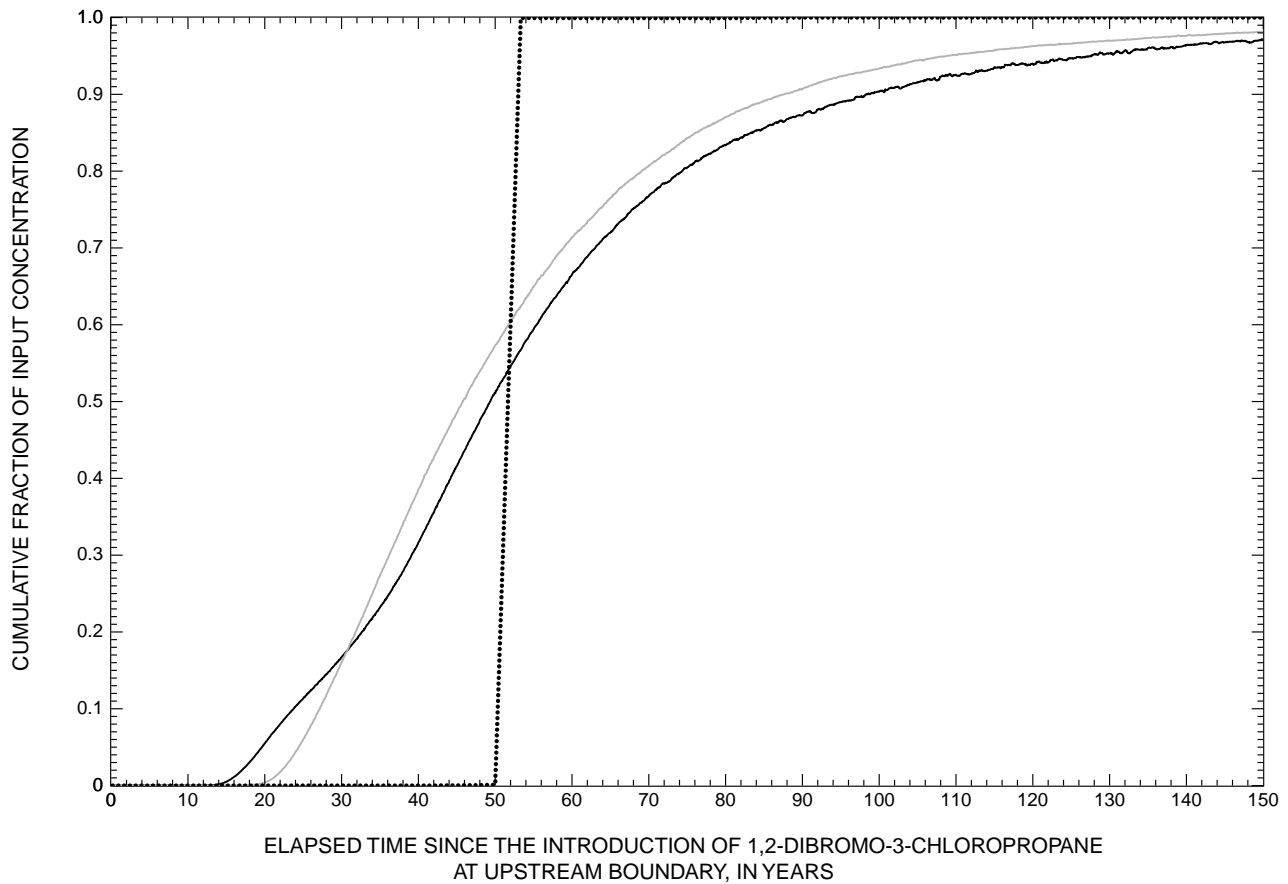
EXPLANATION

——— Most connected case; r1 parameters

——— Least connected case; r1 parameters

·········· Homogeneous

Figure 22. Simulated 1,2-dibromo-3-chloropropane (DBCP) breakthrough curves for transport simulations using a horizontal flow field. Cumulative fraction of input concentration is the fraction of input concentration arriving at cluster site B5 (column 51). Hydraulic conductivity values used in the heterogeneous simulations are in given in table 5.

study area (Gary Weissmann, University of California, written commun., 1998). These calculated values of longitudinal dispersivity are close to the upper limit of the range of measured longitudinal dispersivity values for a scale of about 5,300 m (Domenico and Schwartz, 1990). Although it was demonstrated in the particle-tracking analysis for this current study that the travel times in the deep zone of the model were unrealistically long, calculations of the apparent longitudinal dispersivities for the breakthrough curves for only the shallow and the intermediate zones of the model were nearly the same (1,400 m for both cases). The shallow and intermediate zones of the model are only 52 percent of the thickness of the model, but 71 percent of the simulated DBCP mass entering the transect exits through these zones.

The results of the simulations of dispersion demonstrate that DBCP concentrations are affected by dispersion caused by macro-scale heterogeneity as indicated by the difference in the shape of the breakthrough curves between the heterogeneous and homogeneous simulations and the estimates of apparent longitudinal dispersivity. The dispersion in these simulations may be exaggerated, however, because simulated flow and transport in the two-dimensional model is constrained by the unit depth in the y direction. In reality, the low-permeability hydrogeologic facies may be laterally discontinuous, allowing ground water with DBCP to flow around these layers.

Significance of Simulation Results

The comparison between simulation results and measured DBCP concentration data indicates that, unless DBCP is assumed to decay significantly during transport, the simulated DBCP concentrations are too dispersed to resemble the sharp decrease in the measured DBCP concentrations. The similarity between the measured DBCP concentrations and the concentrations simulated in the breakthrough curve for cluster site B5 in zone INT1 for the 6.1-year half-life simulations (fig. 18) indicates that measured DBCP concentrations reflect rapid transport paths for the period that ground water containing DBCP was recharged. Furthermore, the sharp decrease in measured DBCP concentrations in the early 1980's suggests that a 40-year half-life is too slow because simulated concentrations using a 40-year half-life arrive earlier than expected and because concentrations are greater than half of initial concentrations for the period ending in the 1980's.

Simulation results indicate that the dispersion caused by macro-scale heterogeneity results in decreased DBCP concentrations; however, if DBCP was transported more than about 3 to 4 km across the model transect, the concentrations simulated in the breakthrough curves were more dispersed than indicated by the measured DBCP concentrations (figs. 18 and 19). The long, gradual decrease in concentrations and arrival times of maximum concentrations for simulations with a 40-year half-life (or longer) do not resemble the data for the measured

Table 9. Breakthrough arrival times of 1,2-dibromo-3-chloropropane (DBCP) at cluster site B5 for selected proportions of the total DBCP mass specified at the upgradient boundary in transport simulations and average velocity

[Arrival time greater than 150 years indicates that 99 percent of the mass had not passed the observation cells at 150 years, which is the end of the simulation time. >, actual value is greater than value shown]

Arrival time of DBCP mass, in years					Average velocity, meters per year
1 percent	15 percent	50 percent (mean breakthrough)	85 percent	99 percent	
Most connected (r1-most dispersion test)					
16	28	49	84	>150	116
Least connected (r1-least dispersion test)					
21	30	46	76	>150	110
Homogeneous					
50	51	52	53	53	110

concentrations, except for a simulation with a 6.1-year half-life and a relatively short travel path. For this simulation, the breakthrough curves had a slightly concave, tailing shape, and the arrival times of maximum concentrations more closely resembled the measured concentration data.

The unrealistically long, gradual decrease in concentrations and the late arrival of maximum concentrations in the 40-year half-life and conservative transport simulations may partly be attributed to the assigned upgradient boundary sources of DBCP. Some contribution from upgradient is expected because of the widespread detections of DBCP in wells at depths greater than about 40 m below land surface and because of the predominantly horizontal ground-water flow direction. Furthermore, the simulated dispersion may be exaggerated because the simulated flow and transport in the two-dimensional model is constrained by the unit depth in the y direction. DBCP travel times may be influenced by the pumping of large-volume production wells that can induce sufficient vertical gradients to transport DBCP rapidly downward to the well screens. The influence of the three-dimensional flow paths and the pumping wells was not modeled explicitly; however, the ground-water travel times determined from the CFC-estimated recharge dates indicate that the simulated travel times to the intermediate zones are within reasonable ranges.

The DBCP transport model accounts for transport and first-order decay processes affecting DBCP concentrations other than macro-scale dispersion, which is modeled explicitly. The possibility that measured DBCP concentrations reflect the effects of a 6.1-year half-life does not conflict with the lack of evidence of transformation of DBCP to BAA. The apparent DBCP decay is caused by dispersion and other processes, such as ground-water pumping and reapplication of irrigation water or different chemical or biological transformation pathways. The model does not explicitly account for the effects of removal of DBCP by a pumping well or reapplication as irrigation water, but these processes are represented indirectly in the first-order decay term. Because the DBCP concentrations on the simulated breakthrough curves resemble the measured DBCP concentrations only when transport time is short or when DBCP is significantly decayed along the long transport pathways, dispersion alone cannot cause the decrease in measured DBCP concentrations.

Assuming the breakthrough curve at cluster site B5 for the 6.1-year half-life simulations (fig. 18A) represents a reasonable approximation of the processes affecting DBCP concentrations in ground water, a duration time for DBCP concentrations that remain greater than the MCL of 0.2 µg/L can be estimated by evaluating the length of a simulation time in which concentrations were greater than the MCL. The maximum measured concentration is about 10 times the maximum simulated concentration for the 6.1-year half-life simulation for zone INT1 at cluster site B5; the simulated concentrations were multiplied by a factor of 10 because the maximum simulated concentration is a linear function of the model input concentrations. Using these estimated concentrations and assuming that the initial input concentrations of DBCP were equivalent to the maximum measured concentrations, DBCP may persist at concentrations greater than the MCL for 70 years after the initial input of DBCP at the water table.

SUMMARY AND CONCLUSIONS

This report presents the results of a study of the transport and fate of DBCP in ground water in the eastern San Joaquin Valley, California. The hydrogeologic investigation assesses the relative importance of chemical transformation, dispersion caused by macro-scale heterogeneity, and ground-water pumping and reapplication of irrigation water in affecting DBCP concentrations in the aquifer. The results of this study are relevant to the understanding of the underlying physical and chemical processes that influence the concentrations of DBCP in the aquifer.

Twenty monitoring wells were installed during 1994–95 at six sites along a 4.6-km transect and ground-water samples were collected and analyzed for DBCP and its primary transformation product, BAA. Ground-water samples also were collected and analyzed for concentrations of CFCs and tritium to provide a quantitative estimate of the age of ground water in the aquifer. The estimated ages of the ground-water samples were then used to evaluate whether computed advective travel times in a series of two-dimensional, steady-state simulations were similar to actual travel times in the aquifer. Two steady-state flow solutions were used in a series of transport simulations incorporating dispersion and first-order decay to evaluate the relative importance of the processes of

chemical transformation, macro-scale dispersion, and in a relative sense, ground-water pumping and reapplication of irrigation water on DBCP concentrations.

DBCP was detected in at least one ground-water sample from 13 of the 20 wells (65 percent) monitored for this study; concentrations ranged from less than 0.03 to 6.4 μg/L. Concentrations were greater than the MCL of 0.2 μg/L in samples from 11 of the 13 wells with DBCP detections; these wells, however, are not used for drinking-water supply. Ground-water samples from the monitoring wells at shallow and intermediate depths generally contained the highest concentrations of DBCP, nitrate, and specific conductance. DBCP was not detected in any ground-water samples from wells with depths greater than 70 m. Nitrate and DBCP concentrations were positively correlated. The co-occurrence of nitrate and DBCP may reflect the susceptibility of individual wells to contamination controlled by factors, such as sediment texture and distance from the contaminant source to the well, that affect travel time through the subsurface.

Ground-water recharge dates estimated from concentrations of CFC-11 and CFC-12 in ground-water samples from the 20 monitoring wells along the monitoring well transect indicate that ground water near the water table was recharged within the past 10 years and that ground water in the deepest wells was recharged as much as 55 years before sampling. Ground-water age generally increases with depth because a longer time is required for ground water to move deeper in the flow system. Ground-water recharge dates and concentrations of DBCP, nitrate, tritium, and specific conductance in samples from the shallow monitoring wells were more variable along the transect than in the deep monitoring wells, likely resulting from different land-use practices, local ground-water pumping, and heterogeneity in sediment texture and increased mixing as solutes travel to the deeper parts of the aquifer.

Nitrate concentrations and specific conductance were negatively correlated with travel time, indicating that the highest nitrate concentrations and specific conductance occur in the most recently recharged ground water. DBCP concentrations, however, were not significantly correlated with travel time; this lack of correlation may be caused by the spatial and temporal patterns of DBCP application relative to the application of nitrogen fertilizers.

Initial concentrations of DBCP, calculated from CFC-estimated travel times and a half-life of 6.1 years, shows three distinct pulses of DBCP with similar peak concentrations. The first pulse occurs in the 1950's, which is consistent with the reported date that DBCP application began. Maximum initial concentrations, calculated using a 6.1-year half-life, are about 50 μg/L, which is similar to maximum concentrations in ground water sampled from wells in the study area during the early 1980's. Maximum DBCP concentrations in the aquifer may have been higher than 50 μg/L, however, because the ground-water samples were collected from long-screened irrigation, municipal, and domestic wells in which high concentrations in the discrete zones of the aquifer may have been diluted by zones containing low concentrations. For comparison, a longer half-life of 40 years results in lower calculated maximum concentrations than those calculated for the 6.1-year half-life. In contrast to the initial concentrations of DBCP, the estimated initial concentrations of nitrate show that nitrate concentrations in recharge increased with time, assuming that nitrate is transported conservatively in this well-oxygenated ground-water system.

BAA, a stable end product of DBCP transformation by dehydrohalogenation followed by hydrolysis, was not detected at or above 0.03 μg/L in any ground-water samples from the 20 monitoring wells. The lack of detection of BAA in ground water indicates that the half-life for this reaction is very long and that previous laboratory studies do not accurately reflect the rate of transformation of DBCP to BAA in the aquifer. DBCP transformation to BAA is not a significant process affecting DBCP concentrations in the aquifer.

Tritium concentrations in samples of ground water recharged between 1961 and 1970 were lower than expected, and concentrations in the samples of ground water recharged in 1986, 1991, and 1992 were higher than expected compared with the tritium concentrations in precipitation for those years. The anomalous tritium concentrations indicate that the tritium concentrations may be affected by the process of ground-water pumping and reapplication of irrigation water. As ground water is pumped and then reapplied at land surface for irrigation, the CFC concentrations quickly reequilibrate with the concentrations of CFCs in the atmosphere. Because the equilibration rate for tritium is slow relative to CFCs, the tritium concentrations remain unchanged.

A conceptual two-dimensional numerical flow and transport modeling approach was used during this study to test hypotheses addressing dispersion, transformation rate, and in a relative sense, effects of ground-water pumping and reapplication of irrigation water on DBCP concentrations in the aquifer. The flow and transport simulations, which represent hypothetical steady-state flow conditions in the aquifer, were used to refine the conceptual understanding of the aquifer system. The numerical, finite-difference ground-water flow model MODFLOW was used to simulate the distribution of hydraulic heads and ground-water flow rates along the monitoring well transect. The model of the transect was discretized into a grid of finite-difference cells and simulated as a vertical plane of unit width in the y direction with no flow orthogonal to the x-z plane. A hydraulic conductivity distribution was specified in the horizontal (x) and vertical (z) directions on the basis of the distribution of hydrogeologic facies generated using a transition-probability based indicator approach. Two distributions were selected from a series of 50 equiprobable realizations of the hydrogeologic facies—the "most" and the "least" connected distributions in terms of the degree of horizontal interconnection of high permeability categories (gravel and coarse sand or gravel categories). The flow simulation results were calibrated to match the approximate horizontal and vertical hydraulic gradients in the study area. Ground-water path lines and advective travel times for each flow simulation were calculated using the program MODPATH. Calculated particle travel times were compared with the travel times estimated from the CFC concentrations to determine whether the results of the flow model reasonably represent the hydrologic system along the monitoring well transect.

In spite of the inherent limitations of the two-dimensional, steady-state flow model in representing the ground-water flow system in the study area, the boundary conditions and "average" parameters used in the model did provide a reasonable approximation of the flow system for depths of less than 55 m below land surface. The model, however, did not accurately represent the flow system for depths greater than 55 m below land surface possibly because the model is two-dimensional and therefore, during the simulations, water was forced to flow through the large proportion of low-permeability hydrogeologic facies at greater depths resulting in extremely long particle travel times.

Because most of the wells in the study area that were sampled for DBCP are screened at depths less than 55 m below land surface, the lack of an accurate representation of the flow system for depths greater than 55 m below land surface is not expected to significantly affect the understanding of the processes affecting DBCP transport and fate.

A series of transport simulations was done to evaluate the combined effects of dispersion owing to macro-scale heterogeneity and first-order decay on DBCP concentrations in the model transect using the three-dimensional solute-transport model MT3D. Simulated DBCP concentrations were compared with measured concentrations in the ground-water samples from production wells in the Fresno area. The comparison among simulation results and measured DBCP concentration data indicates that, unless DBCP is assumed to decay significantly during transport, the simulated DBCP concentrations are too dispersed to resemble the measured DBCP concentrations, which showed a sharp decrease in concentrations. The simulation results indicate that dispersion caused by macro-scale heterogeneity results in decreased DBCP concentrations; however, when DBCP was transported more than about 3 to 4 km across the model transect, the DBCP concentrations on the simulated breakthrough curves were more dispersed than the concentrations on the measured DBCP curves. The long, gradual decrease in the computed concentrations and the arrival times of maximum concentrations for simulations with a 40-year half-life (or longer) do not resemble the measured concentration data, whereas the simulation with a 6.1-year half-life and a relatively short travel path resembles the measured data more closely.

The unrealistically long, gradual decrease in concentrations and the late arrival of maximum concentrations in the 40-year half-life and conservative transport simulations may partly be attributed to the assigned upgradient boundary sources of DBCP. Some contribution from upgradient is expected because of the widespread detections of DBCP in wells at depths greater than about 40 m below land surface and because of the predominantly horizontal ground-water flow direction. The influence of the three-dimensional flow paths and the pumping wells were not modeled explicitly; however, the ground-water travel times determined from the CFC-estimated recharge dates indicate that the simulated travel times to the intermediate depth zones are within reasonable ranges.

The DBCP transport model accounts for transport and first-order decay processes affecting DBCP concentrations other than macro-scale dispersion, which is modeled explicitly. The possibility that measured DBCP concentrations reflect the effects of a 6.1-year half-life does not conflict with the lack of evidence of transformation of DBCP to BAA. The apparent DBCP decay may be caused by other processes, such as ground-water pumping and reapplication of irrigation water or different chemical or biological transformation pathways. The model does not explicitly account for the effects of removal of DBCP by ground-water pumping and reapplication of irrigation water, but these processes are represented indirectly in the first-order decay term. Because the simulated breakthrough curves resemble curves for the measured DBCP concentrations only when transport time was short or when DBCP had decayed significantly along the long transport pathways, dispersion alone cannot cause the decrease in measured DBCP concentrations. Assuming that the breakthrough curve for cluster site B5 for the 6.1-year half-life simulations represents a reasonable approximation of the processes affecting DBCP concentrations in ground water and assuming that the initial input concentrations of DBCP were equivalent to the maximum measured concentrations, DBCP may persist in the aquifer system in the study area at concentrations greater than the MCL for 70 years after the initial input of DBCP at the water table.

REFERENCES CITED

Alexander, R.B., and Smith, R.A., 1990, County-level estimates of nitrogen and phosphorus fertilizer use in the United States, 1945 to 1985: U.S. Geological Survey Open-File Report 90-130, 12 p.

Anderson, M.P., and Woessner, W.W., 1992, Applied groundwater modeling: simulation of flow and advective transport: New York, Academic Press, 381 p.

Bertoldi, G.L., Johnston, R.H., and Evenson, K.D., 1991, Ground-water in the Central Valley, California—A Summary report: U.S. Geological Survey Professional Paper 1401-A, 44 p.

Biggar, J.W., Nielsen, D.R., and Tillotson, W.R., 1984, Movement of DBCP in laboratory soil columns and field soils to groundwater: Environmental Geology, v. 5, no. 3, p. 127–131.

Bloom, R.A., and Alexander, Martin, 1990, Microbial transformation of 1,2-dibromo-3-chloropropane (DBCP): Journal of Environmental Quality, v. 19, p. 722–726.

Bouwer, Herman, 1978, Groundwater hydrology: New York, Mc-Graw Hill, Inc., 480 p.

Bouwer, Herman, and Rice, R.C., 1976, A slug test for determining hydraulic conductivity of unconfined aquifers with completely or partially penetrating wells: Water Resources Research, v. 12, no. 3, p. 423–428.

Burlinson, N.E., Lee, L.A., and Rosenblatt, D.H., 1982, Kinetics and products of hydrolysis of 1,2-dibromo-3-chloropropane: Environmental Science and Technology, v. 16, no. 9, p. 627–632.

Bu, X., and Warner, M.J., 1995, Solubility of chlorofluorocarbon 113 in water and seawater: Deep Sea Research, v. 42, p. 1151–1161.

Burow, K.R., Weissmann, G.S., Miller, R.D., and Placzek, Gary, 1997, Hydrogeologic facies characterization of an alluvial fan near Fresno, California, using geophysical techniques: U.S. Geological Survey Open-File Report 97-46, 15 p.

Burow, K.R., Shelton, J.L., and Dubrovsky, N.M., 1998a, Occurrence of nitrate and pesticides in ground water beneath three agricultural land-use settings in the eastern San Joaquin Valley, California: U.S. Geological Survey Water-Resources Investigations Report 97-4284, 51 p.

Burow, K.R., Stork, S.V., and Dubrovsky, N.M., 1998b, Nitrate and pesticides in ground water in the eastern San Joaquin Valley, California: Occurrence and trends: U.S. Geological Survey Water-Resources Investigations Report 98-4040A, 33 p.

Busenberg, Eurybiades, and Plummer, L.N., 1992, Use of chlorofluorocarbons (CCl_3F and CCl_2F_2) as hydrologic tracers and age-dating tools-The alluvium and terrace system of central Oklahoma: Water Resources Research, v. 28, no. 9, p. 2257–2283.

California Department of Food and Agriculture, 1973, Pesticide use data: Computer tapes available from California Department of Food and Agriculture, Sacramento, CA 95814.

California Department of Pesticide Regulation, 1992, Sampling for pesticide residues in California well water: 1992 well inventory data base, cumulative report 1986–1992: Seventh Annual Report to the Legislature, State Department of Health Services, Office of Environmental Health Hazard Assessment, and the State Water Resources Contorl Board, Report number EH 93-02, 222 p.

———1993, Sampling for pesticide residues in California well water: 192 well inventory data base, 1993 update: Eighth Annual Report to the Legislature, State Department of Health Services, Office of Environmental Health Hazard Assessment, and the State Water Resources Contorl Board, Report number EH 93-06, 167 p.

———1994, Sampling for pesticide residues in California well water: 1992 well inventory data base, 1994 update: Ninth Annual Report to the Legislature, State Department of Health Services, Office of Environmental Health Hazard Assessment, and the State Water Resources Control Board, Report number EH 94-06, 151 p.

California Department of Water Resources, 1971, Land use in California: An index to surveys conducted by the California Department of Water Resources, 1950–1970: California Department of Water Resources Bulletin 176, 16 p.

———1986, Crop water use in California: California Department of Water Resources Bulletin 113-4, 116 p.

California State University, Fresno Foundation, 1994, Strategy for mitigation of DBCP contamination of Kings ground water basin: Contract report prepared for California State Water Resources Control Board, No. 1-234-250-0, variously paged.

Carle, S.F., 1997, Implementation schemes for avoiding artifact discontinuities in simulated annealing: Mathematical Geology, v. 29, no. 2, p. 231–244.

Carle, S.F., and Fogg, G.E., 1996, Transition probability-based indicator geostatistics: Mathematical Geology, v. 28, no. 4, p. 453–476.

———1997, Modeling spatial variability with one- and multi-dimensional continuous-lag Markov chains: Mathematical Geology, v. 29, no. 7, p. 891–918.

Carle, S.F., LaBolle, E.M., Weissmann, G.S., VanBrocklin, David, and Fogg, G.E., 1998, Geostatistical simulation of hydrostratigraphic architecture, a transition probability/Markov approach, in Concepts in Hydrogeology and Environmental Geology: SEPM (Society for Sedimentary Geology), Special Publication No. 1., p. 147–170.

Castro, C.E., and Belser, N.O., 1968, Biodehalogenation; Reductive dehalogenation of the biocides ethylene dibromide, 1,2-dibromo-3-chloropropane, and 2,3-dibromobutane in soil: Environmental Science and Technology, v. 2, no. 3, p. 298–303.

Cehrs, D., Soenke, S., and Bianchi, W.C., 1980, A geologic approach to artificial recharge site selection in the Fresno-Clovis area, California: U. S. Department of Agriculture Technical Bulletin 1604, 73 p.

Cohen, D.B., 1986, Ground water contamination by toxic substances, a California assessment: Washington D.C.,

American Chemical Society Symposium Series 3.5, v. 315, p. 499–529.

Cooper, H.H, Bredehoeft, J.D., and Papadopulos, S.S., 1967, Response of a finite-diameter well to an instantaneous charge of water: Water Resources Research, v. 3, p. 263–269.

Cooper, H.H., and Jacob, C.E., 1946, A generalized graphical method for evaluating formation constants and summarizing well field history: Transactions of the American Geophysical Union, v. 27, p. 526–534.

Coplen, T.B., Kendall, Carol, and Davis, G.H., 1985, Oxygen and hydrogen stable isotopes measurements of ground waters of the central west side of the San Joaquin Valley, California: U.S. Geological Survey Open-File Report 85-490, 21 p.

Coplen, T.B., Wildman, J.D., and Chen, J., 1991, Improvements in the gaseous hydrogen-water equilibration technique for hydrogen isotope ratio analysis: Analytical Chemistry, v. 63, p. 910–912.

Craig, H., 1961, Isotopic variations in meteoric waters: Science, v. 133, p. 1702-1703.

Davis, G.H., and Coplen, T.B., 1989, Late Oceanside paleohydrogeology of the western San Joaquin Valley, California, as related to structural movements in the central Coast Ranges: Boulder, Colo., Geological Society of America Special Paper 234, 40 p.

Davis, G.H., Green, J.H., Olmsted, F.H., and Brown, D.W., 1959, Ground-water conditions and storage capacity in the San Joaquin Valley, California: U.S. Geological Survey Water-Supply Paper 1469, 287 p.

Deeley, G.M., Reinhard, Martin, and Stearns, S.M., 1991, Transformation and sorption of 1,2-dibromo-3-chloropropane in subsurface samples collected at Fresno, California: Journal of Environmental Quality, v. 20, no. 3, p. 547–556.

Domagalski, J.L., 1997, Pesticides in surface and ground water of the San Joaquin-Tulare basins, California: Analysis of available data, 1966 through 1992: U.S. Geological Survey Water-Supply Paper 2468, 74 p.

Domagalski, J.L, and Dubrovsky, N.M., 1991, Regional assessment of nonpoint-source pesticide residues in ground water, San Joaquin Valley, California: U.S. Geological Survey Water-Resources Investigations Report 91-4027, 64 p.

Domenico, P.A., and Schwartz, F.W., 1990, Physical and chemical hydrogeology: New York, John Wiley and Sons, 824 p.

Fishman, M.J., 1993, Methods of analysis by the U.S. Geological Survey National Water Quality Laboratory—Determination of inorganic and organic constituents in water and fluvial sediments: U.S. Geological Survey Open-File Report 93-125, 127 p.

Fishman, M.J., and Friedman, L.C., 1985, Methods for determination of inorganic and organic substances in water and fluvial sediments: U.S. Geological Survey Open-File Report 85-495, 709 p.

Fogg, G.E., 1990, Architecture and interconnectedness of geologic media: role of the low-permeability facies in flow and transport, in Neuman, S.P., and Neretnieks, Ivars, eds., 1990, Hydrogeology of Low Permeability Environments: Proceedings of the 28th International Geological Congress, v. 2, July 9-19, 1989, Washington D.C., p. 19–40

Freeze, R.A., and Cherry, J.A., 1979, Groundwater: Englewood Cliffs, New Jersey, Prentice-Hall, 604 p.

Fresno Irrigation District, 1993, Ground-water elevation map, January, 1993: Fresno, California, Fresno Irrigation District, scale 1 inch = 2.5 miles.

Gilliom, R.J., Alley, W.M., and Gurtz, M.E., 1995, Design of the National Water-Quality Assessment Program: Occurrence and distribution of water-quality conditions: U.S. Geological Survey Circular 1112, 33 p.

Gronberg, J.M., Dubrovsky, N.M., Kratzer, C.R., Domagalski, J.L., Brown, L.R., and Burow, K.R., 1998, Environmental setting and study design for assessing water quality in the San Joaquin-Tulare basins, California: U.S. Geological Survey Water-Resources Investigations Report 97-4205, 45 p.

Halmann, M., Hunt, A.J., and Spath, D., 1992, Photodegradation of dichloromethane, tetrachloroethylene and 1,2-dibromo-3-chloropropane in aqueous suspensions of TiO_2 with natural, concentrated and simulated sunlight: Solar Energy Materials and Solar Cells, v. 26, p. 1–16.

Hem, J.D., 1989, Study and interpretation of the chemical characteristics of natural water: U.S. Geological Survey Water-Supply Paper 2254, 263 p.

International Atomic Energy Agency, 1981, Statistical treatment of environmental isotope data in precipitation: International Atomic Energy Agency Technical Report Series No. 2, 2 p.

Journel, A.G., and Huijbregts, C.J., 1978, Mining geostatistics: London, Academic Press, 600 p.

Kipp, K.L., Jr., 1986, Adaptation of the Carter-Tracy water influx calculation to groundwater flow simulation: Water Resources Research, v. 22, no. 3, p. 423–428.

Konikow, L.F., and Bredehoeft, J.D., 1978, Computer model of two-dimensional solute transport and dispersion in ground water: U.S. Geological Survey Techniques of Water-Resources Investigations, book 7, chap. C2, 90 p.

Koterba, M.T., Wilde, F.D., and Lapham, W.W., 1995, Ground-water data-collection protocols and procedures for the National Water-Quality Assessment Program: Collection and documentation of water-quality samples and related data: U.S. Geological Survey Open-File Report 95-399, 113 p.

Lehmann, E.L., 1975, Nonparametrics, statistical methods based on ranks: Oakland, Calif., 457 p.

Litton, G.M., and Guymon, G.L., 1993, Laboratory experiments evaluating the transport and fate of DBCP in Hanford sandy loam: Journal of Environmental Quality, v. 22, p. 311–325.

Loague, K., Lloyd, D., Nguyen, A., Davis, S.N., and Abrams, R.H., 1998a, A case study simulation of DBCP groundwater contamination in Fresno County, California, 1. leaching through the unsaturated subsurface: Journal of Contaminant Hydrology, v. 29, no. 2, p. 109–136.

Loague, K., Abrams, R.H., Davis, S.N., Nguyen, A., and Stewart, I.T., 1998b, A case study simulation of DBCP groundwater contamination in Fresno County, California, 2. transport in the saturated subsurface: Journal of Contaminant Hydrology, v. 29, no. 2, p. 137–163.

Madison, R.J., and Brunett, J.O., 1985, Overview of the occurrence of nitrate in ground water of the United States, in National Water Summary 1984—Hydrologic events, selected water-quality trends, and ground-water resources: U.S. Geological Survey Water-Supply Paper 2275, p. 93–105.

McDonald, M.G., and Harbaugh, A.W., 1988, A modular three-dimensional finite-difference ground-water flow model: U.S. Geological Survey Techniques of Water-Resources Investigations, book 6, chap. A1, 586 p.

Michel, R.L., 1989, Tritium deposition in the continental United States, 1953-83: U.S. Geological Survey Water-Resources Investigations Report 89-4072, 46 p.

Mueller, D.K., and Helsel, D.R., 1996, Nutrients in the Nation's waters, too much of a good thing?: U.S. Geological Survey Circular 1136, 24 p.

Muir, K.S., 1977, Ground water in the Fresno area, California: U.S. Geological Survey Water-Resources Investigations Report 77-59, 22 p.

Nightingale, 1972, Nitrates in soil and ground water beneath irrigated and fertilized crops: Soil Science, v. 114, no. 4, p. 300–311.

Nolte, G.S., 1957, The collection and disposal of storm and flood waters in the Fresno metropolitan area—a report for the Fresno Metropolitan Flood Control District, Fresno County, California: Palo Alto, George Nolte, Inc., 83 p.

Owens, L.B., Edwards, W.M., and Van Keuren, R.W., 1992, Nitrate levels in shallow ground water under pastures receiving ammonium nitrate or slow-release nitrogen fertilizer: Journal of Environmental Quality, v. 21, p. 607–613.

Page, R.W., and LeBlanc, R.A., 1969, Geology, hydrology, and water quality in the Fresno area, California: U.S. Geological Survey Open-File Report, 70 p., 21 plates.

Panshin, S.Y., 1997, Determining concentrations of 2-bromoallyl alcohol and dibromopropene in ground water using quantitative methods: U.S. Geological Survey Open-File Report 97-43, 7 p.

Papadopulos, S.S., Bredehoeft, J.D., and Cooper, H.H., Jr., 1973, On the analysis of slug test data: Water Resources Research, v. 9, no. 4, p. 1087–1089.

Peoples, S.A., Maddy, K.T., Cusick, W., Jackson, T., Cooper, C., and Frederickson, A.S., 1980, A study of samples of well water collected from selected areas in California to determine the presence of DBCP and certain other pesticide residues: Bulletin Environmental Contaminant Toxicology, v. 24, no. 4, p. 611-618.

Plummer, L.N., Michel, R.L., Thurman, E.M., and Glynn, P.D., 1993, Environmental tracers for age dating young ground water, *in* Alley, W.M., ed., 1993, Regional ground-water quality: New York, Van Nostrand Reinhold, p. 255–294.

Pollock, D.W., 1989, Documentation of computer programs to compute and display pathlines using results from the U.S. Geological Survey modular three-dimensional finite-difference ground-water flow model: U.S. Geological Survey Open-File Report 89-381, 188 p.

Reilly, T.E., Plummer, L.N., Phillips, P.J., and Busenberg, Eurybiades, 1994, The use of simulation and multiple environmental tracers to quantity groundwater flow in a shallow aquifer: Water Resources Research, v. 30, no. 2, p. 421–433.

Schmidt, K.D., 1972, Nitrate in ground water of the Fresno-Clovis metropolitan area: Ground Water, v. 10., no. 1, p. 50–64.

———1986, DBCP in ground water of the Fresno-Dinuba area, California, *in* Proceedings of the Agricultural Impacts on Ground Water: National Water Well Association Conference, August 11-13, 1986, p. 511–529.

Sudicky, E.A., 1986, A natural gradient experiment on solute transport in a sand aquifer; spatial variability of hydraulic conductivity and its role in the dispersion process: Water Resources Research, v. 22, no. 13, p. 2069–2082.

Teso, R.R., Younglove, T., Peterson, M.R., Sheeks, D.L., III, and Gallavan, R.E., 1988, Soil taxonomy and surveys: classification of aerial sensitivity to pesticide contamination of ground water: Journal of Soil and Water Conservation, v. 43, no. 4, p. 348–352.

Theis, C.V, 1935, The relation between the lowering of the piezometric surface and the rate and duration of discharge of a well using groundwater storage: Transactions of the American Geophysical Union, v. 16, p. 519–524.

U.S. Department of Commerce, Bureau of Census, 1990, 1990 Census of population and housing, public law 94-171.

U.S. Environmental Protection Agency, 1985, Drinking water criteria document for 1,2-dibromo-3-chloropropane (DBCP): U.S. Environmental Protection Agency Document ECAO-CIN-410.

———1989, Seminar publication, transport and fate of contaminants in the subsurface: U.S. Environmental Protection Agency Report EPA/625/4-89/019, 148 p.

———1996, Drinking water regulations and health advisories: Washington D.C., U.S. Environmental Protection Agency Report EPA-822/B-96/002, 11 p.

Walton, W.C., 1962, Selected analytical methods for well and aquifer evaluation: Illinois State Water Survey Bulletin No. 49, 81 p.

Williams, L.E., and Matthews, M.A., 1990, Grapevine, *in* Irrigation of Agricultural Crops, American Society of Agronomy Monograph no. 30, 1218 p.

Zalkin, F., Wilkerson, M., and Oshima, R.J., 1984, Pesticide contamination in the soil profile at DBCP, EDB, simazine, and carbofuran application sites, *in* Pesticide movement to ground water: California Department of Food and Agriculture, Division of Pest Management, Environmental Protection, and Worker Safety, v. 2, 168 p.

Zheng, C., 1992, MT3D a modular three-dimensional transport model version 1.5 documentation and user's guide: S.S. Papadopulos and Associates, Inc., variously paged.

———1993, Extension of the method of characteristics for simulation of solute transport in three dimensions: Ground Water, v. 31, no. 3, p. 456–465.